1989

Heat transfer and combustion in a two-bed fluidized combustor

James Everett Foley
Iowa State University

Order Number 9003515

Heat transfer and combustion in a two-bed fluidized combustor

Foley, James Everett, Ph.D.

Iowa State University, 1989

U·M·I
300 N. Zeeb Rd.
Ann Arbor, MI 48106

Heat transfer and combustion in a two-bed fluidized combustor

by

James Everett Foley

A Dissertation Submitted to the
Graduate Faculty in Partial Fulfillment of the
Requirements for the Degree of
DOCTOR OF PHILOSOPHY

Major: Mechanical Engineering

Approved:

Signature was redacted for privacy.

In Charge of Major Work

Signature was redacted for privacy.

For the Major Department

Signature was redacted for privacy.

For the Graduate College

Iowa State University
Ames, Iowa
1989

TABLE OF CONTENTS

LIST OF FIGURES

LIST OF TABLES

ACKNOWLEDGEMENTS

This work was performed for the United States Department of Energy, through the Morgantown Energy Technology Center, Morgantown, West Virginia, under contract no. DE-AC21-86MC23248. I wish to acknowledge the financial support received from the Iowa State Mining and Minerals Resources Research Institute. I wish to thank the members of my program of study committee, Dr. Patrick Kavanagh, Dr. Thomas Wheelock, Dr. Gerald Colver, Dr. Gregory Maxwell, and Dr. George Burnet, for their helpful suggestions and criticisms in my graduate program. I thank Rod Oathout, Dean DeCock, Nathan Rosenboom, Marlin Kruse, and Roy Johansen for their assistance in performing experiments and analyzing data. I thank David Pflum for helpful discussions concerning fluidized bed modelling and William Buttermore for his expert assistance in fuel analysis and preparation.

I want to express special appreciation to my major professor, Dr. Robert Brown, who must be the hardest working and most understanding person with whom I have had the pleasure of working. I will be honored to be considered one of his peers.

Finally, I wish to give my greatest appreciation to my parents, who provide the love, patience, and encouragement that allow me to set high goals and try to attain them.

NOMENCLATURE

a_b = bubble area-to-volume ratio, m^2/m^3

A_a = cross-sectional area of annular bed, m^2

A_c = cross-sectional area of combustion bed, m^2

A_o = area of distributor plate per orifice, m^2

Ar = Archimedes number = $\frac{\rho_g(\rho_s-\rho_g)gd_p^3}{\mu_g^2}$

c_g = specific heat of fluidizing air, J/kgK

c_{mf} = specific heat of emulsion phase, J/kgK

$\bar{c}_{pa}$ = average specific heat of heat transfer air , J/kgK

$\bar{c}_{pc}$ = average specific heat of combustion air , J/kgK

c_{pw} = specific heat of water, J/kgK

c_s = specific heat of solid particle, J/kgK

C_{CO} = carbon monoxide concentration, $mole/m^3$

C_{O_2} = oxygen concentration, $mole/m^3$

d_b = bubble diameter, m

d_p = average particle diameter, m

d = char particle diameter, m

D = column diameter, m

D_a = annular bed outside diameter, m

D_c	=	combustion bed diameter, m
D_g	=	gas molecular diffusivity, m^2/s
g	=	acceleration due to gravity, m/s^2
$\dot{G}_{CO}$	=	rate of carbon monoxide production, $mole/s$
$\dot{G}_{O_2}$	=	rate of oxygen production, $mole/s$
h	=	heat transfer coefficient, W/m^2K
h_a	=	annular bed convection coefficient, W/m^2K
h_{aiw}	=	radiation heat transfer coefficient between wall and annular bed, W/m^2K
h_{aow}	=	radiation heat transfer coefficient between water wall and annular bed, W/m^2K
h_{av}	=	reciprocal fluidized bed resistance, W/m^2K
h_c	=	combustion bed convection coefficient, W/m^2K
h_{ciw}	=	radiation heat transfer coefficient between wall and combustion bed, W/m^2K
h_f	=	reciprocal film resistance, W/m^2K
h_{fg}	=	latent heat of vaporization, kJ/kg
h_{gc}	=	gas convection coefficient, W/m^2K
h_p	=	reciprocal packet resistance, W/m^2K
h_{pc}	=	particle convection coefficient, W/m^2K
h_w	=	water heat transfer coefficient, W/m^2K
h_{wall}	=	reciprocal wall resistance, W/m^2K
H_c	=	fluidized combustion bed height, m

$\mathbf{H}_f$	=	fluidized bed height, m
$\mathbf{H}_j$	=	water jacket height, m
$\mathbf{H}_{max}$	=	maximum bed expansion height, m
$\mathbf{H}_{min}$	=	fluidized bed height at minimum fluidization, m
$\Delta H_{f_{C'}}$	=	enthalpy of reaction for $C'(s) + O_2 \ - \ C'O_2$, $J/mole$
$\Delta H_{f_{C'O}}$	=	enthalpy of reaction for $C'O + \frac{1}{2}O_2 \ - \ C'O_2$, $J/mole$
$\mathbf{k}_e^o$	=	defluidized bed conductivity, W/mK
$\mathbf{k}_g$	=	gas conductivity, W/mK
$\mathbf{k}_{mf}$	=	minimally fluidized bed conductivity, W/mK
$\mathbf{k}_q$	=	interphase mass transfer coefficient, m/s
$\mathbf{k}_s$	=	solid particle conductivity, W/mK
$\mathbf{L}$	=	characteristic surface height, m
$\mathbf{m}$	=	empirical film coefficient constant
$\mathbf{m}_c$	=	bed carbon loading, kg
$\dot{m}_{dc}$	=	dry coal mass flow rate, kg/hr
$\dot{m}_f$	=	fuel mass flow rate, kg/hr
$\dot{m}_w$	=	water mass flow rate, kg/s
$\mathbf{M}_{C'}$	=	molecular weight of carbon, 12.011 $kg/mole$
$\mathbf{M}_{C'O}$	=	molecular weight of carbon monoxide, 28.011 $kg/mole$
$\mathbf{M}_{H_2O}$	=	molecular weight of water, 18.016 $kg/mole$
$\mathbf{n}$	=	rate of oxygen diffusion to individual char particle, $mole/s$
$\mathbf{N}$	=	number of char particles in bed
$\mathbf{N}_{C'aO}$	=	moles of calcium oxide produced per lbm of fuel

N_{CaSO_4} = moles of calcium sulfate produced per *lbm* of fuel

N_{dg} = moles of dry gas produced per *lbm* of fuel

N_{H_2O} = moles of water produced per *lbm* of fuel

N_{O_2} = moles of oxygen produced per *lbm* of fuel

Pr_w = water Prandtl number

q = heat flux, W/m^2

q_b = boiling water flux, W/m^2

q_{max} = maximum heat flux from combustor, W/m^2

q_{min} = minimum heat flux from combustor, W/m^2

Q_{aa} = energy advection rate from annular bed, W

Q_{ca} = energy advection rate from combustion bed, W

Q_{comb} = total energy release rate of combustor, W

Q_{cond} = energy conduction rate across annular bed, W

Q_{cr} = energy radiated from combustion bed to dividing wall, W

Q_{cw} = energy convected from combustion bed to dividing wall, W

Q_{in} = rate of energy release in bed, W

Q_w = heat transfer rate to water jacket, W

Sh = Sherwood number = $\frac{k_g d}{D_g}$

T_a = annular bed temperature, K

T_c = combustion bed temperature, K

T_g = gas temperature, K

T_{iw} = dividing wall temperature, K

T_o = inlet air temperature, K

T_{ow}	=	water wall temperature, K
T_{sat}	=	saturation temperature of water, K
T_w	=	water temperature, K
u	=	superficial air velocity, m/s
u_b	=	bubble rise velocity, m/s
u_{mf}	=	minimum fluidizatin velocity, m/s
u_{co}	=	air inlet velocity to central bed, m/s
u_{ao}	=	air inlet velocity to annular bed, m/s
U_{beds}	=	overall heat transfer coefficient, W/K
$\dot{V}_c$	=	molar flow rate of unburned carbon, $mole/s$
W_c	=	*lbm* of dry coal per *lbm* of fuel
W_l	=	*lbm* of added limestone per *lbm* of fuel
W_w	=	*lbm* of water in fuel per *lbm* of fuel
Δx	=	annular bed width, m
x	=	percent excess air
X_{CO}	=	mole fraction of CO in exhaust, dry basis
X_{CO_2}	=	mole fraction of CO_2 in exhaust, dry basis
X_{O_2}	=	mole fraction of O_2 in exhaust, dry basis
X_{N_2}	=	mole fraction of N_2 in exhaust, dry basis
X_{SO_2}	=	mole fraction of SO_2 in exhaust, dry basis
Y_c	=	mass fraction of carbon in flyash
Y_{C_f}	=	mass fraction of fixed carbon in coal
Y_{C_t}	=	mass fraction of total carbon in coal

Y_H = mass fraction of hydrogen in coal

ϵ_c = combustion bed emissivity

ϵ_b = bed voidage due to bubbles

ϵ_{bmax} = maximum bubble voidage

ϵ_{iw} = dividing wall emissivity

ϵ_{mf} = bed voidage at minimum fluidization

ϵ_o = defluidized bed voidage

ϵ_{ow} = water jacket wall emissivity

ϵ_a = annular bed emissivity

η = carbon conversion efficiency

μ_g = gas absolute viscosity, Ns/m^2

μ_w = water absolute viscosity, Ns/m^2

ρ_c = char particle density, kg/m^3

ρ_g = gas density, kg/m^3

ρ_{mf} = bed density at minimum fluidization, kg/m^3

ρ_o = inlet air density, kg/m^3

ρ_s = sand particle density, kg/m^3

ρ_v = saturated water vapor density, kg/m^3

ρ_w = water density, kg/m^3

σ = Stefan-Boltzmann constant, 5.67×10^{-8} W/m^2K^4

σ_b = bubble surface tension, N/m

$[i]$ = concentration of species i, $mole/cm^3$

1 INTRODUCTION

Fluidized bed combustion (FBC) has grown with the prospect that it can burn coal and low grade fuels in an environmentally acceptable manner. In 1985, more FBC units were sold than conventional boilers, the first time this has ever happened [1]. The reason for this growth is the ability of fluidized bed combustors to burn a wide variety of low-rank and high-sulfur coals cleanly and efficiently. The United States has a large abundance of these coals [2].

There are many unique characteristics of fluidized bed combustors. The use of a sulfur sorbent as the bed material results in large reductions in the emission of sulfur dioxide. Lower combustion temperatures compared to conventional pulverized coal boilers result in lower emissions of oxides of nitrogen (NO_x) produced from atmospheric nitrogen. Fuel nitrogen is therefore the major source of NO_x formation in FBC [3]. Reductions in NO_x emissions can be realized by feeding larger coal particles, reducing excess air levels, and utilizing staged combustion [4]. The relatively low combustion temperature also promotes optimum sulfur capture efficiency, relaxes the need for exotic boiler construction materials, and eliminates problems with ash slagging. The bed temperature is also spatially uniform; there are no hot spots that could lead to ash sintering.

The ability to burn a wide variety of fuels (high-sulfur or high-ash coals, biomass

fuels, sludge, etc.) is a result of the good gas-solids contact, long fuel residence times, and vigorous mixing found in fluidized beds. The good mixing in the bed leads to high combustion efficiencies. Fluidized beds have high rates of convection heat transfer to surfaces immersed in the bed. Convection coefficients for tubes located in the bed can be more than an order of magnitude than for tubes located in the freeboard region [5]. These high coefficients allow bed heat exchangers to be very compact.

Despite these advantages, technical problems remain that must be overcome before wider markets are developed. Prominent among these difficulties is the poor load turndown capability of fluidized bed combustors. Load turndown is the ability to vary the firing rate of a combustor to match system energy demands. Maximum load turndown ratio is defined as the ratio of maximum to minimum fuel firing rates. Inherent to conventional FBC designs is an inability to produce large variations in heat transfer rate from the fluidized bed. Generally, changes in heat transfer rate are modest and are accompanied by degradation in combustion. Innovative concepts in bed design are required to control heat transfer independent of combustion. This capability is especially important for fluidized beds targeted for coal-fired gas turbine power systems and small-scale boilers and furnaces.

The objective of this research was to investigate a new concept in fluidized bed design that improves load turndown capability. The research consisted of two major phases of work:

1. Development of computational models to predict heat transfer and combustion performance and to aid in the design of a fluidized bed combustor. The heat transfer model includes energy and mass balances on the two-bed com-

bustor and a semi-empirical theory for calculating convection coefficients. The combustion model includes mass balances for reacting species and a simple kinetic model for coal combustion.

2. Construction of the combustor and performance of coal combustion tests. The combustion tests were performed with three different coal-based fuel forms: crushed coal, coal-limestone briquettes, and coal-water-limestone mixture (CWLM).

The research goal was to determine if a load turndown ratio of 10:1 could be obtained for a fluidized bed combustor, while satisfying pollution emission criteria.

2 BACKGROUND

Heat transfer from a fluidized bed to water tubes is determined by three factors:

1. The temperature gradient between bed and water.

2. The heat transfer area.

3. The overall heat transfer coefficient between bed and water.

Boiler application usually sets the water-side temperature; attempts to control load with temperature gradients require large variations in bed temperature. However, even small variations in bed temperature from optimum design values will greatly degrade both sorbent utilization [6] and combustion efficiency [7].

Reduction of heat transfer area has been suggested as a method for reducing loads in FBC. This condition can be accomplished by either reducing fluidization velocity, which contracts bed volume, or by discharging bed material. The former approach is of little practical value because bed contraction is limited to about 30% [8]; the corresponding load turndown is modest at best. Discharging, storing, and reinjecting hot particles is fraught with many technical difficulties and has little to recommend as a method for load turndown. In addition to the above difficulties, both methods for reducing heat transfer area will expose tubes to erosion when they are in the splash zone of the bed. Another method for reducing heat transfer

area requires the air distributor to be partitioned which allows zones of the bed to be independently fluidized. Load turndown is achieved by selectively slumping part of the bed; heat transfer area in defluidized zones is effectively zero. This technique has some undesirable effects on combustion including fuel smoldering and agglomeration in the slumped regions. Although bed slumping is frequently employed in commercial FBC units, turndown capability is rather modest.

Variation of the overall heat transfer coefficient between bed and tubes can also be employed for load turndown control. Heat transfer coefficients in fluidized beds show large variation with fluidization velocity; in principle, turndown ratios exceeding ten can be achieved by reducing fluidization velocity from its maximum heat transfer value to the minimum fluidization condition. However, as Figure 2.1 illustrates, the dependence of heat transfer coefficient on fluidization velocity is strongly nonlinear; since combustion rate is proportional to fluidization velocity, a match between heat release and heat transfer rates is difficult to achieve. Horio et al., 1985 [9], have developed a baffled heat transfer tube with the goal of achieving a linear response in average heat transfer coefficient with changes in fluidization velocity. Although they were successful in obtaining a linear response in the velocity range of 0.3 to 0.5 m/s, this achievement represents only a modest turndown ratio. It is far from evident that a sufficiently linear response can be achieved over larger velocity intervals. In addition, the baffle arrangements produce a linear response at great sacrifice in heat transfer rates.

A more promising approach to improved load turndown is control of heat transfer rate independent of combustion rate [10,11]. The device as described here can be employed in fluidized beds that remove thermal energy around the perimeter of the

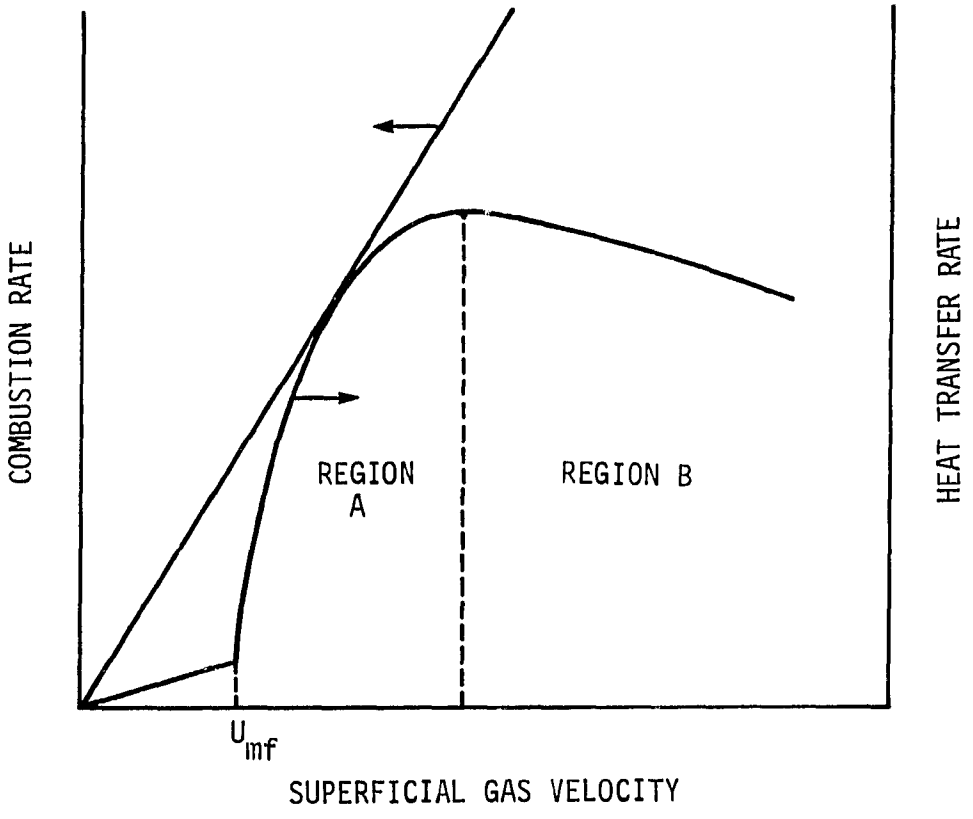

Figure 2.1: Heat transfer rate and combustion rate vs. fluidization velocity

bed, i.e., water jacket or water wall construction; however, the principle can also be applied to any vertical water tube design. Independent control of heat transfer rate and combustion rate is accomplished by surrounding the fluidized bed in which fuel is burned, hereafter called the combustion bed, by another fluidized bed, hereafter called the heat transfer bed, that establishes the overall heat transfer rate from the inner combustion bed. The two beds, physically divided by a wall, are fluidized independently by separate air plenums.

Figure 2.2 illustrates the device in a water jacketed, cylindrical fluidized bed. The central combustion bed is provided with fluidization air through a circular distributor plate from an air plenum which is designed to give even distribution of air through the bed. Coal or other fuel is fed into the combustion bed at a rate determined by the desired heat generation rate, while air flow into this bed is set at a rate consistent with efficient combustion. The heat transfer bed is the annular fluidized bed surrounding the combustion bed. The two beds are separated by a wall constructed of heat resistant material of reasonably high thermal conductivity such as stainless steel. The heat transfer bed is supplied with fluidization air from a plenum separate from the combustion bed plenum. The heat transfer bed is enclosed by a water jacket that removes energy from the combustor in the form of hot water or steam. Overall heat transfer rate from the combustion bed to the water jacket is determined by the heat transfer coefficients associated with the fluidized combustion bed, the conductivity of the wall separating the beds, the heat transfer coefficients at the inner and outer diameters of the heat transfer bed, the conductivity of the water jacket wall, and the convection coefficient of the water in the water jacket. However, control of the overall heat transfer rate will reside in the heat transfer bed and will

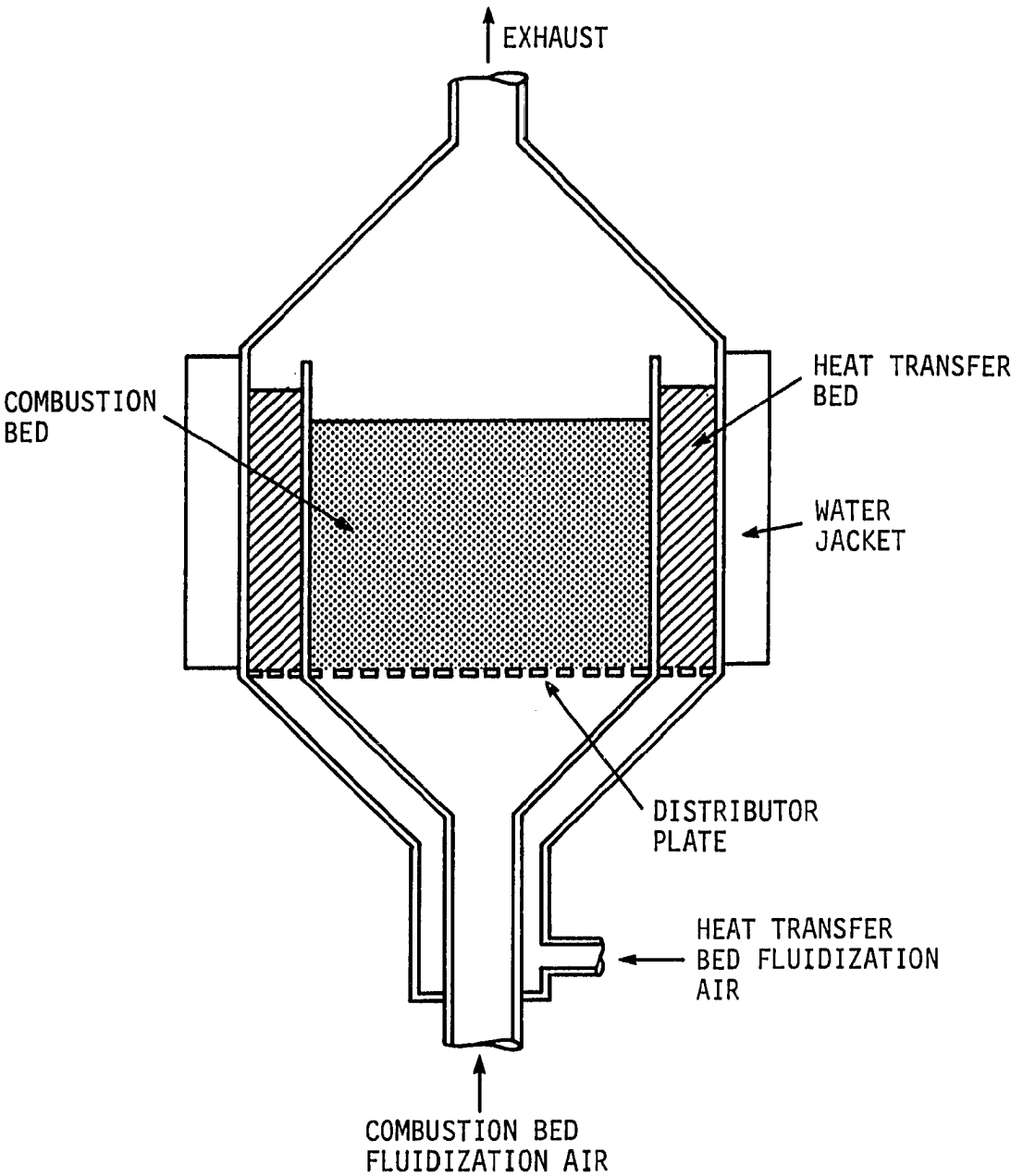

Figure 2.2: Two-bed fluidized combustor

be accomplished by changing the fluidization velocity of air entering this annular bed. The combustion bed can be operated in Region B of Figure 2.1 where heat transfer rate is only a weak function of fluidization velocity; air flow rate to this bed can be chosen consistent with good combustion and independent of heat transfer considerations. The heat transfer bed can be operated in Region A where large variations in heat transfer rate can be achieved. If no air is passed through the heat transfer bed, then it has the poor heat transfer characteristics of packed granular beds. If only sufficient air is passed through the heat transfer bed to just fluidize it, then increased heat transfer due to convection occurs. Heat transfer continues to increase with increasing air flow until enhanced heat transfer characteristic of bubbling fluidized beds is reached; the result is a continuous and large variation in heat transfer rate from the combustor that is controlled independently of combustion rate. A simple analysis provides an estimate of the load turndown capability of this device.

Let q be the heat transfer per unit wall area of the combustor. The load turndown that can be achieved is approximately the ratio of q for full fluidization of the heat transfer bed to q for the slumped heat transfer bed. For steady state operation of the combustor, the maximum heat transfer from the combustion bed can be approximated by:

$$q_{max} = \left(\frac{1}{h_c} + \frac{2}{h_a} + \frac{1}{h_w}\right)^{-1} (T_c - T_w) \tag{2.1}$$

In deriving this equation it is assumed that the combustion and heat transfer beds are uniform in temperature due to vigorous mixing. In addition, the heat transfer bed is assumed to be deep compared to its radial dimension; hence, heat loss associated with energy convected out of the heat transfer bed with fluidization air

is relatively small. In the case of minimum heat transfer from the combustor, the heat transfer bed is completely defluidized:

$$q_{min} = \left(\frac{1}{h_c} + \frac{\Delta x}{k} + \frac{1}{h_w}\right)^{-1} (T_c - T_w) \tag{2.2}$$

Further simplification is obtained if it is assumed that, for the maximum heat transfer condition, the beds are equally fluidized and employ identical bed material. If boiling heat transfer is employed in the water jacket, then:

$$h_a = h_c \ll h_w \tag{2.3}$$

For the minimum fluidization condition:

$$\frac{k_e^o}{\Delta x} \ll h_c \ll h_w \tag{2.4}$$

Hence, the turndown ratio can be approximated by the expression:

$$\frac{q_{max}}{q_{min}} = \frac{1}{3}\frac{h_c \Delta x}{k_e^o} \tag{2.5}$$

For a 2.5 cm wide heat transfer bed of sand with a bulk conductivity of 0.24 W/mK and a typical fluidized bed heat transfer coefficient of 250 W/m^2K, a turndown ratio of about 8 is predicted. The energy convected out of the heat transfer bed with fluidization air does not represent heat loss from the combustor; it can be recovered by heat exchange, employed in preheating fluidization air for the combustion bed, or used in staged combustion in the freeboard [12]. Staged combustion was incorporated in the combustor constructed for this study.

3 HEAT TRANSFER MODEL

The heat transfer model simulates the energy transfer processes in the two-bed fluidized combustor. The model is used to predict combustion bed temperature, combustor heat transfer rates, and load turndown for varying operating conditions. These operating conditions include annular bed width, annular bed particle sizes, annular bed flow velocity, and fuel firing rate.

Several assumptions were employed in model development:

- The central combustion bed is at a uniform temperature, T_c, due to vigorous mixing and large thermal mass.
- The annular bed is also isothermal, at T_a.
- Steady state conditions exist in the combustor.
- The energy released in the bed, Q_{in}, is released uniformly to the central bed.
- Boiling occurs at the water jacket wall with a temperature equal to the saturation temperature of the water.
- Both fluidized beds are opaque and the only radiation effect is from the beds to the wall surfaces. Radiation from the upper bed surface to the freeboard walls can be neglected if the freeboard is assumed to be insulated.

- Heat conduction occurs normal to wall surfaces.
- The dividing wall (between inner and annular beds) and water jacket wall are at uniform temperatures, T_{iw} and T_{ow}, respectively.
- Heat transfer occurs from the annular bed to the fluidization air and to the water jacket.
- Air properties are used for exhaust gases exiting the combustion bed.

3.1 Energy Balance Equations

The mathematical formulation of the model consists of a system of nonlinear algebraic equations describing heat transfer in the combustor due to convection, radiation, and boiling. These equations, derived from energy balances on the combustion bed, dividing wall, heat transfer bed, and water jacket wall, are:

Combustion bed energy balance

$$Q_{in} = \rho_o u_{co} \bar{c}_{pc} A_c (T_c - T_o) + \pi D_c H_j (h_c + h_{ciw})(T_c - T_{iw}) \tag{3.1}$$

Dividing wall energy balance

$$(h_c + h_{ciw})(T_c - T_{iw}) - (h_a + h_{aiw})(T_a - T_{iw}) = 0 \tag{3.2}$$

Annular bed energy balance

$$\frac{\rho_o u_{ao} \bar{c}_{pa} A_a (T_a - T_o)}{\pi H_j} + D_c (h_a + h_{aiw})(T_a - T_{iw}) - D_a (h_a + h_{aow})(T_a - T_{ow}) = 0 \tag{3.3}$$

Water jacket wall energy balance

$$(h_a + h_{aow})(T_a - T_{ow}) = q_b \tag{3.4}$$

Boiling water heat flux

Nucleate pool boiling occurs in the water jacket and is modelled using a correlation developed by Rohsenow and cited by Incropera and DeWitt [13]:

$$q_b = \mu_w h_{fg}\left[\frac{g(\rho_w - \rho_v)}{\sigma_b}\right]^{\frac{1}{2}}\left[\frac{c_{pw}}{c_{sf} h_{fg} Pr_w}\right]^3 (T_{ow} - T_{sat})^3 \tag{3.5}$$

Radiation heat transfer coefficients

The radiation heat transfer coefficients have been linearized and include effects of view factors and emissivities. Here it is assumed that surface areas of wall and bed are equivalent:

$$h_{ciw} = \frac{\sigma(T_{iw}^2 + T_c^2)(T_{iw} + T_c)}{\left(\frac{1}{\epsilon_c} + \frac{1}{\epsilon_{iw}} - 1\right)} \tag{3.6}$$

$$h_{aiw} = \frac{\sigma(T_{iw}^2 + T_a^2)(T_{iw} + T_a)}{\left(\frac{1}{\epsilon_a} + \frac{1}{\epsilon_{iw}} - 1\right)} \tag{3.7}$$

$$h_{aow} = \frac{\sigma(T_{ow}^2 + T_a^2)(T_{ow} + T_a)}{\left(\frac{1}{\epsilon_a} + \frac{1}{\epsilon_{ow}} - 1\right)} \tag{3.8}$$

The preceding equations apply when the annular bed is fluidized. When the annular bed is defluidized, a second set of equations describing conduction across a static bed of particles is used:

Energy released in central bed

$$Q_{in} = \left[\pi D_c H_j (h_c + h_{ciw})(T_c - T_{iw}) + \rho_o u_{co} A_c \bar{c}_{pc}(T_c - T_o)\right] \tag{3.9}$$

Dividing wall energy balance

$$(h_c + h_{ciw})(T_c - T_{iw}) + \left[\frac{2k_e^o}{D_c \ln(\frac{D_c}{D_a})}\right](T_{ow} - T_{iw}) = 0 \tag{3.10}$$

Water wall energy balance

$$Q_{cond} = q_b(\pi D_a H_j) \tag{3.11}$$

Annular bed energy balance

$$Q_{cond} = Q_{in} - \rho_o \left[u_{oc} A_c \bar{c}_{pc}(T_c - T_o) + u_{oa} A_a \bar{c}_{pa}(T_a - T_o)\right] \tag{3.12}$$

3.2 Fluidized Bed Convection Coefficients

Fluidized bed convection coefficients are found theoretically using the two-phase theory of fluidization described by Xavier and Davidson [14]. This theory treats the bed as consisting of a particle-dense phase (emulsion phase) and a particle-lean phase (bubble phase). The bubble phase is created when gas flow in excess of that required for minimum fluidization passes through the bed in the form of voids, or bubbles. The bed convection coefficient is composed of particle convection and gas convection:

$$h_c = h_{pc} + h_{gc} \tag{3.13}$$

Radiation heat transfer is accounted for separately in the energy balance equations given previously. The particle convection coefficient is calculated from a packet resistance in series with a film resistance:

$$h_{pc} = \frac{1 - \epsilon_b}{\left(\frac{1}{h_p} + \frac{1}{h_f}\right)} \tag{3.14}$$

The reciprocal film resistance is:

$$h_f = \frac{mk_g}{d_p} \tag{3.15}$$

The reciprocal packet resistance is:

$$h_p = 2\left[\frac{k_{mf}\rho_{mf}c_{mf}(u-u_{mf})}{\pi L}\right]^{0.5} \tag{3.16}$$

where:

$$L = 0.5d_b \tag{3.17}$$

and the product of density and specific heat of the emulsion phase is:

$$\rho_{mf}c_{mf} = \rho_s(1-\epsilon_{mf})c_s \tag{3.18}$$

The height-average bubble diameter may be calculated from:

$$d_b = 0.54(u-u_{mf})^{0.4}\left[H_f + 4\sqrt{A_o}\right]^{0.8} g^{-0.2} \tag{3.19}$$

and the bed voidage due to bubbles is:

$$\epsilon_b = 1 - \frac{u_b}{u - u_{mf} + u_b} \tag{3.20}$$

The bubble rise velocity is a function of relative bubble size:

$$u_b = 0.71\sqrt{gd_b} \quad \text{if} \quad \frac{d_b}{D} < .125 \tag{3.21}$$

$$u_b = 0.802\sqrt{gd_b}\exp\frac{-d_b}{D} \quad \text{if} \quad .125 \leq \frac{d_b}{D} \leq .60 \tag{3.22}$$

$$u_b = 0.35\sqrt{gd_b} \quad \text{if} \quad \frac{d_b}{D} > .60 \tag{3.23}$$

The thermal conductivity of the emulsion phase is found from:

$$k_{mf} = k_e^o + 0.1\rho_g c_g d_p u_{mf} \tag{3.24}$$

where:

$$k_e^o = k_g\left[\left(\frac{k_s}{k_g}\right)^{(0.28-0.757\log\epsilon_o - 0.057\log(k_s/k_g))}\right] \tag{3.25}$$

The minimum fluidization velocity is:

$$u_{mf} = \frac{25.7\mu_g}{\rho_g d_p}\left[(1 + 5.53 \times 10^{-5} Ar)^{0.5} - 1\right] \tag{3.26}$$

where the dimensionless Archimedes number is given by:

$$Ar = \frac{\rho_g(\rho_s - \rho_g)g d_p^3}{\mu_g^2} \tag{3.27}$$

The gas convection coefficient consists of a bed resistance in series with a wall resistance:

$$h_{gc} = \frac{1}{\left(\frac{1}{h_{av}} + \frac{1}{h_w}\right)} \tag{3.28}$$

where the reciprocal bed resistance is:

$$h_{av} = \left(\frac{4k_{mf}\rho_g c_g u}{\pi H_f}\right)^{0.5} \tag{3.29}$$

and the wall resistance is approximately equal to the film resistance previously calculated:

$$\frac{1}{h_w} = \frac{1}{h_f} \tag{3.30}$$

One additional condition is used in calculating heat transfer coefficients in the annular bed. Since the annular bed is constrained on the top surface by a screen to prevent particle elutriation, there is a maximum height, H_{max}, to which the bed may expand. Therefore, once the bed expands to H_{max}, the following condition restricting bubble voidage applies:

$$\epsilon_{bmax} = 1 - \frac{H_{mf}}{H_{min}} \tag{3.31}$$

3.3 FORTRAN Program

A listing of the FORTRAN program that was written to solve the preceding set of energy balance and convection coefficient equations is shown in Appendix A. The main program solves the energy balance equations, Eqs. 3.1 - 3.12, iteratively. The main program utilizes the following subroutines:

- PROP - evaluates properties of air
- MINFLU - evaluates minimum fluidization velocity, fluidized bed conductivity, and gas convection coefficient
- COEFFA - evaluates convection coefficient for annular heat transfer bed (either a semi-empirical model based on the two-phase theory of fluidization or experimental heat transfer data is used - See Chapter 7.3)
- COEFFC - evaluates convection coefficient for combustion bed using the two-phase theory model

3.4 Heat Transfer Model Predictions

The heat transfer model was used to aid in preliminary design of the two-bed fluidized combustor. Specifically, it was used to determine the effect of annular bed width and annular bed particle size on load turndown. The load turndown is obtained as the ratio of maximum to minimum firing rates in the combustor at constant combustion temperature. The minimum firing rate is obtained at the point where the combustion bed is minimally fluidized and the annular heat transfer bed is static (defluidized). At this condition, the combustion bed will be operated in

a fuel-lean manner, and it is reasonable to assume that 100% of the fuel energy is released in the central bed.

The maximum firing rate is obtained by setting the annular bed air flow rate at the point of maximum convective heat transfer coefficient. The combustion bed air flow rate is set at an expected maximum allowable level. For computational purposes, this maximum superficial velocity is assumed to be $6u_{mf}$, above which significant bed material would be elutriated. Since the combustion bed normally operates sub-stoichiometrically, it is assumed that only 50% of the heat of combustion (Q_{comb}) is released in the bed. The energy released in the bed (Q_{in}) was determined for the maximum and minimum heat transfer cases; the load turndown, then, is calculated as the ratio of maximum Q_{comb} to the minimum Q_{comb}.

Particle size has a large effect on convection coefficients in fluidized beds; a decrease in particle size by a factor of two can double convection coefficients. It was therefore assumed that decreasing particle size would have a large positive effect on load turndown. However, simulations suggested that use of small particles would not have as dramatic an effect on load turndown as might be expected. Figure 3.1 demonstrates that reducing annular bed particle size from 1.0 mm to 0.3 mm increases load turndown from 8.3 to only 9.8 in the case of 1.0 mm particles in the combustion bed, even though convection coefficients in the annular bed increase by a factor of two. The reason for the relatively small effect is as follows. As the air flow through the annular bed becomes large, heat transfer from the combustion bed becomes rate-limiting to the overall heat transfer process. Consequently, the overall heat transfer rate between the combustion bed and the annular bed does not increase dramatically for this range of particle sizes. Nevertheless, there is an

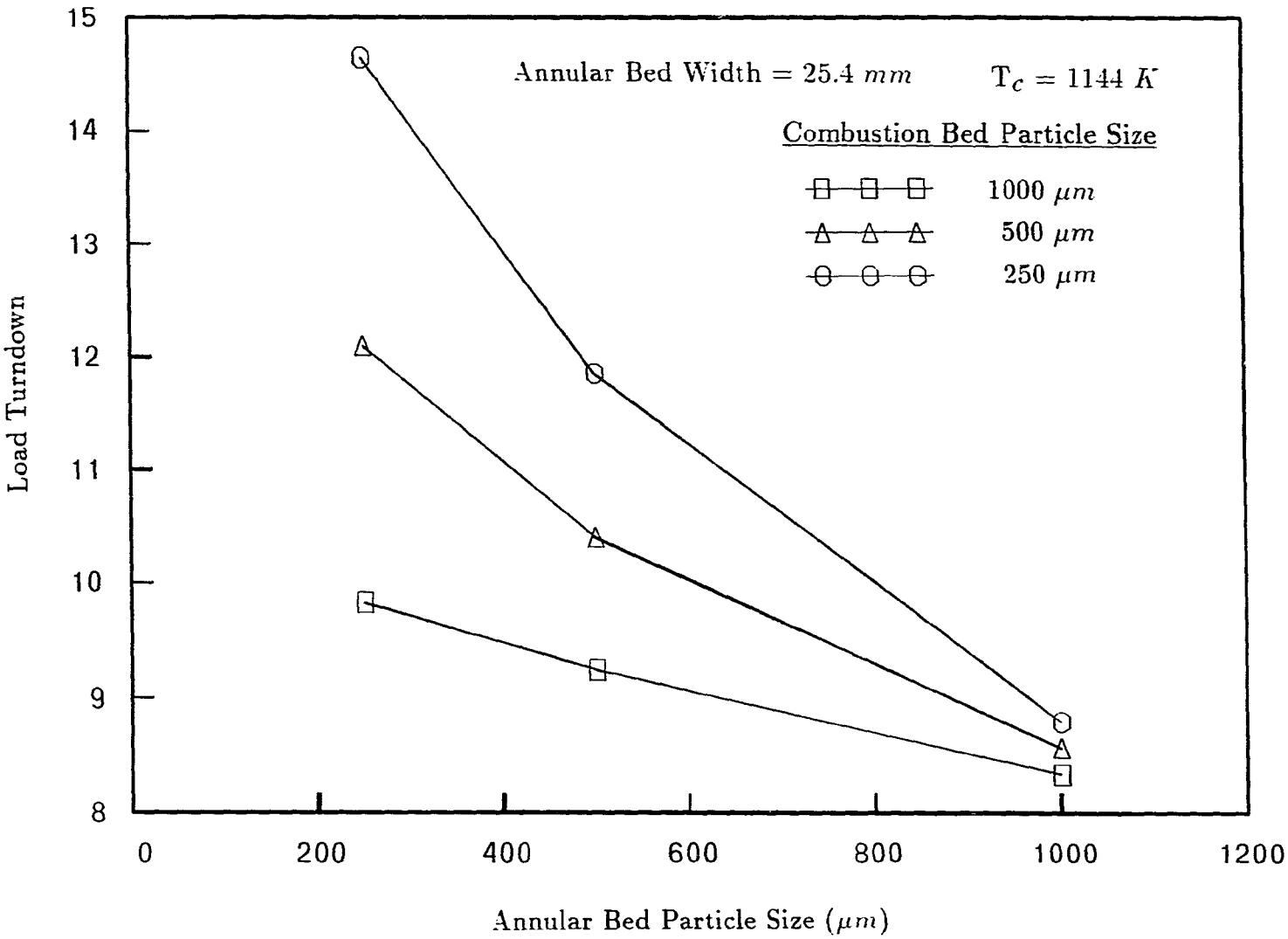

Figure 3.1: Theoretical effect of particle size on load turndown

advantage in using small particles in the annular bed. In addition to the slightly higher load turndown, smaller particles also require a lower air flow rate. Sand sieved to 50 x 70 *mesh* (0.25 *mm* average diameter) was selected as the smallest practical bed material that could be employed in the annular bed. Smaller particles could be too easily entrained in the gas flow by the action of gas bubbles bursting at the surface of the annular bed.

It can also be seen from Figure 3.1 that higher load turndown is achieved with small combustion bed particles. A load turndown of 15 is predicted for 0.25 *mm* combustion bed particles. However, particles smaller than 1.0 *mm* are not practical in the combustion bed because of excessively small particle terminal velocity; low air flow rates result in low firing rates. Therefore, 1.0 *mm* sand particles were selected for use in the combustion bed to allow reasonably high air velocities, and hence, high fuel firing rates.

Simulations also clearly indicated the advantage of a wide annular bed for producing large load turndown. Results shown in Figure 3.2 predict load turndown exceeding 15 with an annular bed width of 65 *mm*. However, the overall diameter of the combustor to be used in experiments was constrained to 254 *mm* by the fixed dimensions of the water jacket prepared for experiments to be performed. Under this constraint, a large annular bed width would have produced an unreasonably small combustion bed volume. Therefore, a 25.4 *mm* width was selected as large enough to achieve a desired load turndown of 10.

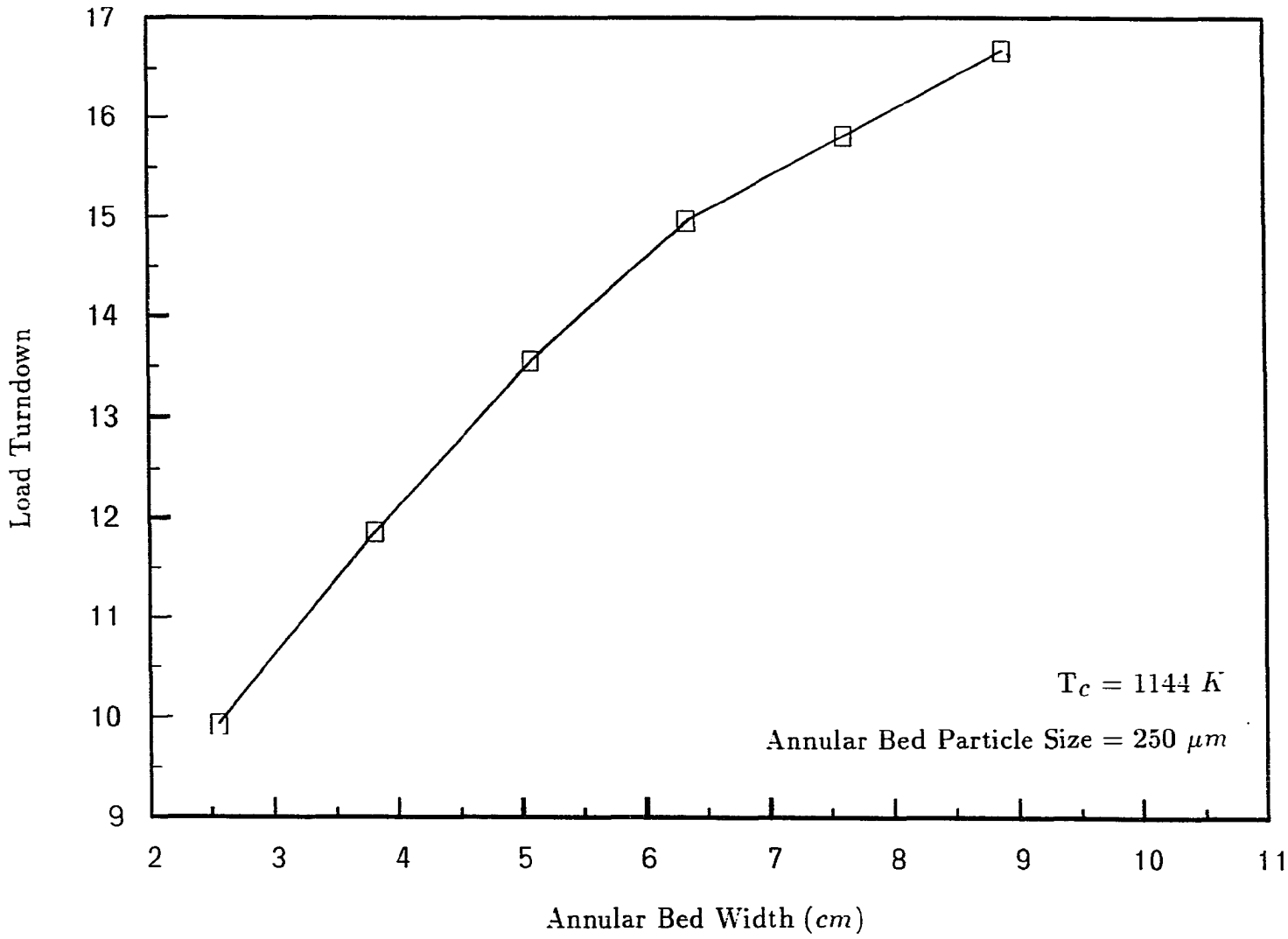

Figure 3.2: Theoretical effect of bed width on load turndown

In summary, the following design parameters were chosen for the two-bed fluidized combustor:

- Combustor bed diameter: 203 mm
- Annular bed width: 25.4 mm
- Combustion bed average particle diameter: 1.00 mm
- Annular bed average particle diameter: 0.25 mm

4 COMBUSTION MODEL

One of the inputs to the heat transfer model is the fraction of fuel burned in the combustion bed. Values ranging from 50% to 100% were assumed in predictions of load turndown in the previous chapter. In order to predict fuel flow rates (and load turndown) more precisely, it is necessary to model the combustion process in the combustion bed. The combustion model consists of species conservation equations for carbon monoxide and oxygen that employ a simple kinetic mechanism for coal combustion.

When coal particles are fed into the combustion bed, they undergo rapid heating and volatile gases are released. The remaining char particles consist mainly of fixed carbon and ash. To model the combustion process, it is necessary to consider the behavior of both volatiles and char.

The mechanism of volatile combustion in fluidized beds is not fully understood [15]. Most models assume that the volatiles are released instantaneously upon fuel entrance to the bed, which is a reasonable assumption since volatiles release usually occurs within seconds upon rapid heating [16].

The rate of char combustion is usually limited by one of the following rates [15]:

1. Film diffusion - diffusion rate of oxygen from the emulsion phase to the char

particle surface

2. Pore diffusion - diffusion rate of oxygen through pores in the char particle

3. Chemical reaction - adsorption and reaction of oxygen at active sites in the char particle to produce gaseous reaction products

The char particle may burn as a constant volume sphere or as a shrinking sphere. In the case of constant diameter, the particle either completely burns up or it reaches a critical porosity, at which time the particle fragments and elutriates from the bed [17]. A particle which burns as a shrinking sphere simply shrinks in diameter as it burns until it is small enough to be elutriated from the bed.

There is evidence that char combustion in fluidized beds is film diffusion rate limited [16]. Pore diffusion and chemical reactions take place rapidly compared to the diffusion of oxygen to the char particle surface. There is also strong evidence that char particles burn with constant diameter [17], and the model that follows assumes constant diameter particles. The following assumptions have been employed in the combustion model development:

- Volatiles are released instantaneously from coal particles entering the bed.
- Volatiles are converted instantaneously to carbon monoxide and water in the emulsion phase.
- The char particle burns with constant diameter where reaction is rate limited by diffusion of oxygen to the particle surface.
- Unburned carbon losses arise only from elutriation of char particles from the bed (no loss from bed overflow).

- The char reacts to form carbon monoxide (CO); the CO does not further react in the particle boundary layer or emulsion phase [18,19].
- Carbon monoxide produced from volatile and char combustion diffuses to the bubble phase where it is converted to carbon dioxide by homogeneous reaction.
- The emulsion phase is well-mixed; gas concentrations are spatially uniform.
- The bubble phase is in plug flow; concentrations of CO and O_2 vary with height in the bubble phase.

4.1 Mathematical Formulation

4.1.1 Emulsion phase model

In the emulsion phase, char reacts with oxygen to form carbon monoxide and the volatiles react to form carbon monoxide and water. Since it is assumed that the carbon portion of the volatiles is converted to carbon monoxide instantaneously, the rate of carbon monoxide production due to volatile combustion is:

$$\dot{G}_{CO_{vol}} = (Y_{C_t} - Y_{C_f})\left(\frac{\dot{m}_{dc}}{M_C}\right) \tag{4.1}$$

where $Y_{C_t} - Y_{C_f}$ (the difference between total and fixed coal carbon content) is the carbon content of volatiles.

The char reaction is given by:

$$C(s) + \frac{1}{2}O_2 \;-\; CO \tag{4.2}$$

The reaction is rate limited by the diffusion of oxygen to the char surface [16]:

$$n = 2\pi d Sh D_g C_{O_{2e}} \tag{4.3}$$

where n is the rate of oxygen diffusion to an individual char particle, D_g is the molecular diffusivity of oxygen, d is the char particle diameter, and $C_{O_{2e}}$ is the concentration of oxygen in the emulsion phase. The Sherwood number, Sh, a measure of the mass transfer at the particle surface, was found by Avedesian and Davidson to have an average value of 1.42 for fluidized beds [16]. A constant value of molecular diffusivity, $D_g = 2.08 \times 10^{-4}$, was assumed. The rate of oxygen consumption in the emulsion phase due to char combustion is then the rate of diffusion per particle multiplied by the number of char particles in the bed:

$$\dot{G}_{O_{2char}} = -nN \tag{4.4}$$

The number of char particles, N, is found from the bed carbon loading divided by the mass per char particle:

$$N = \frac{m_c}{\frac{\pi}{6}\rho_c d^3} \tag{4.5}$$

where ρ_c is the char particle density, in kg/m^3, and m_c is the bed carbon loading, in kg. In principle, carbon loading can be calculated from a population balance on burning particles [8], however, Gregory and Brown [20] found the bed carbon loading to be fairly constant at 0.080 kg for combustor geometry and operating conditions similar to those used in the present experiments. This value is used for these simulations.

Derivation of species conservation equations for both the emulsion phase and bubble phase appear in Appendix B. The resulting equations for the emulsion phase are:

$$\frac{1}{H_c}\left[u_{mf}C'_{O_{2e}} - u_{mf}\left(\frac{T_o}{T_c}\right)C'_{O_{2o}}\right] = \frac{\left(-k_q a_b \epsilon_b \left(C'_{O_{2e}} - \bar{C}'_{O_{2b}}\right) + \frac{\dot{G}_{O_{2e}}}{H_c A_c}\right)}{\left(\epsilon_{mf}(1-\epsilon_b)\right)} \tag{4.6}$$

$$\frac{1}{H_c}\left[u_{mf}C'_{CO_e} - u_{mf}\left(\frac{T_o}{T_c}\right)C'_{CO_o}\right] = \frac{\left(-k_q a_b \epsilon_b \left(C'_{CO_e} - \bar{C}'_{CO_b}\right) - \frac{\dot{G}_{CO_e}}{H_c A_c}\right)}{\left(\epsilon_{mf}(1-\epsilon_b)\right)} \tag{4.7}$$

where $C'_{O_{2o}} = 0.008705\ moles/m^3$ and $C'_{CO_o} = 0$ correspond to concentrations of oxygen and carbon monoxide in air, respectively.

Carbon monoxide is produced in the emulsion phase by both char and volatile combustion. The rate of production due to char combustion is found from the rate of diffusion of oxygen to the char surface (Eq. 4.4). Two moles of CO are produced per mole of oxygen diffusing to the char surface, so the rate of CO production is:

$$\dot{G}_{CO_{char}} = -2\dot{G}_{O_{2char}} = 2nN = 4\pi d N Sh D_g C'_{O_{2e}} \tag{4.8}$$

The rate of carbon monoxide production due to char has a maximum value at steady state fixed by the feed rate of coal:

$$\dot{G}_{CO_{char\ max}} = Y_{C_f}\left(\frac{\dot{m}_{dc}}{M_C}\right) \tag{4.9}$$

where Y_{C_f} is the mass fraction of fixed carbon of the moisture-free coal, M_C is the molecular weight of carbon, and $\dot{m}_{dc}$ is the mass flow rate of dry coal. The

difference between maximum and actual carbon monoxide production due to char represents unburned carbon that is elutriated from the combustion bed.

The rate of oxygen consumption in the emulsion phase is given by:

$$\dot{G}_{O_{2e}} = \dot{G}_{O_{2char}} + \dot{G}_{O_{2vol}} \tag{4.10}$$

The rate of oxygen consumption due to volatile combustion is:

$$\dot{G}_{O_{2vol}} = -\frac{1}{2}\dot{G}_{CO_{vol}} - \frac{1}{2}\dot{G}_{H_2O_{vol}} \tag{4.11}$$

where the production of water due to hydrogen combustion is:

$$\dot{G}_{H_2O_{vol}} = Y_H \left(\frac{\dot{m}_{dc}}{M_{H_2O}} \right) \tag{4.12}$$

where Y_H is the mass fraction of hydrogen in dry coal, and M_{H_2O} is the molecular weight of water.

4.1.2 Bubble phase model

In the bubble phase, carbon monoxide produced in the emulsion phase is oxidized to carbon dioxide. The elementary reaction is thought to be [21]:

$$CO + OH \overset{k_1}{\rightarrow} CO_2 + H \tag{4.13}$$

Accordingly, the irreversible rate of disappearance of CO is:

$$d[CO]/dt = -k_1[CO][OH] \tag{4.14}$$

The concentration of hydroxyl is assumed to be controlled by the three equilibrium reactions:

$$O + H_2 = OH + H \tag{4.15}$$

$$OH + H_2 = H_2O + H \tag{4.16}$$

$$O + O + M = O_2 + M \tag{4.17}$$

where the equilibrium constants are [22]:

$$K_a = \frac{[OH][H]}{[O][H_2]} = 2.239 \exp\left(\frac{-941.1}{T_c}\right) \tag{4.18}$$

$$K_b = \frac{[H_2O][H]}{[H_2][OH]} = 0.2089 \exp\left(\frac{7654.7}{T_c}\right) \tag{4.19}$$

$$K_c = \frac{[O_2]}{[O]^2} = 0.05018 \exp\left(\frac{59561}{T_c}\right) \tag{4.20}$$

Algebraic manipulation of the three above equations leads to an expression for OH concentration:

$$[OH] = \left[\frac{K_a[H_2O][O_2]^{1/2}}{K_b K_c^{1/2}}\right]^{1/2} \tag{4.21}$$

which, when substituted into Eq. 4.14 gives:

$$\frac{d[CO]}{dt} = -\frac{k_1 K_a^{1/2}}{K_b^{1/2} K_c^{1/4}}[CO][H_2O]^{1/2}[O_2]^{1/4} \tag{4.22}$$

Howard et al. [21] found the empirical rate constant, k_1, to be approximately equal to $1.3 \times 10^{14} \frac{cm^3}{mole\ sec}$.

The species conservation equations for the bubble phase (derived in Appendix B) are:

$$\frac{d}{dz}C_{O_{2b}} = \frac{\left(-k_q a_b \epsilon_b \left(C_{O_{2b}} - C_{O_{2e}}\right) + \frac{\dot{G}_{O_{2b}}}{H_c A_c}\right)}{\epsilon_b (u - u_{mf})} \tag{4.23}$$

$$\frac{d}{dz}C_{CO_b} = \frac{\left(-k_q a_b \epsilon_b \left(C_{CO_b} - C_{CO_e}\right) + \frac{\dot{G}_{CO_b}}{H_c A_c}\right)}{\epsilon_b (u - u_{mf})} \tag{4.24}$$

where the subscript e designates emulsion phase and b designates bubble phase. The initial conditions are $C_{O_{2b}} = C_{O_{2o}}$ and $C_{CO_b} = 0$ at $z = 0$. The interphase mass transfer coefficient, k_q, is given by Grace [23] as:

$$k_q = \frac{u_{mf}}{3} + \left(\frac{4D_g \epsilon_{mf} u_b}{\pi d_b}\right)^{\frac{1}{2}} \tag{4.25}$$

The rate of carbon monoxide consumption in the bubble phase is:

$$\dot{G}_{CO_b} = \frac{d[CO]}{dt}\left(\epsilon_b H_c A_c\right) \tag{4.26}$$

Substitution of Eq. 4.22 into the above equation with proper unit conversion yields:

$$\dot{G}_{CO_b} = -\frac{(3.162 \times 10^{-5}) k_1 K_a^{1/2}}{K_b^{1/2} K_c^{1/4}} \left(C_{CO_b}\right)\left(C_{H_2O_b}\right)^{1/2}\left(C_{O_{2b}}\right)^{1/4} \epsilon_b H_c A_c \tag{4.27}$$

The rate of oxygen consumption in the bubble phase is then simply:

$$\dot{G}_{O_{2b}} = \frac{1}{2}\dot{G}_{CO_b} \tag{4.28}$$

4.1.3 Fraction of fuel burned in-bed

With knowledge of the emulsion phase CO concentration and the bubble phase average CO concentration, the fraction of fuel energy released in the bed may be determined. Incomplete combustion of the fuel in the bed has three components:

1. Unburned carbon in char particles
2. Unreacted carbon monoxide advected from emulsion phase
3. Unreacted carbon monoxide advected from bubble phase

These components may be treated as energy losses; the loss due to unburned char in the emulsion phase is:

$$L_1 = \dot{V}_{C'}(\Delta H_{f_{C'}}) \tag{4.29}$$

where $\Delta H_{f_{C'}} = 393520\ kJ/mole$ is the enthalpy of reaction of $C'(s) + O_2 \rightarrow C'O_2$. The molar flow rate of unburned carbon, $\dot{V}_{C'}$, is found as the difference between maximum CO production and actual CO production due to char combustion (Eq. 4.9 - Eq. 4.8); the previous equation becomes:

$$L_1 = \left(\frac{Y_{C'_f} \dot{m}_{dc}}{M_{C'}} - 4\pi d N Sh D_g C'O_{2e} \right) \Delta H_{f_{C'}} \tag{4.30}$$

The loss due to unreacted carbon monoxide in the emulsion phase is:

$$L_2 = \left[C'C'O_e u_{mf} A_c \epsilon_b (1 - \epsilon_{mf}) \right] \Delta H_{f_{C'O}} \tag{4.31}$$

where $\Delta H_{f_{C'O}} = 110530\ kJ/mole$ is the enthalpy of reaction of $C'O + \frac{1}{2}O_2 \rightarrow C'O_2$, and the term in brackets is the molar flow rate of unreacted emulsion phase CO. Likewise, the loss due to unreacted CO in the bubble phase is:

$$L_3 = \left[\bar{C}_{C'O_b} (u - u_{mf}) A_c \epsilon_b \right] \Delta H_{f_{C'O}} \tag{4.32}$$

The percent of fuel burned in-bed is then given by:

$$\% \text{ burned in bed} = \frac{(100) Q_{in}}{\dot{m}_{dc}(LHV)} = 100 \left[1 - \frac{L_1 + L_2 + L_3}{\dot{m}_{dc}(LHV)} \right] \tag{4.33}$$

where LHV is the lower heating value of the coal.

4.2 FORTRAN Program

A FORTRAN program was written to solve the preceding set of equations and a listing appears in Appendix C. The method of solution is:

1. Input bed parameters such as temperature, voidage, and velocity from the heat transfer model or from experimental data.

2. Guess values of emulsion phase oxygen and carbon monoxide concentrations and fuel mass flow rate.

3. Solve equations 4.23 and 4.24 for bubble phase oxygen and carbon monoxide concentration distributions using differential equation solver DIVPAG [24].

4. Solve equations 4.6 and 4.7 (in closed form) for emulsion phase oxygen and carbon monoxide concentrations.

5. Solve equation 4.33 for the percent of fuel burned in-bed, and hence, the fuel mass flow rate.

6. Iterate until convergence is reached.

4.3 Combustion Model Predictions

Preliminary simulations were performed with the combustion model to determine the effect of fuel flow rate and equivalence ratio on the fraction of fuel burned in the combustion bed. The equivalence ratio is defined as the mass flow rate of coal divided by the mass flow rate of coal required for stoichiometric combustion. The stiochiometric requirement is based on the air flow rate entering the combustion bed. The equivalence ratio is directly proportional to coal feed rate for fixed air flow rate. Figure 4.1 is a plot of predicted fraction of fuel burned in-bed vs. coal feed rate for three different equivalence ratios. Assumptions used in these simulations were constant combustion temperature of 1144 K, combustor geometry

as selected by heat transfer modelling (See Page 22), and a coal heating value of 30000 kJ/kg. The plotted equivalence ratios correspond to 73%, 100%, and 167% of stoichiometric air requirements.

At low fuel flow rates (less than 2.0 kg/hr) it is predicted that about 80% of the fuel is burned in-bed. At each plotted equivalence ratio, the fuel flow rate reaches a minimum at the point corresponding to minimum bed fluidization. For example, at an equivalence ratio of 1.37, a reduction in fuel flow rate below about 2.0 kg/hr would defluidize the bed. If the fuel flow rate is further lowered from 2.0 kg/hr, the equivalence ratio will decrease (because air flow rate must be held constant at the minimum fluidization level). In Figure 4.1 if the fuel flow rate is lowered from 2.0 kg/hr (at an equivalence ratio of 1.37) to 1.0 kg/hr the equivalence ratio must decrease to 0.60.

Maximum fuel flow rates are limited by the maximum amount of air that can be admitted to the combustion bed, which is set by the bed particle entrainment velocity. For example, in Figure 4.1 at an equivalence ratio of 1.00, the maximum fuel flow rate is about 6.0 kg/hr. A higher fuel flow rate would require increased equivalence ratio, as the air flow rate would be held constant to prevent excessive elutriation. So, if the fuel flow rate is to be increased to 8.0 kg/hr, the equivalence ratio must be increased to 1.37.

At mid-range fuel flow rates (2 - 6 kg/hr), it is predicted that an increase in equivalence ratio (decrease in air flow rate) will result in an increase in fraction of fuel burned in-bed. One might have expected this trend to be reversed; a decrease in air flow rate decreases oxygen concentration, which decreases combustion rate. This trend suggests that gas residence time (since residence time is proportional to

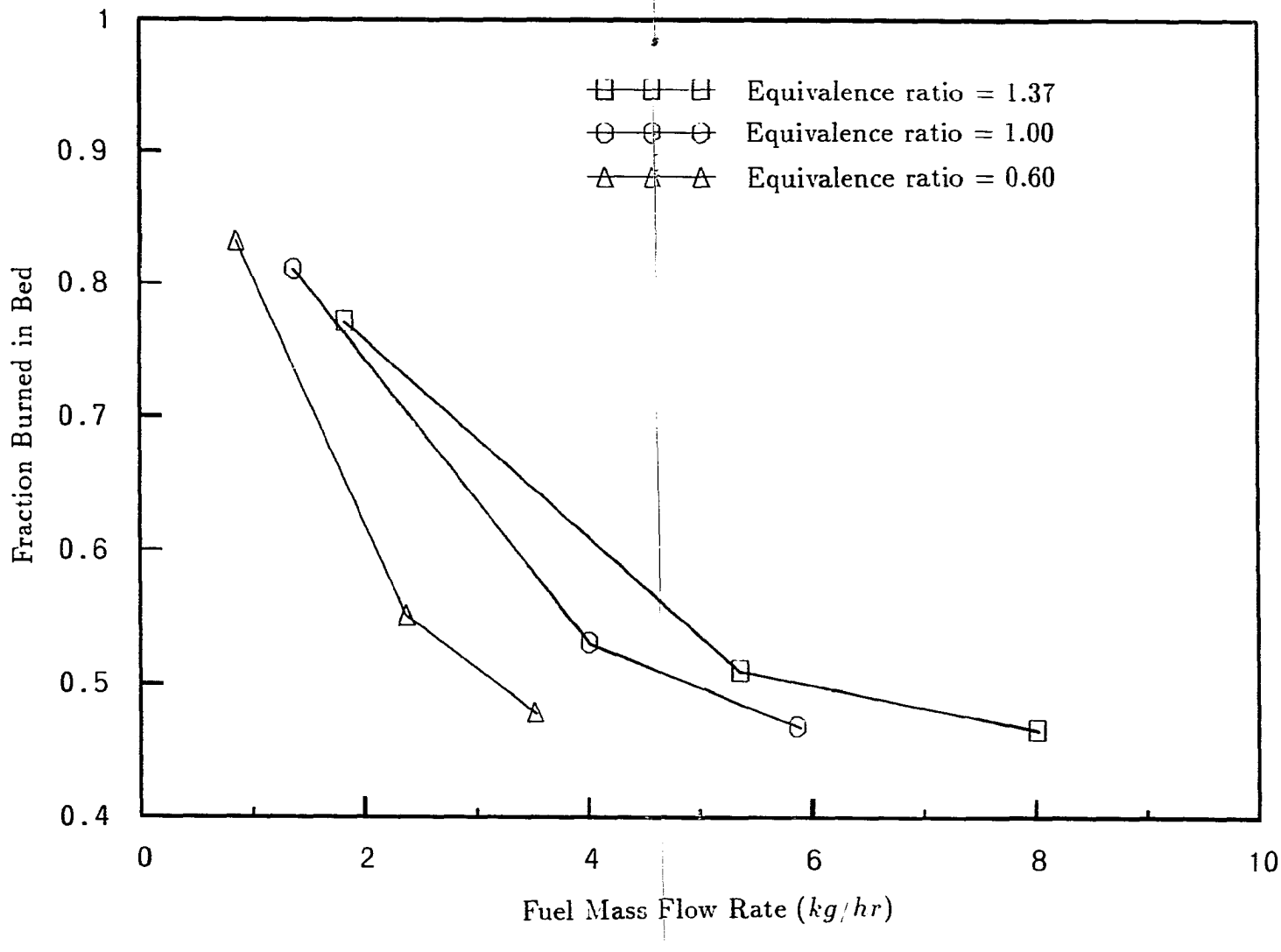

Figure 4.1: Effect of fuel flow rate and equivalence ratio on fraction of fuel burned in-bed

air flow velocity) is a more important factor in in-bed energy release than is oxygen concentration.

In predicting load turndown using the heat transfer model, it was necessary to assume values for percent of fuel burned in-bed at minimum and maximum fuel flow rates (100% and 50% respectively). Combustion model predictions of 84% and 47% for percent burned in-bed, respectively, support these assumptions.

5 EXPERIMENTAL APPARATUS

The combustion system and test rig consisted of the following main components: the two-bed fluidized combustor, the fuel feed system, air and water metering equipment, the flue-gas analysis system, and a microcomputer-based data acquisition system.

5.1 Two-Bed Fluidized Combustor

A section view of the cylindrical two-bed combustor constructed for coal-fired combustion trials is shown in Figure 5.1. The combustor was constructed in four vertical sections. The bottom section consisted of separate plenum chambers serving the combustion bed and heat transfer bed. Air from these plenums flowed through a common distributor plate. The stainless steel distributor was a 12 mm thick, 406 mm diameter plate with 250 uniformly spaced, 0.238 mm drilled holes. To prevent sand backflow in the annular bed and to prevent flame flashback in the combustion bed, 80-*mesh* stainless steel screen was welded to the upper surface of the plate. The water jacket section bolted onto the distributor plate and plenum assembly. The third section, a smaller, ceramic-insulated section, was added immediately above the water-jacketed section. A stainless steel cylinder with an inner diameter of 203 mm, a height of 370 mm, and a wall thickness of 3.175 mm ran the length of

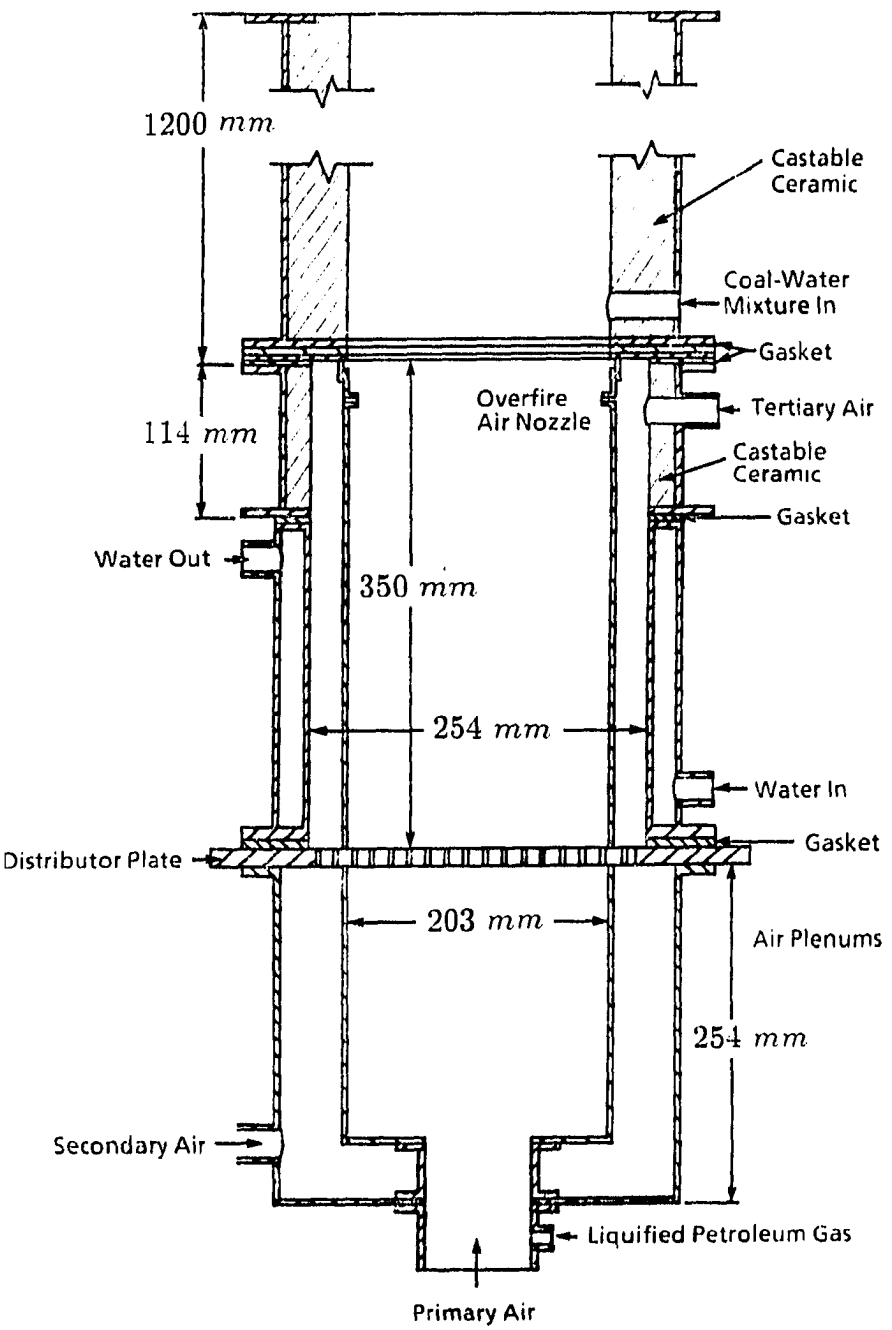

Figure 5.1: Experimental two-bed fluidized combustor

the water-jacketed and insulated sections and divided these combined sections into two concentric beds: the central combustion bed and the annular heat transfer bed. The insulated bed section was not an integral part of the two-bed combustor; it was included in this test combustor to simplify energy balances on the combustor and to allow the measurement of overall heat transfer coefficients in the heat transfer bed. The fourth section of the combustor was a 1.2 m long, 203 mm inside diameter, ceramic-insulated freeboard.

The central combustion bed supported combustion and the annular heat transfer bed controlled the amount of heat transfer to the water jacket. Air used to fluidize the annular bed was exhausted through nozzles to the combustor freeboard immediately above the combustion bed. The eight evenly-spaced 6 mm nozzles were installed on the bed dividing wall at a point 300 mm from the distributor plate. They were positioned in such a manner as to impart swirl to the secondary air as it mixed with gas exiting the central bed. This arrangement, in addition to the insulated freeboard, was expected to promote complete combustion of unreacted gases and coal fines released to the freeboard.

5.2 Fuel Feed System

Dry fuel (including crushed coal and coal briquettes) was fed into the combustor using an auger feeder. The above-bed feed point was through the freeboard at a point 460 mm above the distributor plate. The feeder was an Accurate Model 602 variable-speed solids-auger with a 25 mm-diameter feedscrew. It was calibrated using a scale-and-stopwatch technique. The feeder was modified to allow positive hopper sealing to prevent exhaust gas backflow through the feeder. (The combustor

operated at slight positive pressure due to the pressure drop in the exhaust lines.)

Liquid fuels (e.g., coal-water mixtures) were fed into the bed using a Teel-model positive displacement pump. The coal-water mixture entered the combustor through a water-jacketed 6.4 *mm* stainless steel tube. When the coal-water mixture entered the combustion bed, it tended to form pea-size agglomerates. This phenomenon has been found to increase combustion efficiency since the agglomerates have long in-bed residence times [25]. Figure 5.2 is a schematic of the pumping system. A variable speed electric motor that drives the pump was used for feed rate control. All valves were used on a full-open or full-closed basis to prevent clogging and were not used for flow rate control. The mixture was pumped from a 5-gallon reservoir placed on an Arlyn digital scale having a capacity of 50 *lbs* and a resolution of 0.01 *lbs*. Since the pump was capable of flow rates greatly in excess of desired fuel feed rates, a bypass piping system was used. A small fraction of the fuel flow was sent to the combustor while the balance was recycled back to the fuel reservoir. Since the mass of fuel in the pipes was essentially constant, the fuel feed rate could be calculated as the change in the scale weight reading divided by the elapsed time between readings.

5.3 Air and Water Metering System

Figure 5.3 shows a schematic of the overall experimental set-up. Three air flows entered the combustor: primary air entered the combustion bed, secondary air entered the heat transfer bed, and tertiary air entered the freeboard of the heat transfer bed. Secondary air and tertiary air, taken together, represented overfire air required to burn volatiles and char that escaped into the freeboard above the

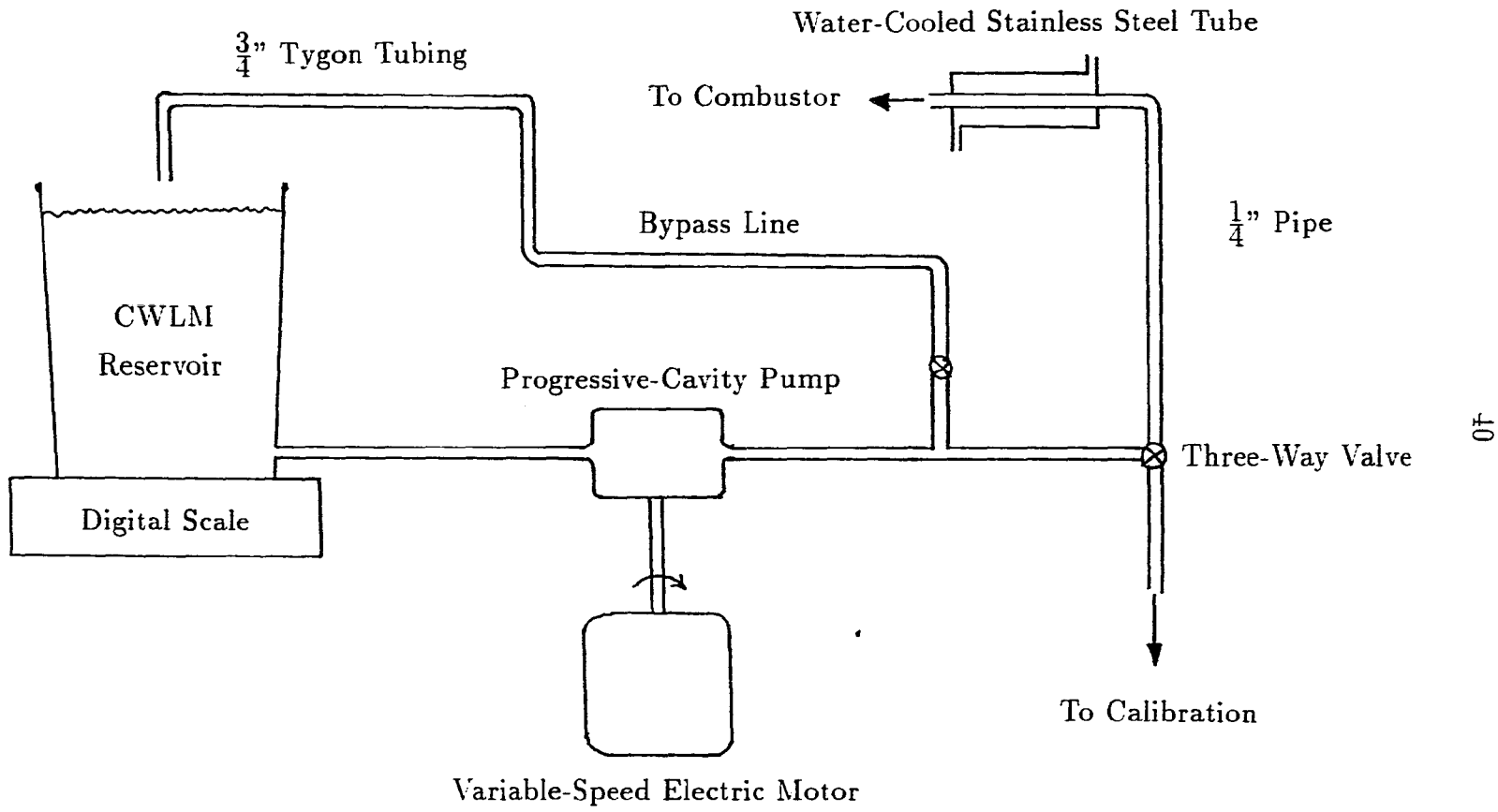

Figure 5.2: Coal-water mixture feed system

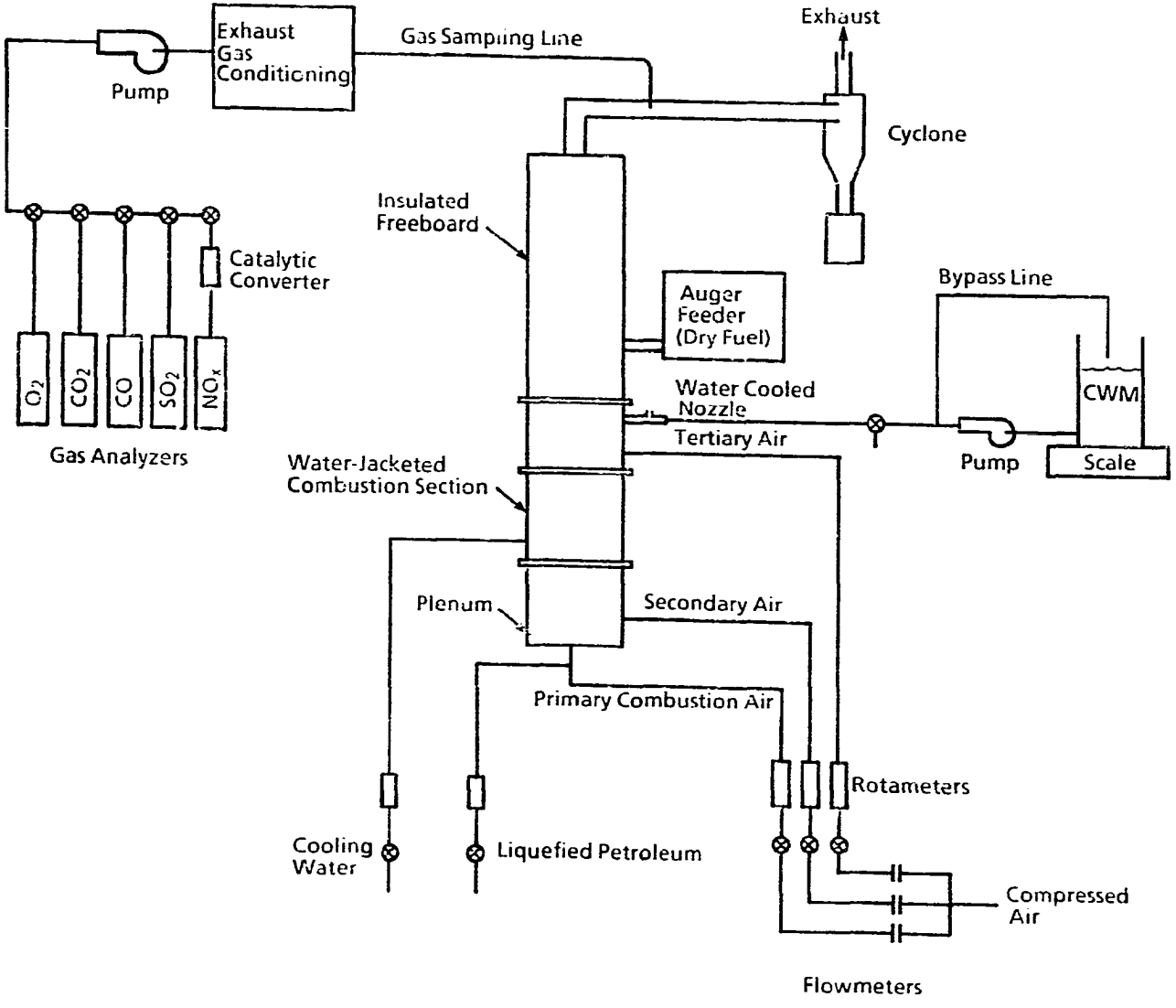

Figure 5.3: Experimental apparatus

combustion bed. These air flows could be measured manually using rotameters or automatically with calibrated orifice meters. The orifice meters were assembled using 1-inch NPT pipe and a drilled stainless steel plate. The orifice meters were calibrated using a laminar flow meter. The water flow rate into the water jacket was read manually using a rotameter. Liquified petroleum gas (LPG) was used to preheat the combustor. The LPG entered the central plenum, mixed with the primary air, and was ignited above the bed with a high-voltage spark transformer. The LPG flow rate is read manually with a rotameter.

A photograph of the experimental apparatus is shown in Figure 5.4. There are two combustors in the photograph; the combustor on the left was used in previous work described in Reference 11. The combustor on the right was used in this work. The dry fuel auger and coal-water mixture pumping system are visible on a movable stand between the two combustors. The control panel is on the right side and faces away from the combustors. Not shown in the photograph are the gas analysis system and microcomputer-based data acquisition.

5.4 Flue-Gas Analysis System

Exhaust gas was sampled through a 6 mm stainless steel tube located in the top of the combustor freeboard. Figure 5.5 is a schematic of the gas sampling and analysis system. The exhaust gas flowed through a heat-tape-wrapped stainless steel tube to a particulate filter, an acid-mist filter, and a Perma-Pure dryer. The dryer removed moisture from the flue-gas stream in a the vapor phase, which prevented condensation of water (and the possible formation of sulfuric acid). The gas flowed through a filter before entering the vacuum pump. The gas was then directed to

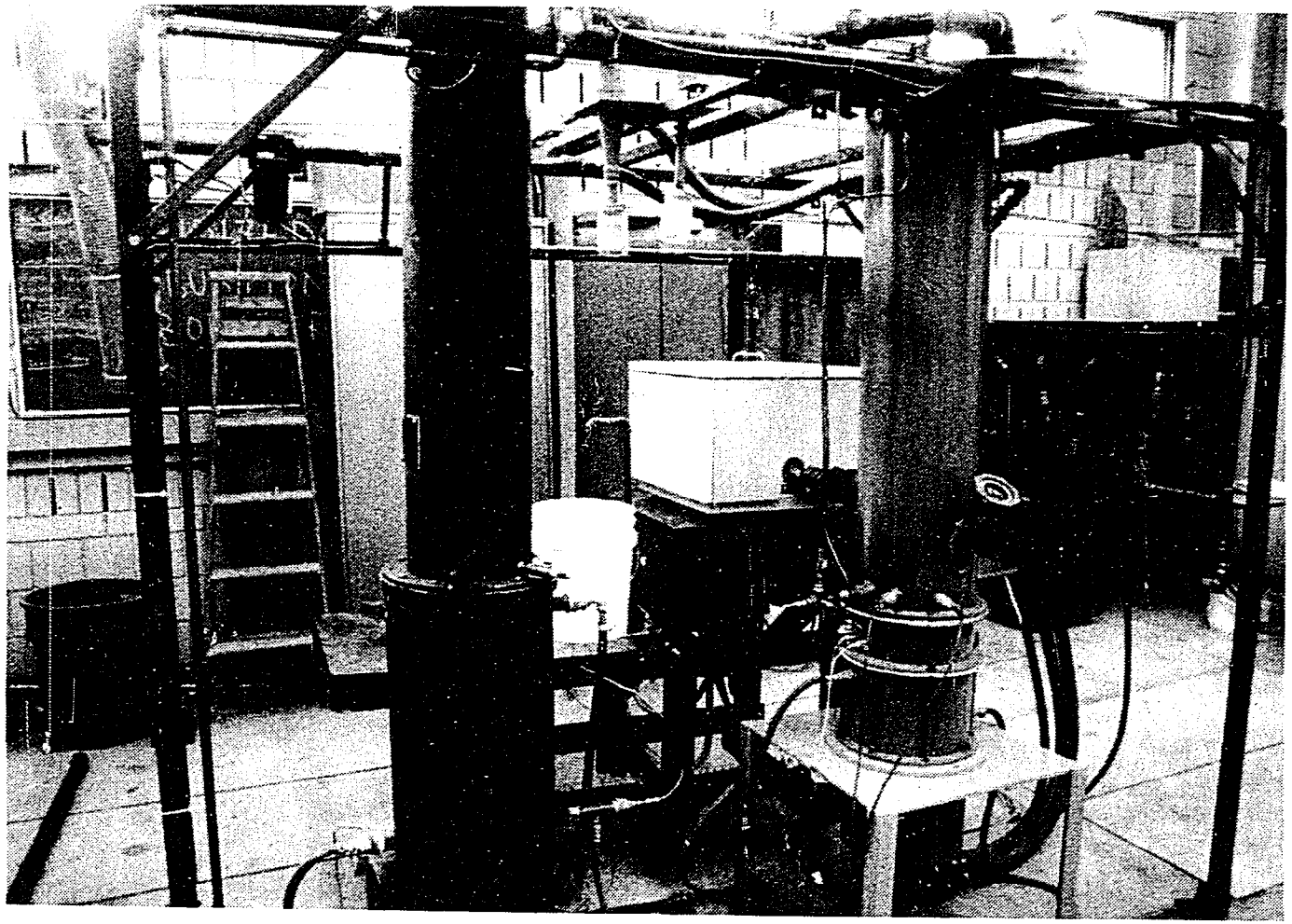

Figure 5.4: Photograph of the experimental apparatus

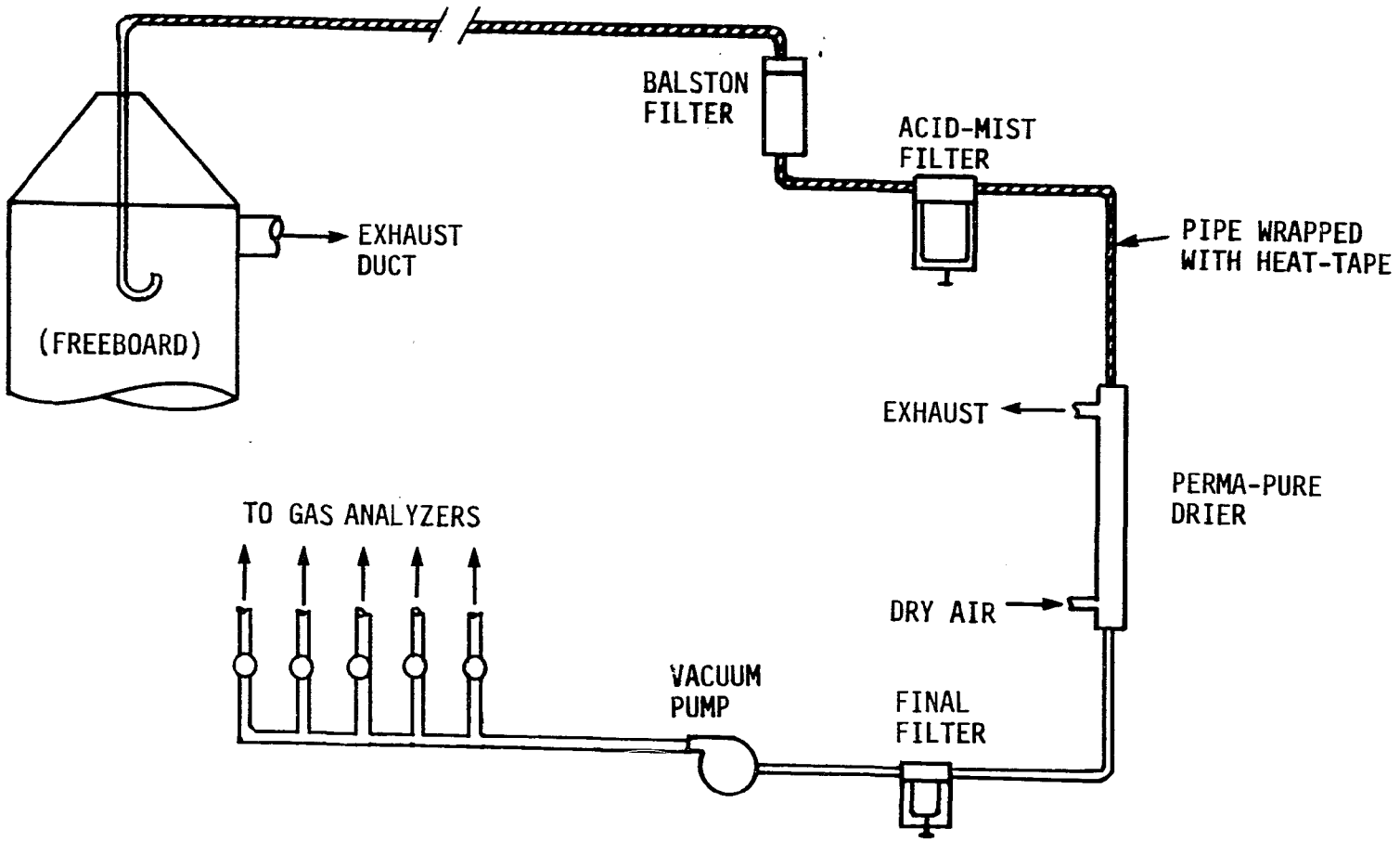

Figure 5.5: Gas sampling system

the gas analyzers via a flow-rate-controlled manifold. The gas stream to the NO analyzer first passed through a heated catalytic converter to reduce NO_2 to NO. Five gas analyzers were used: SO_2, NO, CO_2, CO and O_2 meters. The oxygen meter was a Beckman Model 755 paramagnetic analyzer. The CO_2 and CO meters were Beckman Model 820 non-dispersive infra-red analyzers. Horiba Model VIA-300 and VIA-500 non-dispersive infra-red analyzers were used to measure NO_x and SO_2 respectively.

Solids (ash and unburned carbon) sampling was performed using a 75 *mm* diameter cyclone located downstream of the freeboard as shown in Figure 5.3. The solids sample was collected in a 1-liter glass jar. Cyclone collection efficiency could be periodically tested by performing isokinetic sampling on the exhaust tube. In shakedown combustion trials, it was found that the cyclone collection efficiency was greater than 90% for a variety of operating conditions.

5.5 Data Acquisition System

A Zenith Model Z-158 microcomputer equipped with a 20-megabyte hard disk drive was used for data acquisition and test control. The computer had five expansion slots for slide-in expansion boards. One expansion slot was occupied by a 24-bit, parallel, digital input/output interface board (Metrabyte Model PIO-12). Two 8-channel, high speed, analog-to-digital converter boards (Metrabyte Model DAS-8) occupied two other expansion slots. Figure 5.6 is a schematic of the data acquisition system.

Thermocouple measurements were performed using 3, 16-channel, analog input, sub-multiplexer boards (Metrabyte Model EXP-16) giving a total capacity of 48

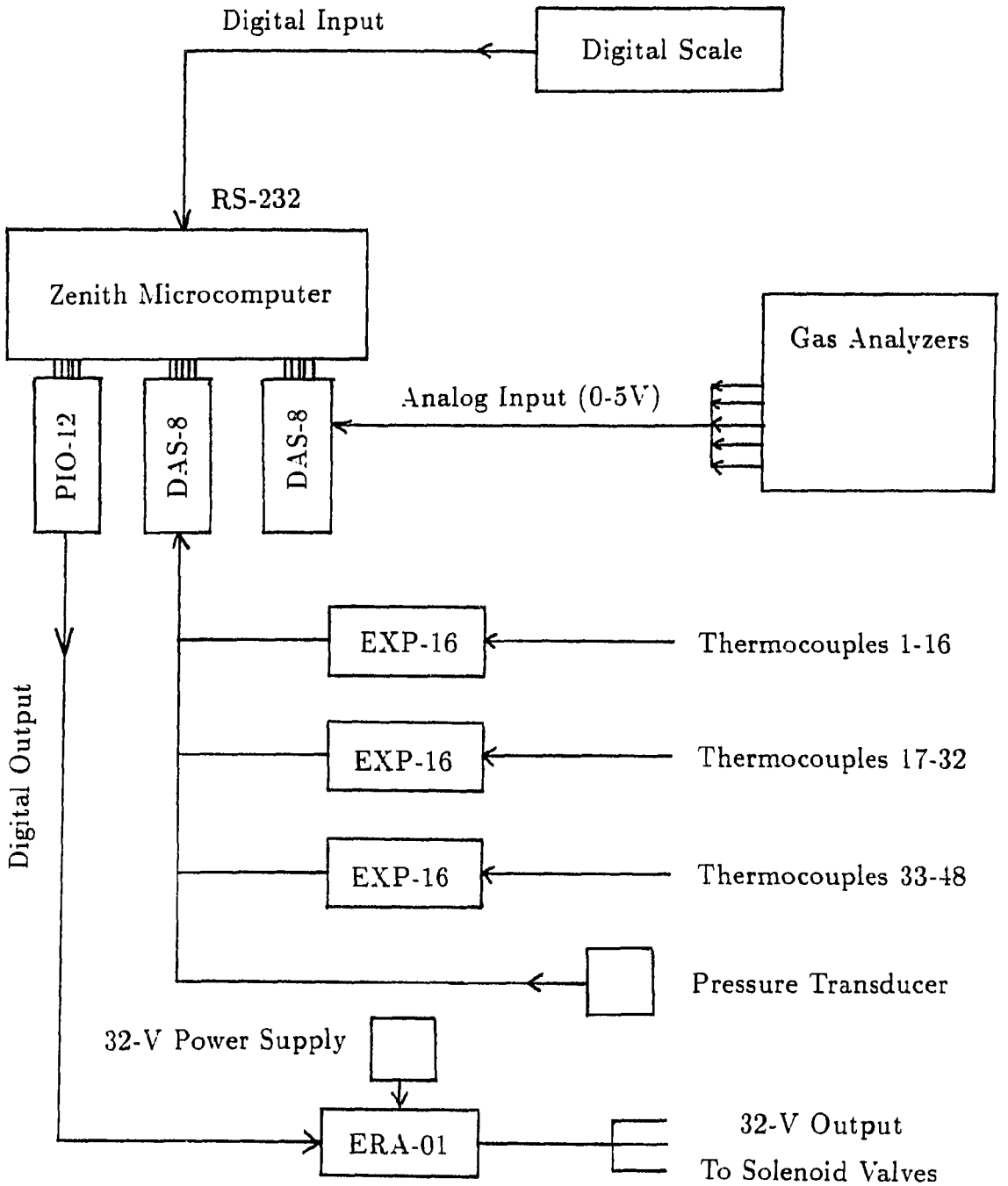

Figure 5.6: Data acquisition system

thermocouples. The EXP-16 boards performed signal amplification, multiplexing, and cold junction compensation, and were connected in parallel to one of the DAS-8 boards. Each EXP-16 occupied one channel of the DAS-8 board.

Thermocouples were used to measure the following temperatures: air and water inlet temperatures, heat transfer and combustion bed temperatures, combustor wall temperatures, and exit temperatures of flue-gas and water. Temperature measurements were made using chromel-alumel (Type K) thermocouples. For surface temperature measurement, the thermocouple wires were individually spot-welded to the metal surfaces to form intrinsic thermocouple junctions. This method of attachment provided a more accurate measurement of the surface temperature compared to attaching a thermocouple bead to the surface. In regions of high temperature, the thermocouple leads were electrically insulated by threading them through ceramic tubes. Thermocouple probes were used for air, water, and bed temperature measurements.

Figure 5.7 is a schematic of the pressure measurement system. The orifice meter pressure drops were measured using a Schaevitz Model P3061 LVDT (linear variable displacement transformer) pressure transducer. The analog electrical output of the transducer was connected to one of the DAS-8 channels. Pressure drops of multiple orifice meters were read from the single transducer using a computer-controlled solenoid-valve manifold system. Pressure taps from each orifice meter were connected to Humphrey Model M31E1 solenoid valves. The solenoids were activated by the computer using an electromechanical relay board (Metrabyte Model ERA-01), connected to the PIO-12 interface board. A given pressure drop could then be measured by activating the corresponding set of solenoid valves.

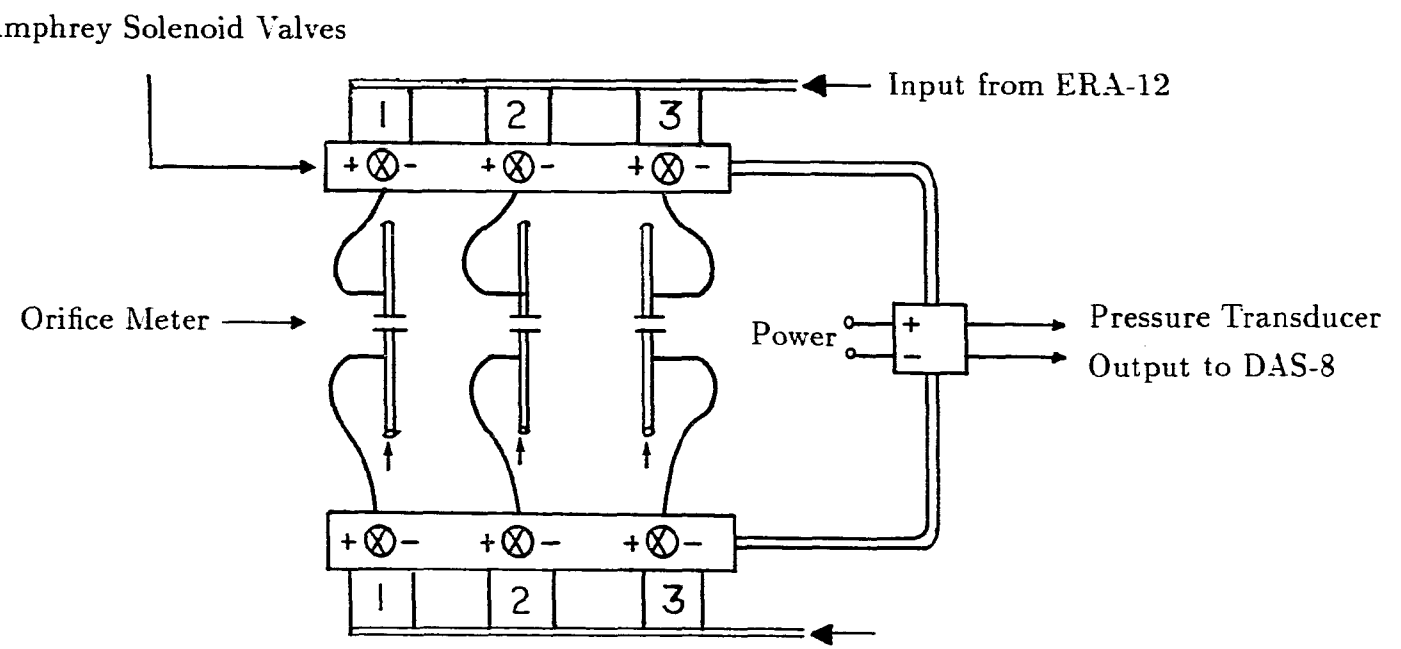

Figure 5.7: Pressure measurement system

6 EXPERIMENTAL PROCEDURE

6.1 Load Turndown Tests

A series of load turndown tests were planned with the two-bed combustor. These tests were designed to determine the maximum load turndown while operating at constant combustion temperature. Tests were planned for three different coal-based fuel forms: double-screened crushed coal, coal-limestone briquettes, and coal-water-limestone mixture (CWLM). In addition to determining load turndown, emissions of sulfur dioxide and nitrogen oxide were monitored to evaluate the effectiveness of limestone and low bed temperature on pollution control. Mass and energy balances were then performed on each set of test data to determine carbon conversion efficiency, fraction of fuel energy released in-bed, and overall heat transfer coefficients.

6.2 Fuel Preparation

A 3200-pound bulk sample of coal was obtained from the Rapatee mine of the Midland Coal Company in Fulton County, Illinois. The sample consisted of freshly-mined, washed Illinois No. 5 seam coal, 1.5-inch in top-size. The coal was obtained directly from coal load-out facilities at the mine/preparation plant, loaded in a truck, covered with a tarpaulin, and transported to preparation facilities at Iowa

State University.

Two representative bulk samples were obtained by cone-and-quartering from the 3200-pound bulk sample. One sample (1200 *lb*) was used for briquette and coal-water mixture formulation and the second sample (2000 *lb*) was crushed for dry coal tests.

The 1200-pound sample was ground in a Holmes Model 45 impact pulverizer fitted with a 0.0625-inch perforated screen. This pulverizer produced a coal product with a top size of approximately 40 *mesh* (0.425 *mm*). This pulverized sample was then divided by riffling into equal portions and stored in plastic bags, under argon, in lined 55-gallon steel drums. An analytical sample was also obtained from the pulverized coal by splitting and grinding to minus 60 *mesh* (0.250 *mm*). Ultimate and proximate analyses were performed on this sample and the results appear in Table 6.1.

The 2000-pound representative bulk sample was sieved to produce a particle size range of approximately 10.0 *mm* by 1.0 *mm*. This size range was selected so that the largest particles could be accurately metered into the combustor with an auger feeder and that the smallest particles were large enough not to elutriate from the combustor. After sieving, oversize material was reduced in a Brawn 3-inch jaw crusher to obtain the largest quantity of coal in the desired size range while producing a minimum of fines. Approximately 1200 pounds of 10.0 *mm* by 1.0 *mm* coal resulted from this operation. An analytical sample of this screened coal was also prepared to determine if loss of fines changed the coal analysis. The analysis was performed and the results were not significantly different than those shown in Table 6.1 for the pulverized coal sample.

Table 6.1: Illinois No. 5 coal analysis

Proximate analysis (%)		
	As received	Moisture-free
Moisture	10.8	0.0
Ash	10.1	11.3
Volatile matter	36.6	41.0
Fixed carbon	42.5	47.7
Ultimate analysis (%)		
	As received	Moisture-free
Carbon	69.47	77.88
Hydrogen	4.56	3.76
Nitrogen	1.33	1.49
Oxygen	11.86	2.57
Sulfate sulfur	.07	.08
Pyritic sulfur	.96	1.08
Organic sulfur	1.65	1.84
Total sulfur	2.68	3.00
HHV (kJ/kg)	26,493	29,701
LHV (kJ/kg)	25,770	28,891
Free swelling index (FSI)	4	—

A 500-pound sample of Mississippian-age Gilmore City limestone was obtained from Ames, Iowa in Story County. It was prepared for use in briquettes and coal-water mixtures by crushing in the Holmes Model 45 pulverizer. The pulverizer was fitted with the same 0.0625-inch screen used for coal grinding and produced a limestone product with a top-size of about 20 *mesh* (0.850 mm).

A K.R. Komarek Model B-100 roll-briquetter was used to prepare the coal-limestone briquettes. Preliminary tests were performed with the briquetter to select the briquette forming parameters: roll pressure = 1500 *psi*, roll speed = 3, and screw speed = 2-3. Pre-gelatinized corn starch was selected for use in the briquette binder. The binder was produced by mixing 22% of corn starch by weight with water in an electric blender. Limestone was mixed with the pulverized coal to produce a mixture with a calcium-to-sulfur molar ratio (Ca/S) of 2.0. From the coal sulfur analysis, it can be determined that 16.7 *kg* of limestone must be added to every 100 *kg* of as-received coal. However, the inherent calcium content of the coal (CaO in ash) accounts for about 11% of this amount. Therefore, it was necessary to add only 14.9 *kg* of limestone to every 100 *kg* of coal. The binder mixture was then added to the coal-limestone mixture at an addition rate of 11% by weight. After hand-mixing the coal-limestone-binder mixture, approximately 200 *kg* of briquettes were prepared. The elliptical briquette had dimensions of 20 mm x 12 mm x 8 mm. The moisture-free composition of the briquettes was 83.2% moisture-free coal, 13.9% limestone, and 2.95% corn starch.

The coal-water-limestone mixture was prepared using the same limestone addition rate as for briquettes. Water was added to the coal-limestone mixture at a rate of 1.13 *kg* of water per *kg* of coal. Approximately 200 *kg* of CWLM were prepared

in an emulsifier-mixer (powered by a 10-hp electric motor) for 10 minutes. The resulting mixture had the following composition: 49.7% dry coal, 8.3% limestone, and 42.0% water by weight; the solids loading was therefore 58%. This was the highest attainable solids loading that resulted in an easily-pumpable mixture. Both the CWLM and briquettes were stored in sealed 5-gallon buckets until needed for combustion tests.

6.3 Start-Up Procedure

The start-up procedure for each combustion test consisted of a series of equipment checks and combustor preheat. First, the gas sampling system was activated. This allowed the heat-taped lines to come up to operating temperature; also, the gas analyzers were used to monitor L-P gas combustion during preheat. The cooling water flow was started and the ignition spark was turned on. The computer was activated to monitor air flow rates, temperatures, and exhaust gas composition.

The combustor was preheated by burning L-P gas in the bed. Combustion bed air flow was set at about 30 *scfm* (standard cubic feet per minute). Air flow through the heat transfer bed was set at about 4 *scfm* to purge any L-P gas that might infiltrate this bed. The L-P flow rate was set at 0.75 cfm and ignition occurred within 5-10 seconds. The fuel burned at the surface of the bed initially, but began to burn within the bed as the bed temperature increased. Air and L-P flow rates were steadily decreased as the bed temperature rose. When the bed temperature reached 900 K, the coal feed was started. Then, as the temperature increased to about 1050 K, the L-P flow was turned off. The coal feed and combustion air flow rates were set at desired levels of energy release rate and bed stoichiometry.

The heat transfer bed air flow rate was set at a level to achieve a combustion bed temperature of 1140 K. To decrease combustion bed temperature the heat transfer air flow rate was lowered; to increase bed temperature the air flow rate was raised. The combustor was operated for 30-60 minutes before data acquisition began to allow steady state conditions to be reached.

6.4 Data Acquisition

Once steady state conditions were achieved for a particular test, the data acquisition program was started. The program was written in BASIC and was stored on the computer hard disk drive. The program controlled the collection of temperature, flow rate, and exhaust gas composition data and wrote these data to a data file on the hard drive once every minute. Each recorded temperature was a one-minute average of 12 5-second-interval readings. The gas concentrations and air flow rates were read once every minute, as they ded not fluctuate greatly at steady state. Steady state data were recorded for 30-60 minutes for each test. Uncertainty in temperature measurement was $\pm 20K$. Uncertainties in air flow rate measurement and in gas composition were $\pm 5\%$. The coal feed rate was determined to be certain within $\pm 5\%$.

6.5 Ash Analysis

An ash sample was collected for every test by opening the cyclone collection valve once test equilibrium was achieved. The sample was collected for 10-30 minutes depending on the exhaust gas flow rate. The sample was collected in a one-liter jar.

A 25 gram sample of the collected ash was dried in an oven, reweighed, and placed in an ashing oven at $800^{o}C$ for 2 hours. When the sample had cooled, it was weighed and the weight loss was calculated. It was assumed that unburned carbon accounted for all of the weight loss. The carbon conversion efficiency could then be calculated by performing a carbon balance on the combustor; details on combustion mass balances are found in Appendix D.

6.6 Coal Feed Rate Determination

Coal feed rate into the combustor ranged between 1 and 10 kg/hr. These low flow rates were very difficult to measure on-line accurately. Before a test, the auger feeder was calibrated to provide an estimate of the feed rate during a test. However, for a more accurate measure of the fuel feed rate, it was determined after a test from a mass balance on the combustor. It was calculated based on accurately measured values of air flow rate, exhaust gas composition, and unburned carbon elutriation loss. See Appendix D for details on combustor mass balances.

7 RESULTS

7.1 Load Turndown

Load turndown tests were performed for the three fuel forms: crushed coal, coal-limestone briquettes, and coal-water-limestone mixture (CWLM). Test data obtained for the crushed coal are shown in Table 7.1. A load turndown of 12.4 (obtained from the ratio of maximum fuel flow of 9.21 *kg/hr* to the minimum fuel flow rate of 0.74 *kg/hr*) at constant combustion bed temperature (1155 $\pm$ 25 K) was achieved. The temperature was held constant by admitting the proper amount of air through the heat transfer bed (secondary air flow) after the combustion fuel flow and air flow rates were set. Overall excess air is obtained as the ratio of total air flow to stoichiometric air flow rate. Percent of fuel burned in-bed is obtained from an energy balance on the combustion bed.

The combustor was designed for air-staged firing. The combustion bed was operated sub-stoichiometrically to suppress NO_x formation. Overfire air was injected above the bed to complete fuel combustion at fuel lean conditions. This overfire air consisted of air exiting the heat transfer bed (secondary air) as well as air bypassing the heat transfer bed (tertiary air). The target value of excess air was 20% with a combustion bed equivalence ratio of 1.30 (77% of stoichiometric air). It was not possible to hold the excess air level at 20% for the lowest firing rates to avoid

Table 7.1: Load turndown test results for crushed coal

Run	Fuel Feed Rate (kg/hr)	Secondary Air Flow (kg/hr)	Bed Temperature (K)	Bed Equivalence Ratio	Overall Excess Air (%)
A1	0.74	0.0	1133	0.44	126
A2	1.28	0.0	1172	0.71	67
A3	1.87	11.1	1156	1.30	42
A4	5.43	11.3	1144	1.52	5
A5	7.19	14.4	1161	1.37	10
A6	7.08	19.1	1172	1.05	50
A7	9.21	31.2	1178	1.36	18

O_2 (%)	CO_2 (%)	CO (%)	SO_2 (ppm)	NO_x (ppm)	kg NO_x per GJ
10.6	7.9	0.051	—	300	0.24
7.4	10.9	0.029	—	325	0.19
5.6	12.4	0.034	1480	210	0.10
1.3	16.9	0.078	2385	435	0.16
3.9	15.9	0.070	1976	510	0.20
6.3	12.1	0.015	2000	520	0.27
3.8	15.2	0.037	2380	440	0.18

Total Air Flow [a] (kg/hr)	Carbon Conversion Efficiency (%)	Percent Fuel Burned in Bed	Annular Bed Temperature (K)
15.4	95	100	675
19.5	95	71	803
24.2	94	71	694
52.4	95	51	656
72.7	96	50	658
97.1	97	57	638
100.0	95	52	610

[a] Sum of primary, secondary, and tertiary air.

defluidization of the combustion bed. The excess air level ranged from 5% to 50% for the five highest firing rates (Runs A3-A7). This wide range was the result of an inability to accurately meter coal with the auger feeder. In subsequent tests, it was decided to use air flow rates in conjunction with exhaust gas analysis to set excess air level.

No limestone was added to the bed for these trials with dry coal. The sulfur emissions of 1480 ppm to 2385 ppm are in the range expected for the coal. Expected sulfur retention due to inherent calcium content was 11%; observed values ranged from 0% to 23%. The accuracy of sulfur balances was about 15%. Emissions of NO_x ranged from 0.10 to 0.27 kg/GJ.

Load turndown test results for briquettes are shown in Table 7.2. A load turndown of 9.4 was achieved at constant combustion bed temperature (1110 $\pm$ 35 K). A test to determine conventional load turndown (the load turndown that could be obtained with a conventional one-bed design) is shown as table entry Run B6. Conventional load turndown is defined as the ratio of maximum to minimum firing rate with the annular bed defluidized, regardless of firing rate. Combustion bed temperature was allowed to rise no higher than in the two-bed turndown trials. The convention load turndown obtained from this test was only 5.3; this is compared to 9.4 obtained with the annular bed fluidized.

Test results for CWLM are shown in Table 7.3. A load turndown of 9.0 was achieved at constant combustion temperature (1110 $\pm$ 45 K). Again, the temperature was maintained constant by adjusting secondary air flow through the annular heat transfer bed for each firing rate.

Although a load turndown of 12.4 was achieved for crushed coal, turndown

Table 7.2: Load turndown results for briquettes

Run	Fuel Feed Rate (kg/hr)	Secondary Air Flow (kg/hr)	Bed Temperature (K)	Bed Equivalence Ratio	Overall Excess Air (%)
B1	1.08	0.0	1073	0.70	44
B5	3.46	5.3	1091	1.27	20
B4	4.85	8.6	1109	1.27	22
B3	5.77	11.0	1144	1.13	35
B2	10.10	30.6	1141	1.32	24
B6	5.69	0.0	1142	0.74	48

O_2 (%)	CO_2 (%)	CO (%)	SO_2 (ppm)	NO_x (ppm)	kg NO_x per GJ	kg S per GJ
5.9	12.2	0.102	194	236	0.12	0.104
4.6	14.3	0.008	368	271	0.12	0.166
4.2	14.3	0.010	704	337	0.14	0.321
5.0	13.2	0.024	1170	342	0.16	0.586
5.0	14.6	0.024	936	313	0.14	0.437
7.2	11.8	0.022	706	353	0.18	0.394

Total Air Flow [a] (kg/hr)	Carbon Conversion Efficiency (%)	Percent Fuel Burned in Bed	Sulfur Capture (%)	Annular Bed Temperature (K)
12.5	91	74	90	711
33.4	90	57	84	587
47.5	90	58	68	600
62.2	92	62	42	617
100.0	95	51	57	597
67.7	92	56	61	762

[a] Sum of primary, secondary, and tertiary air.

Table 7.3: Load turndown results for CWLM

Run	Fuel Feed Rate (kg/hr)	Secondary Air Flow (kg/hr)	Bed Temperature (K)	Bed Equivalence Ratio	Overall Excess Air (%)
C2	2.49	0.0	1064	0.76	31
C1	5.28	4.1	1106	1.32	14
C3	22.29	30.8	1152	1.43	8

O_2 (%)	CO_2 (%)	CO (%)	SO_2 (ppm)	NO_x (ppm)	kg NO_x per GJ	kg S per GJ
5.1	13.2	0.190	151	272	0.12	0.074
5.0	14.6	0.024	936	313	0.08	0.088
7.2	11.8	0.022	706	353	0.10	0.326

Total Air Flow [a] (kg/hr)	Carbon Conversion Efficiency (%)	Percent Fuel Burned in Bed	Sulfur Capture (%)	Annular Bed Temperature (K)
16.8	91	53	93	693
30.8	91	40	91	680
123.2	94	38	68	603

[a] Sum of primary, secondary, and tertiary air.

was limited to about 9.0 for briquettes and CWLM. One possible explanation for this is evident by re-examining the minimum fuel flow rates in Tables 7.1, 7.2, and 7.3. For the crushed coal case, 100% of the fuel is burned in the bed, while for briquettes and CWLM only 74% and 53% respectively is burned in the bed. A greater percentage of fuel burned in the bed allows lower fuel firing rates to maintain the same combustion temperature. Lower minimum firing rates and correspondingly larger turndown would probably have resulted with briquettes and CWLM if leaner stoichiometries had been allowed with these fuels.

Load turndown ratio is best defined as the ratio of maximum to minimum firing rates for a combustor. In developing Equation 2.5 it was necessary to employ an alternative, but nearly equivalent, definition of load turndown; that is, load turndown was defined as the ratio of maximum to minimum heat transfer rates between the combustion bed and water jacket. The overall heat transfer coefficient between combustion bed and water jacket, U_{beds}, can be defined as the total heat transfer rate per unit wall area to the heat transfer bed divided by the temperature gradient between the combustion bed and water jacket. The subscript "beds" is used here to emphasize that the overall heat transfer coefficient is limited by the convection coefficients in the fluidized beds. Figure 7.1 is a plot of overall heat transfer coefficient versus annular bed air flow rate for the coal combustion tests. The ratio of maximum to minimum overall heat transfer coefficient represents this alternative definition of load turndown ratio. The value of 7.0 obtained from Figure 7.1 is in good agreement with calculations using Equation 2.5. This alternative definition of load turndown assumes that the same fraction of fuel is burned in-bed for both maximum and minimum fuel flow rates. It was predicted by the

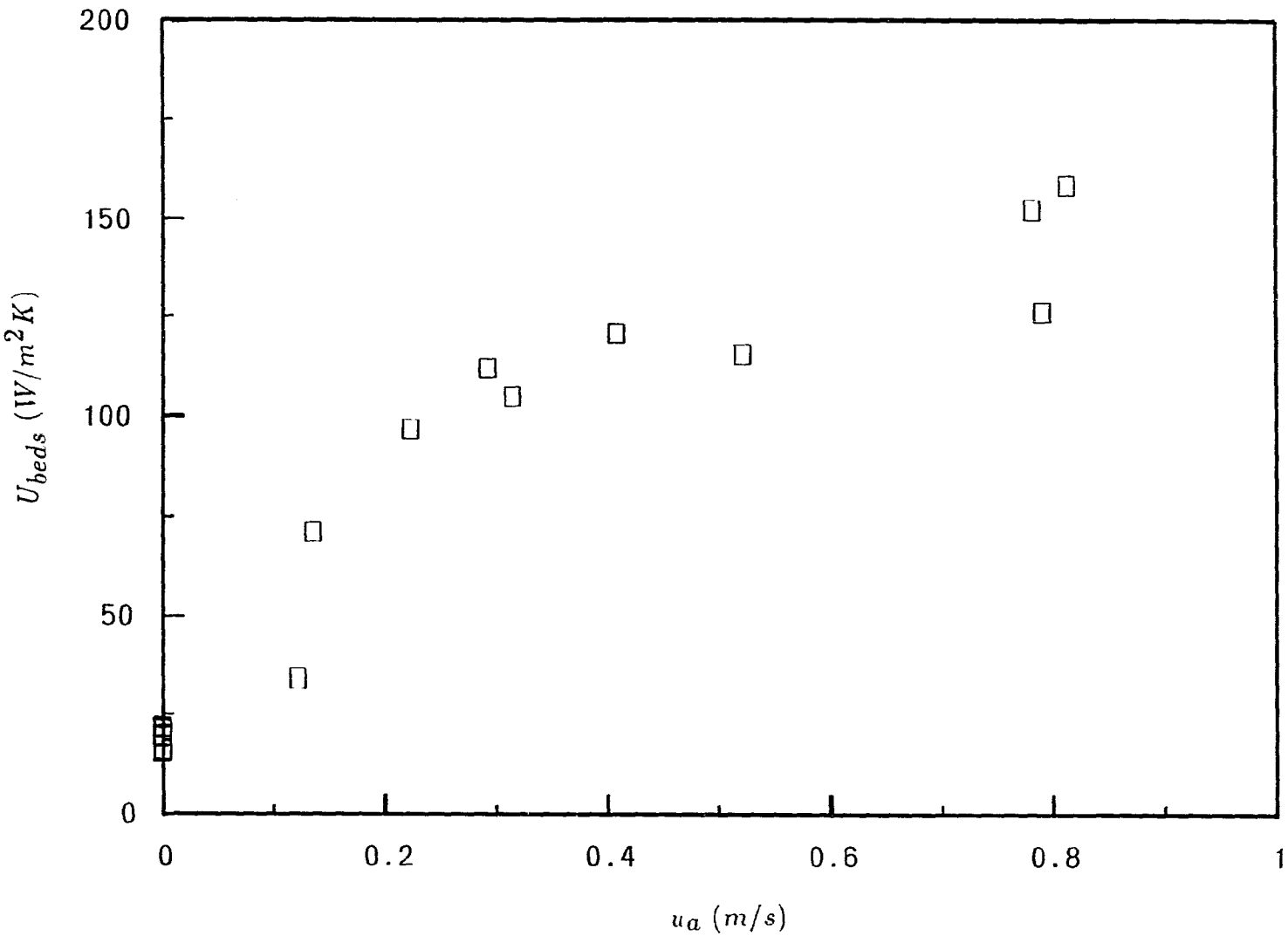

Figure 7.1: Overall heat transfer coefficient vs. fluidization velocity

combustion model and observed in the combustion tests that a higher fraction of fuel is burned in-bed for low fuel flow rates than for high fuel flow rates. For this reason, higher load turndowns were observed in the combustion tests than predicted by heat transfer considerations alone.

7.2 Emissions

Both the briquettes and the CWLM were formulated with a calcium-to-sulfur molar ratio of 2.0. Sulfur dioxide emission reduction of 42% to 93% was observed in the load turndown tests; emissions ranged from 0.07 to 0.59 $kg\ S/GJ$. Most tests met the EPA New Source Performance Standards of 0.52 kg/GJ [26]. The effect of combustion bed temperature on sulfur retention is shown in Figure 7.2. The data is compared to experimental results of Stantan [27] who found the optimal temperature for sulfur retention to be close to 1100 K. In contrast, the optimum bed temperature in these tests was found to be no higher than 1050 K. This discrepancy with results of other researchers possibly arises from the fact that limestone in briquettes and CWLM more closely follows the temperature history of fuel particles, in which it is incorporated, than the bulk bed material. Since fuel particles burn at temperatures 50 to 200 K higher than the bed [28], the optimal bed temperature for sulfur retention is expected to be somewhat lower for fuel forms that contain limestone. Furthermore, higher sulfur retention than that reported by Stantan was observed. This result, as well, is probably related to the intimate contact of limestone with coal briquettes and CWLM.

The effect of combustion bed temperature on emissions of NO_x is illustrated in Figure 7.3. The general trend is for increased emissions of NO_x with increasing bed

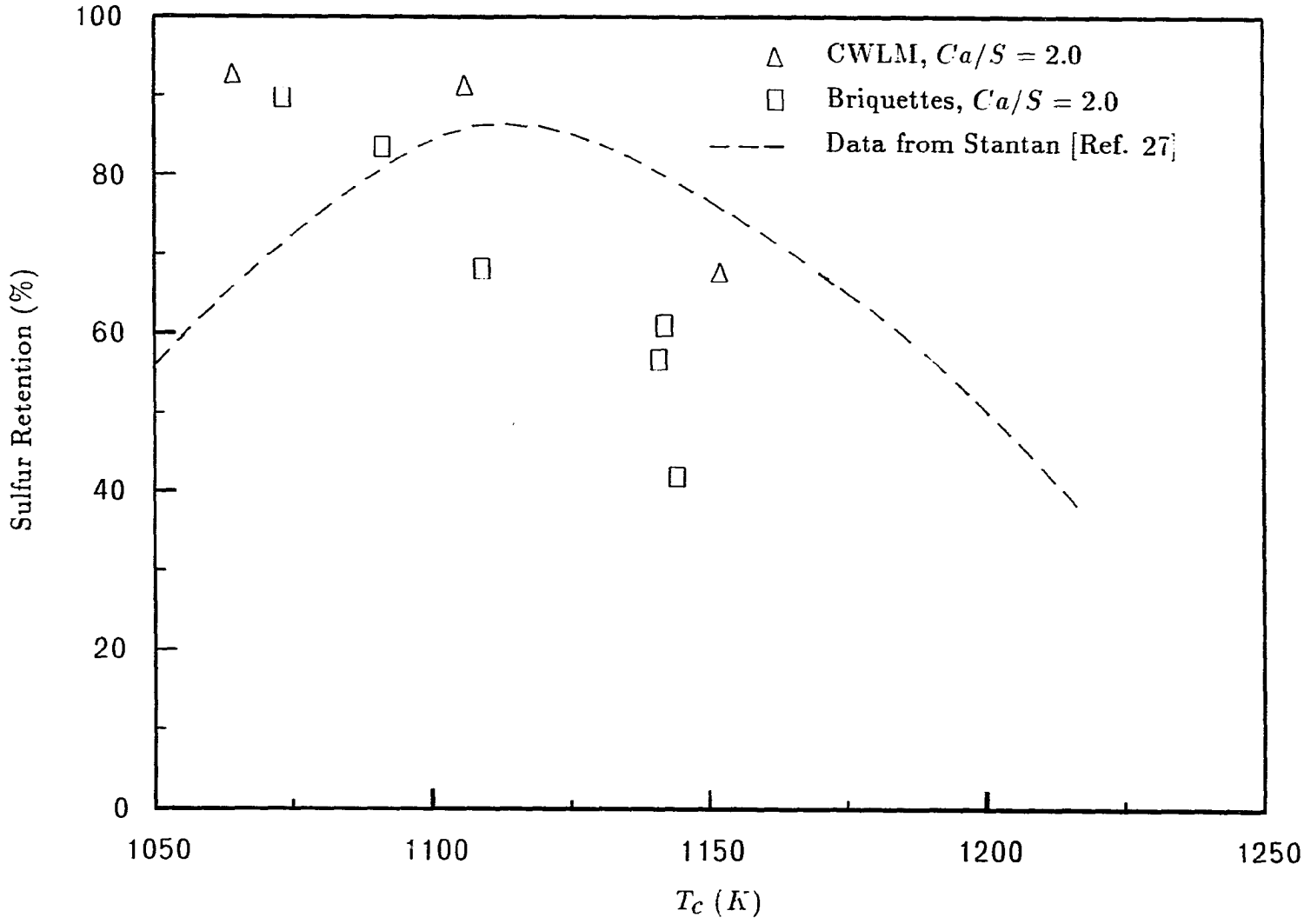

Figure 7.2: Sulfur retention vs. combustion bed temperature

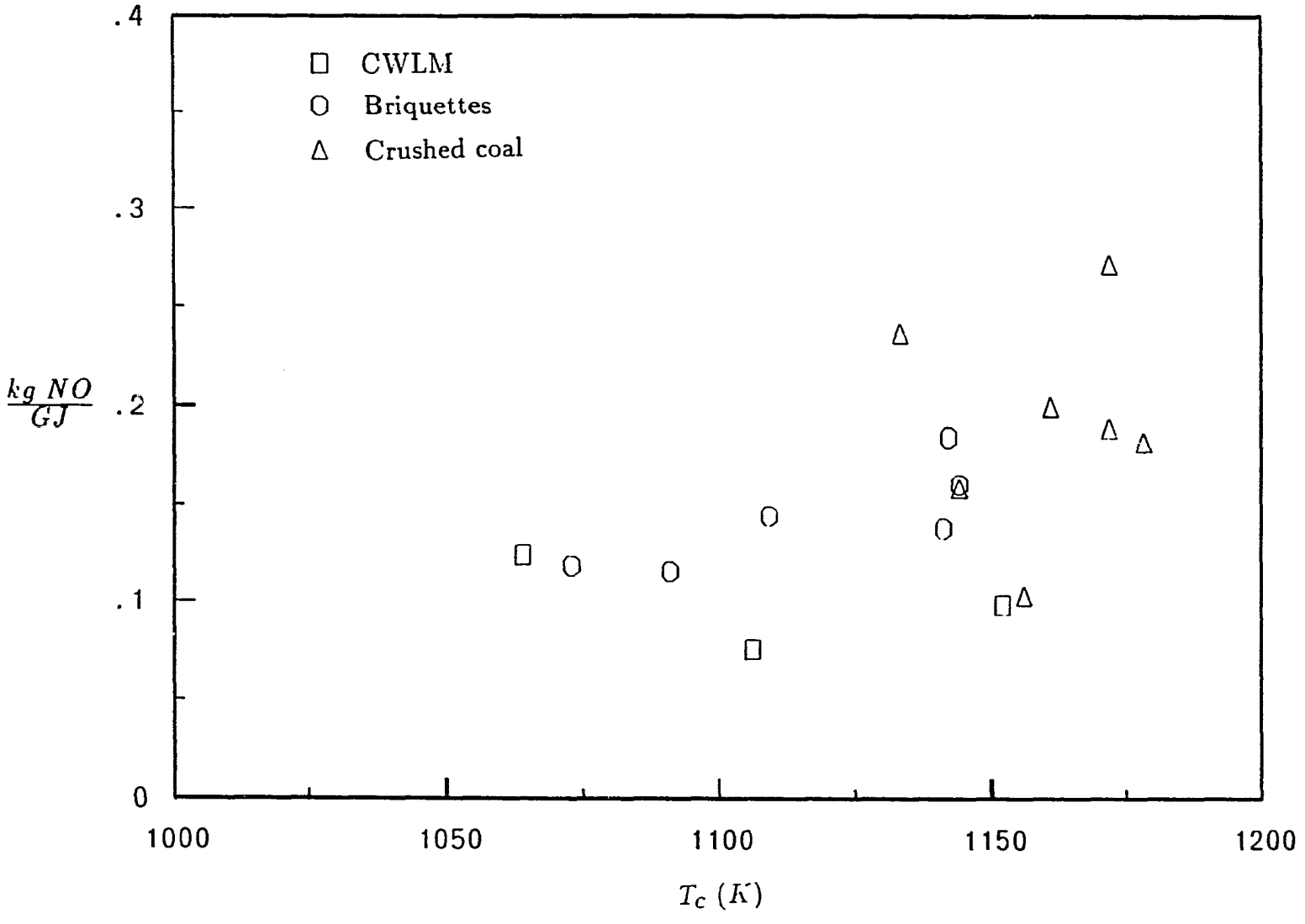

Figure 7.3: Nitrogen oxide emission vs. combustion bed temperature

temperature, as expected. However, NO_x formation also increases with combustion bed excess air. Experimental observations agree qualitatively with other researchers who concluded that, to minimize NO_x emissions, the combustion bed should be operated sub-stoichiometrically at low combustion bed temperatures [12,3,29]. Emissions of NO_x ranged from 0.08 to 0.27 kg/GJ. Most tests met the EPA New Source Performance Standards of 0.26 kg NO_x/GJ [26].

7.3 Estimate of Largest Practical Combustor

Calculations were performed to estimate the largest practical combustor which could employ this two-bed design. The following assumptions were used:

- Annular bed width is 2.5 cm.
- The overall heat transfer coefficient between combustion bed and water jacket is 150 W/m^2K (see Figure 7.1).
- Fuel consists of dry coal with a heating value of 23258 kJ/kg that requires 11.25 kg air per kg of coal for 20% excess air.
- Water jacket wall temperature is 373 K and combustion bed temperature is 1144 K.
- Combustion bed is operated sub-stoichiometrically and 50% of fuel energy is released in the combustion bed.
- The combustor geometry is cylindrical, and bed height is limited to 1 m due to pressure drop considerations.

The heat transfer rate from the combustor wall can be equated to the energy release in the bed and the following solution is obtained:

- Combustion bed diameter = 1.43 m.
- Total combustor heat load = 1.04 MW.

Larger units could be obtained by using a modular system composed of several smaller combustors.

7.4 Comparison with Heat Transfer Model

Experimental results obtained for briquettes (See Table 7.2) have been compared to simulation predictions. Figure 7.4 plots firing rate in the combustor versus secondary air flow through the heat transfer bed for constant combustion temperature. Model prediction and experimental results show two major discrepancies. First, the model predicts a sudden increase in sustainable firing rate when secondary air flow is increased to the minimum fluidization velocity of the annular bed. In contrast, the experimental results show a more gradual increase in firing rate with increasing secondary air flow. Second, the model under-predicts the amount of energy that can removed from the combustor at the highest secondary air flow rates. Both of these discrepancies apparently arise from the convection coefficients calculated for the annular bed from the two-phase theory of fluidization.

Most heat transfer correlations that have been developed for fluidized beds assume that the bed is either slugging or bubbling. Slugging occurs when large bubbles with a diameter on the order of the bed width form, and travel up through the bed as one large slug. Bubbling beds have more distinct, smaller bubbles that rise up

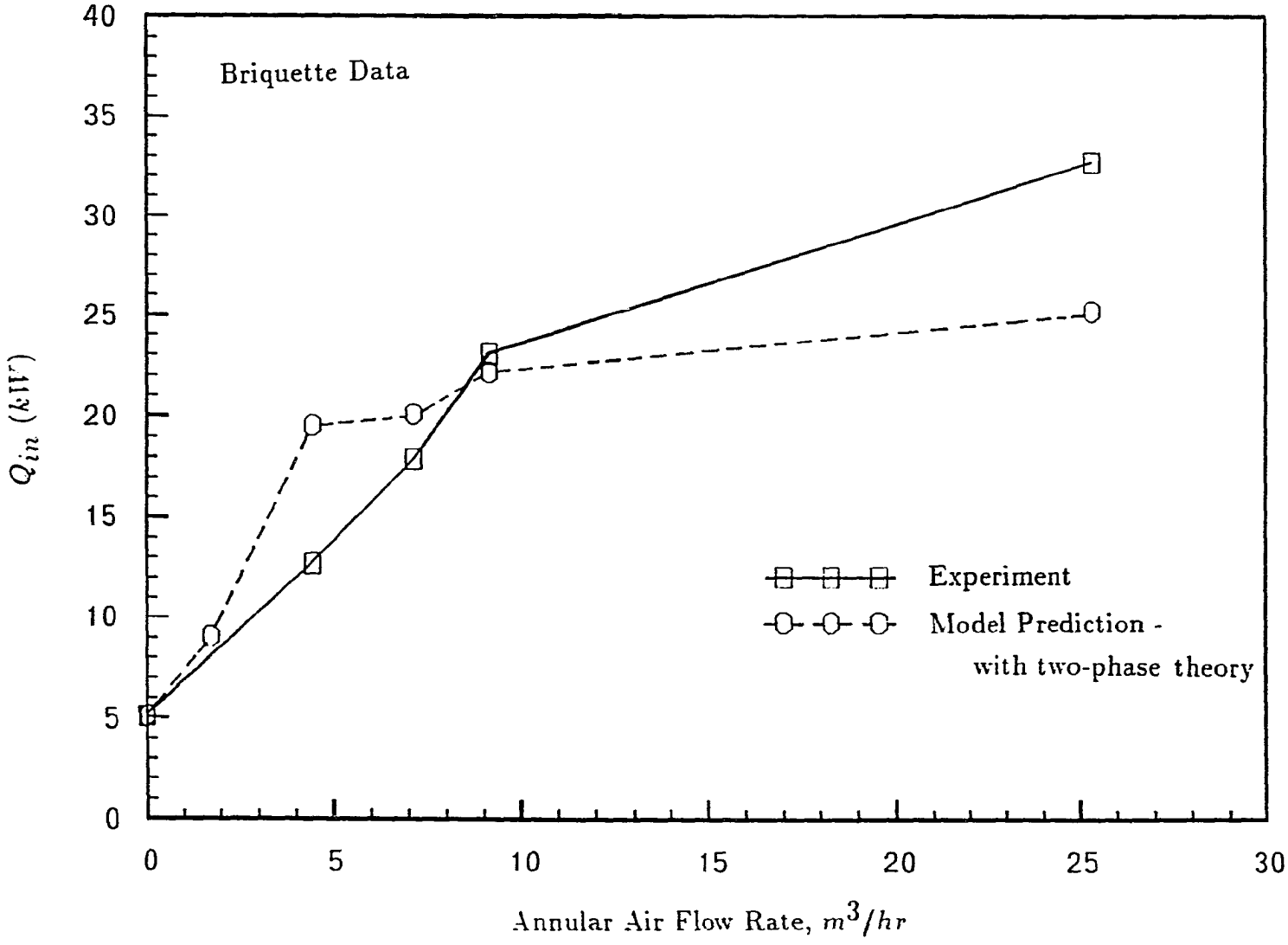

Figure 7.4: Energy released in-bed vs. annular air flow rate – experiment vs. two-phase theory prediction

through the bed. The aspect ratio of a fluidized bed is equal to its height divided by its width. The two-phase theory of fluidization that was used to predict heat transfer coefficients was expected to yield accurate results for low aspect-ratio slugging beds. However, although the heat transfer bed operates in the slugging regime, the unusually high aspect ratio may alter the hydrodynamics enough to make the two-phase theory invalid. For the annular heat transfer bed with a fluidized height of 0.25 m, the aspect ratio is 10. Pflum et al. [30] compared experimentally-obtained convection coefficients in high-aspect ratio fluidized beds to two-phase theory predictions. Their findings suggested two major differences between experiment and theory: measured convection coefficients were significantly higher than predicted by two-phase theory and increased more gradually with fluidization velocity than predicted by the two-phase theory. Figure 7.5 shows a comparison of their experimental and predicted values of convection coefficient versus fluidizing velocity. These experimental data were employed in the computer model in place of two-phase theory values.

Convection coefficients for the combustion bed were still calculated using the two-phase theory. Since this bed has a low aspect-ratio, the two-phase theory was expected to predict convection coefficients accurately. Also, the convection coefficient in the combustion bed becomes rate-limiting only at the highest annular air flow rates. Figure 7.6 shows energy released in the combustion bed versus annular air fluidizing velocity using the experimental convection coefficients. It can be seen that significant improvement has been obtained over Figure 7.4. There is still some discrepancy in the mid-range flow rates of 4-10 m^3/hr. A possible explanation for this discrepancy is non-uniform air distribution in the annular bed. If one zone of

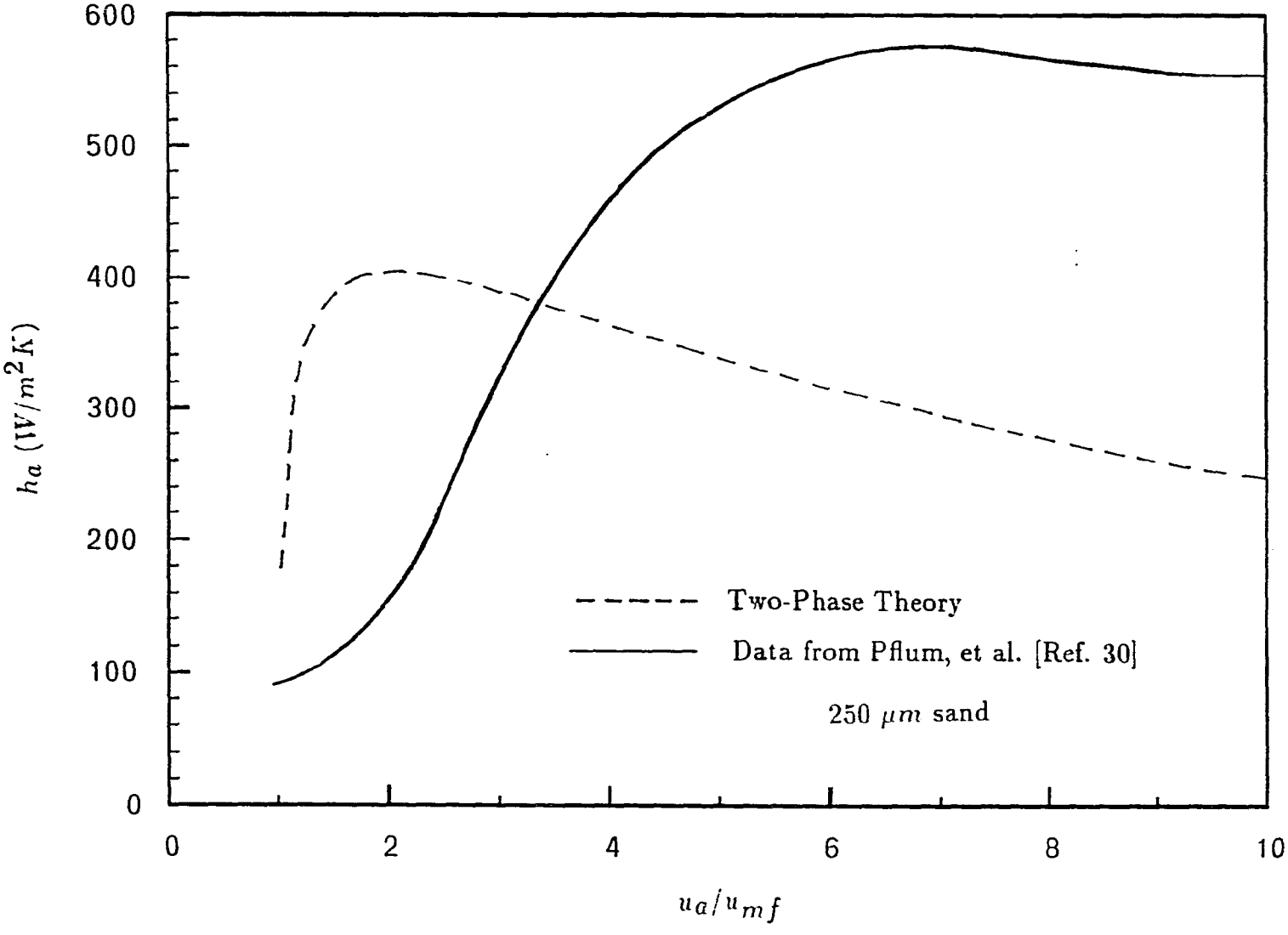

Figure 7.5: Convection coefficient vs. fluidization velocity – experimental data

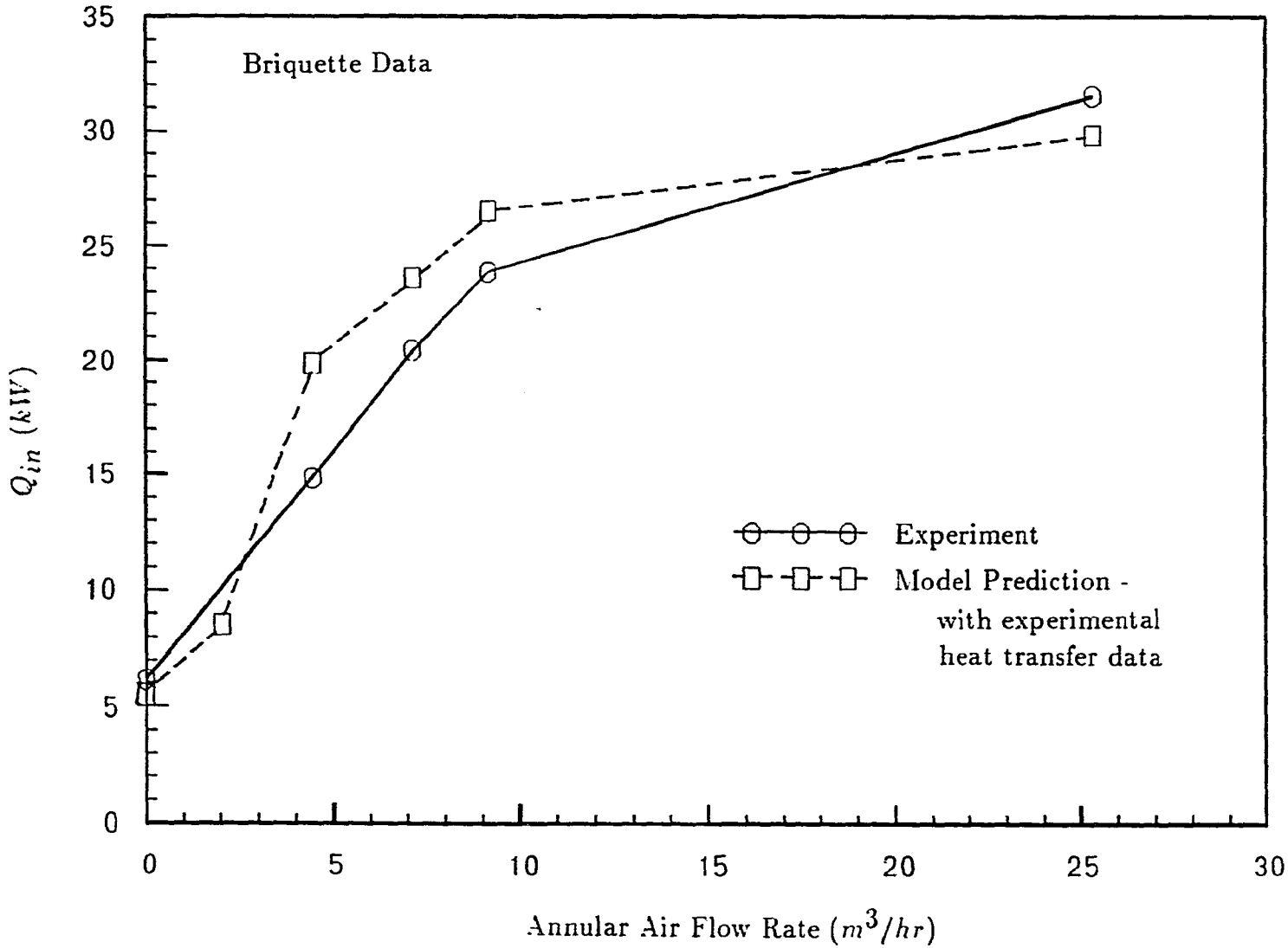

Figure 7.6: Energy released in-bed vs. annular air flow rate – experiment vs. experimental heat transfer data

the annular bed fluidizes before the rest of the bed, a more linear response in firing rate with changes in fluidization velocity is expected. Then, as more air is admitted to the annular bed, the firing rate should reach a maximum as the heat transfer coefficient in the combustion bed becomes rate-limiting to the overall heat transfer process.

7.5 Comparison with Combustion Model

Experimental results obtained for crushed coal (See Table 7.1) have been compared to combustion model predictions. The combustion model was executed as follows:

1. Bed temperature and air flow rates were used as input parameters to the heat transfer model.

2. Output data from the heat transfer model (including energy released in-bed, air velocity, bubble diameter and rise velocity, and bed voidage) were used as input parameters to the combustion model.

The combustion model then predicts percent of fuel energy released in-bed, coal mass flow rate, and incomplete combustion energy loss due to unburned carbon and unreacted carbon monoxide.

Figure 7.7 shows a plot of predicted fraction of fuel burned in-bed vs. experimental values from crushed coal tests. It can be seen that the best agreement is for the four cases where the combustion bed was operated with an equivalence ratio greater than 1.05; these cases represent the higher fuel flow rates. Model predictions

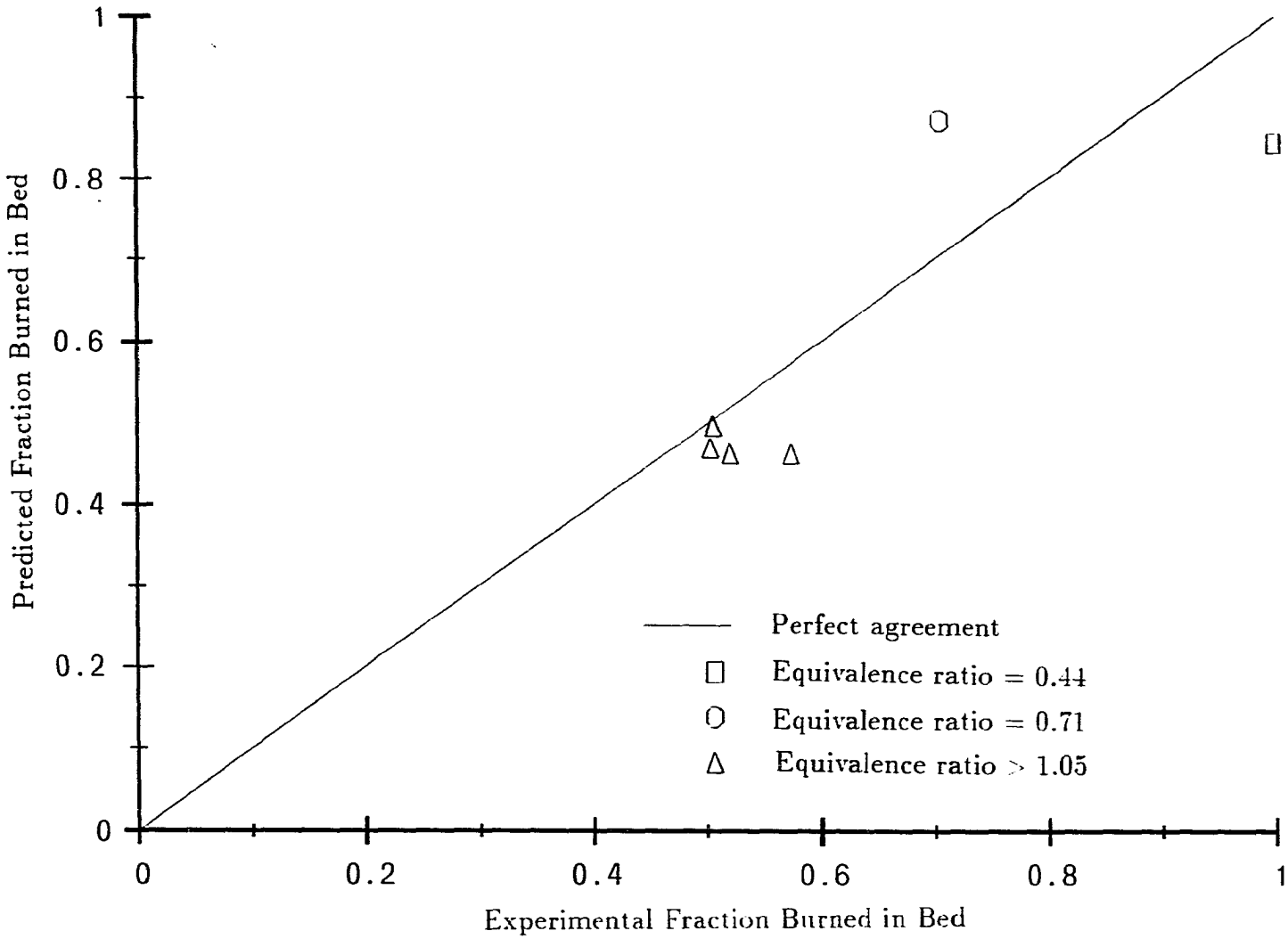

Figure 7.7: Fraction of fuel burned in bed - predicted vs. observed

are in poor agreement for the other two cases; these represent the lowest fuel firing rates.

Figure 7.8 is a bar graph showing combustion model predictions of fraction of fuel burned in-bed, fraction of incomplete combustion due to unburned carbon monoxide, and fraction due to unburned carbon, for three different coal mass flow rates. At a fuel flow rate of 0.90 kg/hr, 85% of the fuel is burned in-bed and 15% leaves the bed in the form of unburned carbon monoxide. No loss due to unburned carbon is predicted. At the highest fuel flow rate of 9.5 kg/hr, 46% of the fuel is burned in-bed, 1% leaves the bed in the form of unburned carbon monoxide, and 53% of the incomplete combustion loss is due to unburned carbon.

At the lowest fuel flow rate, the combustion bed is nearly minimally fluidized and is operated with high excess air. It is reasonable to expect that the char would burn completely to carbon monoxide. Also, because the model assumes that carbon monoxide burns only in the bubble phase, some unburned carbon monoxide would be expected (because near minimum fluidization, bubble phase volume is much less than emulsion phase volume). In the test case where 100% combustion in-bed was observed, some of this predicted unburned carbon monoxide must be burning in the emulsion phase.

At high fuel flow rates, it is predicted that the major source of incomplete in-bed combustion is unburned carbon. Loss due to unburned carbon monoxide is essentially zero. These predictions agree with those made by Walsh [17], who compared his fluidized bed combustion model to experimental data of others. Walsh's model assumes that carbon monoxide formed during char oxidation is rapidly consumed and that the major source of incomplete combustion is due to elutriated

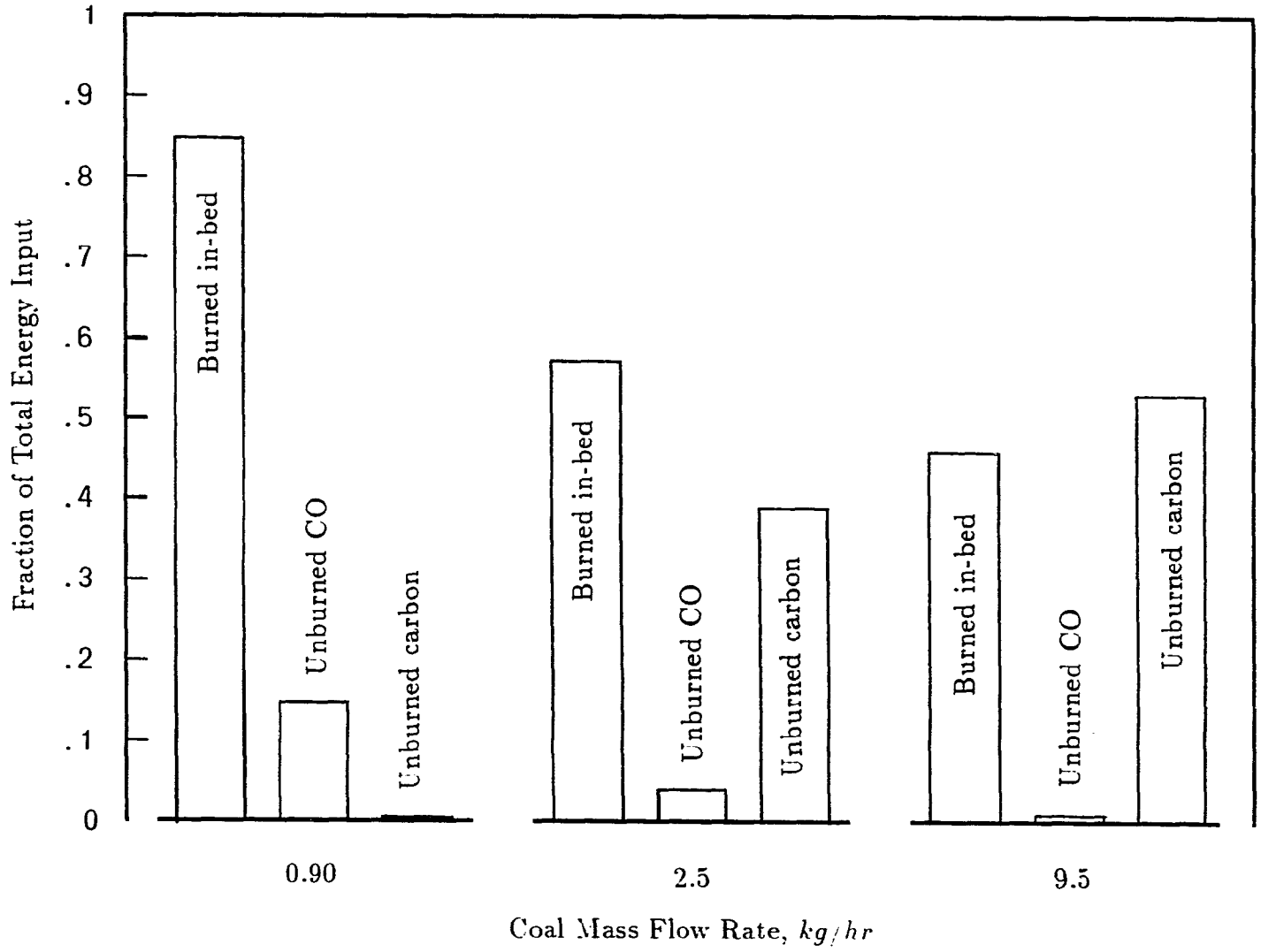

Figure 7.8: Predicted fraction of fuel burned in-bed and sources of incomplete combustion vs. fuel mass flow rate

unburned carbon. Carbon fines continue to burn in the freeboard; unburned carbon exiting the freeboard represents overall combustor carbon loss. In the present combustion experiments, it was observed that unburned carbon exiting the freeboard was usually between 3% and 10%. Since it is predicted that about 50% of the carbon elutriates from the bed, significant freeboard combustion must be taking place. Overfire air and the insulated freeboard used in the combustion tests encourage freeboard combustion.

If char particles burn as shrinking spheres, unburned carbon loss would be very small (since the carbon fines would be much less massive than the char particles). Walsh argued that char particles burn as constant diameter particles until the reach a critical porosity. Then, the particles fragment and elutriate from the bed. This would result in large amounts of elutriated carbon from the bed. The present combustion model supports the fragmentation theory, as up to 60% of unburned carbon is predicted.

Table 7.4 shows combustion model predictions of coal mass flow rate. The first column is measured coal feed rate, the second column is combustion model prediction using the heat transfer (HT) model prediction of energy released in-bed (Q_{in}), and the third column is combustion model prediction using measured values of Q_{in}. In the second column, it is seen that, as with the heat transfer model, the best agreement is at minimum and maximum fuel flow rates. Predictions based on experimental values of energy release in-bed (column 3) offer slightly better agreement. However, this slight improvement is at the expense of the model becoming more dependent on experimental data.

Table 7.4: Fuel flow rate - combustion model predictions vs. experimental data

Actual Coal Feed Rate (kg/hr)	Predicted Coal Feed Rate (with Q_{in} from HT model) (kg/hr)	Predicted Coal Feed Rate (with measured Q_{in}) (kg/hr)
0.66	1.04	0.91
1.13	0.93	0.95
4.84	6.38	4.93
6.37	7.47	6.89
6.28	8.35	7.97
8.21	8.56	9.47

8 CONCLUSIONS

Control of heat transfer rate independent of combustion conditions in a fluidized bed combustor is possible using a two-bed design. The second bed (heat transfer bed) surrounds the combustion bed and is independently fluidized. The heat transfer bed establishes the overall heat transfer coefficient between the combustion bed and water jacket. A load turndown of 12 was achieved in the two-bed fluidized combustor when burning crushed coal, while holding combustion temperature constant. Slightly lower turndown ratios were observed for coal-limestone briquettes and coal-water-limestone mixture (CWLM), and were attributed to slightly different operating conditions. Emissions of NO_x ranged from 0.08 to 0.27 $kg\ NO/GJ$. Emissions of SO_2 ranged from 0.074 to 0.586 $kg\ S/GJ$ for briquettes and CWLM, which translates to 42% to 93% sulfur retention.

The heat transfer model predictions were in reasonable agreement with experimental observations. The two-phase theory heat transfer predictions were not sufficiently accurate for the high aspect-ratio annular fluidized bed, so experimental heat transfer data was used. Simple calculations showed that the largest practical combustor employing this two-bed, water-wall design would be 1.43 m in diameter, with 1.04 MW thermal output.

The combustion model predictions were in reasonable agreement with exper-

imental observations. The model predicted well in cases of high fuel flow rates and poorly in cases where the combustion bed was minimally fluidized. Combustion model predictions support the fragmentation theory, whereby char particles burn at constant diameter until reaching a critical porosity, when they fragment and elutriate from the bed. For most cases, the major source of incomplete in-bed combustion was due to elutriated unburned carbon.

Recommendations for future work include:

1. A more detailed analysis of the combustion process in fluidized beds. The effect of operating parameters such as excess air and fuel flow rate on percent of fuel burned in bed needs to be determined.

2. A more fundamental study of heat transfer coefficients in high aspect ratio fluidized beds. This study is needed to explain why observed heat transfer coefficients were higher than predicted by two-phase theory.

9 BIBLIOGRAPHY

[1] Merritt, Paul, C. "New Coal-Burning Systems are on the Threshold." *Coal Age* 91 (1986): 105-106.

[2] Green, L., Jr. "Utilization of Medium-Sulfur Slurry Fuels by a Fluid-Bed Calcium-Sulfur Contactor." Proc. 2nd Annual Pittsburgh Coal Conference, Pittsburgh, Pennsylvania, 1985.

[3] Hampartsoumian, E.; and Gibbs, B. M. "NO_x Formation and Reduction in Fluidized Bed Combustors." *J. Inst. of Energy* 57 (1984): 402-410.

[4] Keairns, D. L.; Altiner, H. K.; Hamm, J. R., Ahmed, M. M.; Weeks, K. D.; Bachovchin, D. M.; Kececioglu, I.; Ulerich, N. H.; and Yang, W. C. "Advanced Atmospheric Fluidized Bed Combustion Design: Internally Circulating AFBC." Final Report. USDOE, DOE/MC/19329-1405, 1983.

[5] Biyikli, S.; Tuzla, K.; and Chen, J. C. "Heat Transfer around a Horizontal Tube in Freeboard Region of Fluidized Beds." *AIChE J.* 29, No. 5 (1983): 712-716.

[6] Roberts, A. G.; Stantan, J. E.; Wilkins, D. M.; Beacham, B.; and Hoy, H. R. "Fluidized Bed Combustion of Coal and Oil Under Pressure." *Inst. Fuel Symp. Series* 1 (1975): 23-28.

[7] Anson, D. "Fluidized Bed Combustion of Coal for Power Generation." *Prog. Energy Combustion Science* 2 (1976): 61-82.

[8] Kunii, D.; and Levenspiel, O. *Fluidization Engineering.* Malabar, Florida: Robert E. Krieger Publishing Company, Inc., 1969.

[9] Horio, M.; Hayashi, H.; and Morishita, K. "A Novel In-Bed Heat Transfer Tube Capable of Decreasing h_w Linearly with Load Turndown." *Proc. Eighth Int. Conf. on Fluidized Bed Combustion*, Houston, Texas, 1985.

[10] Brown, R. C.; and Buttermore, W. H. "A Method for Improving Load Turndown in Fluidized Bed Combustors." U. S. Patent No. 4,762,090, 1988.

[11] Brown, R. C.; and Foley, J. E. "A New Method for Improving Load Turndown in Fluidized Bed Combustors." *Industrial and Engineering Chemistry Research* 27 (1988): 24-30.

[12] Gibbs, B. M.; Pereira, F. J.; and Beer, J. M. "The Influence of Air Staging on the NO Emission from a Fluidized Bed Combustor." *Sixteenth Symposium (International) on Combustion* 16 (1977): 461-474.

[13] Incropera, F. P.; and DeWitt, D. P. *Fundamentals of Heat and Mass Transfer.* 2nd edition. New York: John Wiley and Sons, Inc., 1985.

[14] Xavier, A. M.; and Davidson, J. F. "Heat Transfer in Fluidization: Convective Heat Transfer in Fluidized Beds." In *Fluidization*. 2nd edition. Edited by J. F. Davidson, R. Clift, and D. Harrison. New York: Academic Press, 1985.

[15] Essenhigh, R. H. "Coal Combustion," in *Coal Conversion Technology.* Edited by C. Y. Wen and E. S. Lee. Reading, Massachusetts: Addison-Wesley Publishing Company, 1979, pp. 171-312.

[16] Avedesian, M. M.; and Davidson, J. F. "Combustion of Carbon Particles in a Fluidized Bed." *Trans. Instn. Chem. Engrs.* 51 (1973): 121-131.

[17] Walsh, P. M. "The Efficiency of Bituminous Coal Combustion in Bubbling Atmospheric Pressure Fluidized Beds." *Proc. Tenth Int. Conf. on Fluidized Bed Combustion.* San Francisco, California 10 (1989): 765-773.

[18] Roberts, P. T.; Shirvill, L. C.; and Cowley, L. T. "Bed Carbon Loadings in Fluid Bed Combustion." *Combustion and Flame* 69 (1987): 243-247.

[19] Turnbull, E.; and Davidson, J. F. "Fluidized Combustion of Char and Volatiles from Coal." *AIChE J.* 30 (1984): 881-889.

[20] Gregory, J. W.; and Brown, R. C. "Mechanisms of Coal-Water Mixture Combustion in Fluidized Beds." *Proc. Tenth Int. Conf. on Fluidized Bed Combustion*, San Francisco, California 10 (1989): 77-84.

[21] Howard, J. B.; Williams, G. C.; and Fine, D. H. "Kinetics of Carbon Monoxide Oxidation in Postflame Gases." *14th Symposium (International) on Combustion* 14 (1973): 975-986.

[22] Eraslan, A. N.; and Brown, R. C. "A Simple Iterative Procedure for Reducing Stiffness and Computer Memory in Reactive Flow Problems." *Computer Methods in Applied Mechanics and Engineering* 64 (1987): 61-77.

[23] Grace, J. R. "Fluid Beds as Chemical Reactors." in *Gas Fluidization Technology.* Edited by D. Geldart, New York: John Wiley and Sons Ltd., 1986, pp. 285-339.

[24] IMSL Math Library Subroutines, "DIVPAG - An Initial Value Problem Solver." New York: IMSL, Inc., 1987.

[25] McHale, E. T. "Review of CWF Combustion Technology." *Energy Progress* 5, No. 1 (1985): 15-24.

[26] Organisation for Economic Cooperation and Development. *Emission Standards for Major Air Pollutants.* Member Countries, Paris, France, 1984.

[27] Stantan, J. E. "Sulfur Retention in Fluidized Bed Combustion." In *Fluidized Beds: Combustion and Applications.* Edited by J. R. Howard. Essex, England: Applied Science Publishers, 1983, pp. 199-226.

[28] Basu, P. "Burning Rate of Carbon in Fluidized Beds." *Fuel* 56 (1977): 390-392.

[29] Salan, T. F.; Sibtain, S. F.; and Gibbs, B. M. Reduction of NO_x by Staged Combustion Combined with Ammonia Injection in a Fluidized Bed Combustor: Influence of Fluidizing Velocity and Excess Air Levels." *Proc. Tenth Int. Conf. on Fluidized Bed Combustion*, San Francisco, California 10 (1989): 69-76.

[30] Pflum, D. L.; Brown, R. C.; and Maxwell, G. M. "A Resistance Wire Technique Applied to Heat Transfer Measurements in High Aspect Ratio Fluidized Beds." *Proc. 26th National Heat Transfer Conference*, Philadelphia, Pennsylvania, 1989.

10 APPENDIX A. HEAT TRANSFER COMPUTER MODEL LISTING

```
C     This program solves the system of equations for temperature
C     and heat transfer in a two-bed fluidized bed combustor.

C     The equations for calculating heat transfer coefficients in
C     a fluidized bed are contained in the subroutine COEFFC for the
C     center bed and COEFFA for the annular heat transfer bed.

C     The subroutine MINFLU evaluates minimum fluidization velocity and
C     PROP determines air properties.

C     LAST UPDATE:  6/20/89 by Jim Foley

      DOUBLE PRECISION AORIF, EPSB,EPSIW,EPSOW,EPSP,CPS,EMFA,EMFC
      DOUBLE PRECISION EOA,EOC,RHOS,RMUW,HFG,G,RHOL,RHOV,SIG,CPW
      DOUBLE PRECISION CSF,PRANW,RJUNK1,RJUNK2,DPC,DPA,BOILC,PI
      DOUBLE PRECISION ABAREA,CBAREA,AHDEAD,CHDEAD,CPNOT,HJACK
      DOUBLE PRECISION SAIW,SAOW,RHONOT,GPMW,UOVERUMF,CSCFM,COAL
      DOUBLE PRECISION ASCFM,AFRAT,DPAM,DPCM,DBC
      DOUBLE PRECISION VFBIW,VFPIW,VFPOW,UBIW,UPIW,UPOW,DC,DA
      DOUBLE PRECISION UNOT,UHTNOT,MAIR,MHTAIR,UAIR,UHTAIR
      DOUBLE PRECISION CPAIR,RHOAIR,RMUAIR,RKAIR,PRAIR
      DOUBLE PRECISION CPHT,RHOHT,RMUHT,RKHT,PRHT
      DOUBLE PRECISION ARA,UMFHT,KEO,HGCA,ARC,UMFC,KEOC,HGCC
      DOUBLE PRECISION EC,EBC,UBC,HEIGHTC,HPCC,HB
      DOUBLE PRECISION HA,FLUX,QCOND
      DOUBLE PRECISION TNOT,QIN,TB,TIW,TP,TOW,TW
      DOUBLE PRECISION VAL(5),ERR(5),TEST,TOL
      DOUBLE PRECISION QCWALL,QCAIR,QCRAD,QARADI,QARADO,QWALLI
```

```
      DOUBLE PRECISION QWALLO,QHTAIR,QH2O,RATIOC,RATIOA,UABEDS
      CHARACTER*3 HUH
      INTEGER FLAGDP,IFLAGHT,IFLAGA,IQUES

C     INPUT DATA FOR FLUIDIZED BED :

      DATA AORIF, EPSB, EPSIW, EPSOW, EPSP,
     *     CPS,   EMFA, EMFC,  EOA,   EOC,
     *     RHOS,  RMUW, HFG,   G,     RHOL,
     *     RHOV,  SIG,  CPW,   CSF,   PRANW
     *   /2.0268D-04, 0.8D0,     0.40D0,     0.40D0,   0.90D0,
     *     800.0D0,   0.476D0,   0.476D0,    0.40D0,   0.40D0,
     *     2600.0D0,  279.0D-06, 2257.0D+03, 9.806D0,  957.9D0,
     *     0.5955D0,  58.9D-03,  4217.0D0,   0.0130D0, 1.76D0 /

      DATA TNOT,  DA,    AHDEAD, CHDEAD,
     *     CPNOT, HJACK, RHONOT, GPMW
     *    /294.0D0,  0.254D0,  0.229D0, 0.178D0,
     *     1007.0D0, 0.2286D0, 1.19D0,  1.50D0 /

      PRINT*,'WHAT IS THE ANNULAR BED PARTICLE DIAMETER ? '
      PRINT*,'   IN MICRONS : '
      PRINT*,' '
      READ(5,*) DPAM
      DPA = DPAM*1.0D-06
      PRINT*,'WHAT IS THE CENTRAL BED PARTICLE DIAMETER ? '
      PRINT*,'   IN MICRONS : '
      READ(5,*) DPCM
      DPC = DPCM*1.0D-06
      PRINT*,' INPUT CENTRAL BED DIAMETER (IN INCHES) : '
      PRINT*,' FOR EXAMPLE:  5,7, OR 8 INCHES  . . . '
      PRINT*,' '
      READ(5,*) DC

      DC = DC*0.02540D0
      BOILC = RMUW*HFG*DSQRT( G*(RHOL-RHOV)/SIG )*
     *        ( (CPW/(CSF*HFG*PRANW))**3 )
      PI = 4.0D0*DATAN(1.0D0)
      ABAREA = (  DA*DA - DC*DC )*PI/4.0D0
```

```
      CBAREA = PI*DC*DC/4.0D0
      SAIW = PI*HJACK*DC
      SAOW = PI*HJACK*DA
      WRITE(6,10)
      WRITE(6,20) DC,DPCM,CHDEAD
      WRITE(6,30) DPAM,AHDEAD

 10       FORMAT('1',X,'TWO-BED FLUIDIZED BED COMBUSTOR SIMULATION')
 20       FORMAT(' ',/,/,/,X,'COMB BED DIAMETER : ',F6.3,' m',/,X,
     *      'COMB BED PARTICLE SIZE : ',F7.1,' MICRONS',/,X,
     *      'COMB BED DEAD HEIGHT :',F6.3,' m')
 30       FORMAT(' ',/,X,'ANNULAR BED PARTICLE SIZE : ',F7.1,' MICRONS'
     *      ,/,X, 'ANN BED DEAD HEIGHT : ',F6.3,' m',//,X,
     *      'UNITS ARE AS FOLLOWS: ',/,6X,'U (m/s)  Q (kW)  V (scfm) ',
     *      'UA (W/K)  h (W/m2K)   T (K)   A/F (scfm/kW)',/,X )


C  INPUT AIRFLOWS AND (BED TEMPERATURE OR ENERGY RELEASED IN BED)

 5     PRINT*,'INPUT U/Umf FOR ANNULAR BED  :'
       PRINT*,'       '
       READ(5,*) UOVERUMF
       PRINT*,'   '
       PRINT*,'  INPUT PRIMARY (combustion bed) AIRFLOW (scfm)  :'
       PRINT*,'    '
       READ(5,*) CSCFM
       PRINT*,'    '

 50    PRINT*,'DO YOU KNOW :  1)  Combustion Temperature  '
       PRINT*,'          OR :  2)  QIN     '
       READ(5,*) II
       IF (II.NE.1.AND.II.NE.2) THEN
          PRINT*,'MUST BE 1 OR 2!'
          GOTO 50
       ELSE
          CONTINUE
       ENDIF

       IF (II.EQ.1) THEN
```

```
      PRINT*,'INPUT TBED (K)'
      READ(5,*) TB

   ELSE

      PRINT*,'QIN (kW)'
      READ(5,*) QIN
      QIN = QIN*1000.0D0
      TB = 1144.0D0              !INITIAL GUESS

   ENDIF


C  CALCULATE RADIATION VIEW FACTORS :

      VFBIW = 5.68D-08 / ( 1.0D0/EPSB+1.0D0/EPSIW-1.0D0 )
      VFPIW = 5.68D-08 / ( 1.0D0/EPSP+1.0D0/EPSIW-1.0D0 )
      VFPOW = 5.68D-08 / ( 1.0D0/EPSP+1.0D0/EPSOW-1.0D0 )


C  MAKE INITIAL GUESSES

      TEST = 5.0D0
      TOL = 0.00005D0              !CONVERGENCE CRITERION
      TW = 300.0D0                 !AVERAGE WATER TEMP.
      TOW = 373.1D0                !WATER WALL TEMP.
      TP = 670.0D0                 !HT ANNULAR BED TEMP.
      TIW = 900.0D0                !INSERT WALL TEMP.

C  CALCULATE INITIAL VALUES OF RADIATION COEFFICIENTS

      UBIW = VFBIW*(TB*TB+TIW*TIW)*(TB+TIW)     !W/m2K
      UPIW = VFPIW*(TP*TP+TIW*TIW)*(TP+TIW)
      UPOW = VFPOW*(TP*TP+TOW*TOW)*(TP+TOW)

      UNOT = CSCFM*4.7195D-04/CBAREA        !m/sec
      MAIR = CSCFM*RHONOT*4.7195D-04        !kg/sec
      UMFHT = 0.0500D0                      !m/sec
```

```
      IF (UOVERUMF.GE.1.00D0) THEN    !ANNULAR BED IS FLUIDIZED

         IF (II.EQ.1) THEN            !COMBUSTION TEMP. IS KNOWN

          DO 100 WHILE(TEST.GT.TOL)

            CALL PROP ( TP,RHOHT,CPHT,RMUHT,RKHT,PRHT,IFLAGHT )
            CALL PROP ( TB,RHOAIR,CPAIR,RMUAIR,RKAIR,PRAIR,IFLAGA )

            UHTAIR = UOVERUMF*UMFHT                !m/sec
            UHTNOT = UHTAIR*TNOT/TP                !m/sec
            MHTAIR = UHTNOT*RHONOT*ABAREA          !kg/sec
            UAIR = UNOT*TB/TNOT                    !m/sec

            CALL MINFLU (UHTAIR,RHOHT,CPHT,RKHT,RMUHT,EOA,DPA,RHOS,
     *                   AHDEAD,PI,ARA,UMFHT,KEO,HGCA)
            CALL MINFLU (UAIR,RHOAIR,CPAIR,RKAIR,RMUAIR,EOC,DPC,RHOS,
     *                   CHDEAD,PI,ARC,UMFC,KEOC,HGCC)

            CALL COEFFC ( UAIR,CPAIR,RHOAIR,RMUAIR,RKAIR,DPC,CPS,RHOS,
     *                    EOC,EMFC,CHDEAD,DC,AORIF,UMFC,EC,EBC,UBC,DBC,
     *                    HEIGHTC,HGCC,HPCC,HB )
            CALL COEFFA ( DPA,UOVERUMF,HGCA,HA,FLAGDP )

            CPAIR = 0.50D0*(CPNOT+CPAIR)
            CPHT = 0.50D0*(CPNOT+CPHT)

            VAL(1) = QIN
            VAL(2) = TIW
            VAL(3) = TP
            VAL(4) = TOW

            QIN = MAIR*CPAIR*(TB-TNOT) + SAIW*(HB+UBIW)*(TB-TIW)
            TIW = (  (HB+UBIW)*TB + (HA+UPIW)*TP    ) /
     *           (  (HB+UBIW)    + (HA+UPIW)       )
            TP  = ( MHTAIR*CPHT*TNOT + SAIW*(HA+UPIW)*TIW +
     *              SAOW*(HA+UPOW)*TOW  ) /
     *           ( MHTAIR*CPHT + SAIW*(HA+UPIW) + SAOW*(HA+UPOW) )
```

```
            FLUX = (HA+UPOW)*(TP-TOW)
            TOW = 373.0D0 + (FLUX/BOILC)**(1.0D0/3.0D0)

            ERR(1) = DABS( (QIN-VAL(1))/QIN )
            ERR(2) = DABS( (TIW-VAL(2))/TIW )
            ERR(3) = DABS( (TP -VAL(3))/TP  )
            ERR(4) = DABS( (TOW-VAL(4))/TOW )
            TEST = 0.0D0

            DO 99 I=1,4
               IF (ERR(I).GT.TEST) TEST=ERR(I)
 99         CONTINUE
 100      CONTINUE


C        ***************************************************************

         ELSE                          !QIN IS KNOWN

          DO 200 WHILE (TEST.GT.TOL)

            CALL PROP ( TP,RHOHT,CPHT,RMUHT,RKHT,PRHT,IFLAGHT )
            CALL PROP ( TB,RHOAIR,CPAIR,RMUAIR,RKAIR,PRAIR,IFLAGA )
            UHTAIR = UOVERUMF*UMFHT                !m/sec
            UHTNOT = UHTAIR*TNOT/TP                !m/sec
            MHTAIR = UHTNOT*RHONOT*ABAREA          !kg/sec
            UAIR = UNOT*TB/TNOT                    !m/sec
            CALL MINFLU (UHTAIR,RHOHT,CPHT,RKHT,RMUHT,EOA,DPA,RHOS,
     *                   AHDEAD,PI,ARA,UMFHT,KEO,HGCA)
            CALL MINFLU (UAIR,RHOAIR,CPAIR,RKAIR,RMUAIR,EOC,DPC,RHOS,
     *                   CHDEAD,PI,ARC,UMFC,KEOC,HGCC)

            CALL COEFFC ( UAIR,CPAIR,RHOAIR,RMUAIR,RKAIR,DPC,CPS,RHOS,
     *                    EOC,EMFC,CHDEAD,DC,AORIF,UMFC,EC,EBC,UBC,DBC,
     *                    HEIGHTC,HGCC,HPCC,HB )
            CALL COEFFA ( DPA,UOVERUMF,HGCA,HA,FLAGDP )

            CPAIR = 0.50D0*(CPNOT+CPAIR)
            CPHT = 0.50D0*(CPNOT+CPHT)
```

```
            TP = 0.50D0*(TIW+TOW)

            VAL(1) = TB
            VAL(2) = TIW
            VAL(3) = TP
            VAL(4) = TOW

            TB = ( QIN + MAIR*CPAIR*TNOT + SAIW*(HB+UBIW)*TIW ) /
     *           (  MAIR*CPAIR + SAIW*(HB+UBIW)  )
            TIW = ( (HB+UBIW)*TB + (HA+UPIW)*TP  ) /
     *            ( (HB+UBIW) + (HA+UPIW)  )
            TP = ( MHTAIR*CPHT*TNOT + SAIW*(HA+UPIW)*TIW +
     *             SAOW*(HA+UPOW)*TOW  ) /
     *           ( MHTAIR*CPHT + SAIW*(HA+UPIW) + SAOW*(HA+UPOW) )
            FLUX = (HA+UPOW)*(TP-TOW)
            TOW = 373.0D0 + (FLUX/BOILC)**(1.0D0/3.0D0)

            ERR(1) = DABS( (TB -VAL(1))/TB  )
            ERR(2) = DABS( (TIW-VAL(2))/TIW )
            ERR(3) = DABS( (TP -VAL(3))/TP  )
            ERR(4) = DABS( (TOW-VAL(4))/TOW )
            TEST = 0.0D0

            DO 199 I=1,4
               IF (ERR(I).GT.TEST) TEST=ERR(I)
 199        CONTINUE
 200      CONTINUE

C         ************************************************************

         ENDIF

      ELSE                              !ANNULAR BED IS DEFLUIDIZED

         IF (II.EQ.1) THEN              !COMBUSTION TEMP. IS KNOWN

          DO 300 WHILE (TEST.GT.TOL)

            CALL PROP ( TP,RHOHT,CPHT,RMUHT,RKHT,PRHT,IFLAGHT )
```

```
      CALL PROP ( TB,RHOAIR,CPAIR,RMUAIR,RKAIR,PRAIR,IFLAGA )

      UHTAIR = UOVERUMF*UMFHT                !m/sec
      UHTNOT = UHTAIR*TNOT/TP                !m/sec
      MHTAIR = UHTNOT*RHONOT*ABAREA          !kg/sec
      UAIR = UNOT*TB/TNOT                    !m/sec

      CALL MINFLU (UHTAIR,RHOHT,CPHT,RKHT,RMUHT,EOA,DPA,RHOS,
     *              AHDEAD,PI,ARA,UMFHT,KEO,HGCA)
      CALL MINFLU (UAIR,RHOAIR,CPAIR,RKAIR,RMUAIR,EOC,DPC,RHOS,
     *              CHDEAD,PI,ARC,UMFC,KEOC,HGCC)

      CALL COEFFC ( UAIR,CPAIR,RHOAIR,RMUAIR,RKAIR,DPC,CPS,RHOS,
     *               EOC,EMFC,CHDEAD,DC,AORIF,UMFC,EC,EBC,UBC,DBC,
     *               HEIGHTC,HGCC,HPCC,HB )

      CPAIR = 0.50D0*(CPNOT+CPAIR)
      CPHT = 0.50D0*(CPNOT+CPHT)
      TP = 0.50D0*(TIW+TOW)
      VAL(1) = QIN
      VAL(2) = TIW
      VAL(3) = TOW

      TP = 0.50D0*(TIW+TOW)
      QIN = MAIR*CPAIR*(TB-TNOT) + SAIW*(HB+UBIW)*(TB-TIW)
      TIW = (  (-2.0D0*KEO/(DLOG10(DC/DA)))*TOW +
     *     DC*(HB+UBIW)*TB - MHTAIR*CPHT*(TP-TNOT)/(PI*HJACK)  )/
     *       ( (-2.0D0*KEO/(DLOG10(DC/DA))) + DC*(HB+UBIW) )
      QCOND = - ( 2.0D0*PI*HJACK*KEO*(TIW-TOW) )/(DLOG10(DC/DA))
      TOW = ( QCOND/(BOILC*PI*DA*HJACK) )**(1.0D0/3.0D0)
     *        + 373.0D0

      ERR(1) = DABS( (QIN-VAL(1))/QIN )
      ERR(2) = DABS( (TIW-VAL(2))/TIW )
      ERR(3) = DABS( (TOW-VAL(3))/TOW )
      TEST = 0.0D0

      DO 299 I=1,3
         IF (ERR(I).GT.TEST) TEST=ERR(I)
```

```
 299        CONTINUE
 300      CONTINUE

C         ************************************************************

          ELSE                              !QIN IS KNOWN

           DO 400 WHILE (TEST.GT.TOL)

             CALL PROP ( TP,RHOHT,CPHT,RMUHT,RKHT,PRHT,IFLAGHT )
             CALL PROP ( TB,RHOAIR,CPAIR,RMUAIR,RKAIR,PRAIR,IFLAGA )

             UHTAIR = UOVERUMF*UMFHT                !m/sec
             UHTNOT = UHTAIR*TNOT/TP                !m/sec
             MHTAIR = UHTNOT*RHONOT*ABAREA          !kg/sec
             UAIR = UNOT*TB/TNOT                    !m/sec

             CALL MINFLU (UHTAIR,RHOHT,CPHT,RKHT,RMUHT,EOA,DPA,RHOS,
     *                    AHDEAD,PI,ARA,UMFHT,KEO,HGCA)
             CALL MINFLU (UAIR,RHOAIR,CPAIR,RKAIR,RMUAIR,EOC,DPC,RHOS,
     *                    CHDEAD,PI,ARC,UMFC,KEOC,HGCC)
             CALL COEFFC ( UAIR,CPAIR,RHOAIR,RMUAIR,RKAIR,DPC,CPS,RHOS,
     *                     EOC,EMFC,CHDEAD,DC,AORIF,UMFC,EC,EBC,UBC,DBC,
     *                     HEIGHTC,HGCC,HPCC,HB )

             CPAIR = 0.5ODO*(CPNOT+CPAIR)
             CPHT = 0.5ODO*(CPNOT+CPHT)

             VAL(1) = TB
             VAL(2) = TIW
             VAL(3) = TP
             VAL(4) = TOW

             TP = 0.5ODO*(TIW+TOW)
             TB = ( QIN + MAIR*CPAIR*TNOT + SAIW*(HB+UBIW)*TIW ) /
     *            (  MAIR*CPAIR + SAIW*(HB+UBIW)  )
             TIW = (  (-2.ODO*KEO/(DLOG10(DC/DA)))*TOW +
     *           DC*(HB+UBIW)*TB - MHTAIR*CPHT*(TP-TNOT)/(PI*HJACK)  )/
     *             ( (-2.ODO*KEO/(DLOG10(DC/DA))) + DC*(HB+UBIW) )
```

```
            QCOND = - ( 2.0D0*PI*HJACK*KE0*(TIW-TOW) )/(DL0G10(DC/DA))
            TOW = ( QCOND/(B0ILC*PI*DA*HJACK) )**(1.0D0/3.0D0)
     *              + 373.0D0

            ERR(1) = DABS( (TB -VAL(1))/TB  )
            ERR(2) = DABS( (TIW-VAL(2))/TIW )
            ERR(3) = DABS( (TP -VAL(3))/TP  )
            ERR(4) = DABS( (TOW-VAL(4))/TOW )
            TEST = 0.0D0

            DO 399 I=1,4
               IF (ERR(I).GT.TEST) TEST=ERR(I)
 399        CONTINUE
 400      CONTINUE

C         ************************************************************

         ENDIF

      ENDIF

****************** IF ANNULAR BED IS FLUIDIZED ******************

      IF (U0VERUMF.GE.1.00D0) THEN

      ASCFM  = MHTAIR*1763.67D0
      RATI0A = U0VERUMF
      RATI0C = UAIR/UMFC
      QIN    = QIN*1.0D-03
      QCWALL = HB*HJACK*PI*DC*(TB-TIW)*1.0D-03
      QCAIR  = MAIR*CPAIR*(TB-TN0T)*1.0D-03
      QCRAD  = UBIW*(TB-TIW)*HJACK*PI*DC*1.0D-03
      QARADI = UPIW*(TIW-TP)*HJACK*PI*DC*1.0D-03
      QWALLI = HA*HJACK*PI*DC*(TIW-TP)*1.0D-03
      QWALL0 = HA*HJACK*PI*DA*(TP-TOW)*1.0D-03
      QARAD0 = UP0W*(TP-TOW)*HJACK*PI*DA*1.0D-03
      QHTAIR = MHTAIR*CPHT*(TP-TN0T)*1.0D-03
      QH20   = FLUX*HJACK*PI*DA*1.0D-03
      UABEDS = 1000.0D0*(QH20+QHTAIR)/(TB-TP)
```

```
      AFRAT  = CSCFM/QIN

      ELSE

************** IF ANNULAR BED IS DEFLUIDIZED


      QCAIR  = MAIR*CPAIR*(TB-TNOT)*1.0D-03
      QCRAD = UBIW*HJACK*PI*DC*(TB-TIW)*1.0D-03
      QHTAIR = MHTAIR*CPHT*(TP-TNOT)*1.0D-03
      QH2O = HJACK*PI*DA*BOILC*( (TOW-373.0)**3 )*1.0D-03
      QIN = QIN*1.0D-03
      QCWALL = HB*(TB-TIW)*HJACK*PI*DC*1.0D-03
      QWALLI = HA*(TIW-TP)*HJACK*PI*DC*1.0D-03
      RATIOC = UAIR/UMFC
      RATIOA = UOVERUMF
      UABEDS = 1000.0D0*(QH2O+QHTAIR)/(TB-TP)
      AFRAT  = CSCFM/QIN

      ENDIF

999   CONTINUE

      WRITE(6,501) TB,QIN,RATIOC,HB
      WRITE(6,502) TIW,QH2O,CSCFM,AFRAT
      WRITE(6,503) TP, QCAIR, RATIOA, HA
      WRITE(6,504) TOW, QHTAIR, ASCFM, UABEDS

      WRITE(7,721) QIN,TB,RATIOA,QCRAD,QCAIR,QCWALL
      WRITE(7,722) QWALLI, QARADI, QHTAIR, QWALLO, QARADO
      WRITE(7,723) QH2O
      WRITE(7,724)

      WRITE(8,*) UAIR
      WRITE(8,*) UMFC
      WRITE(8,*) UBC
      WRITE(8,*) DBC
      WRITE(8,*) TNOT
      WRITE(8,*) TB
```

```
      WRITE(8,*) EBC
      WRITE(8,*) EMFC
      WRITE(8,*) HEIGHTC
      WRITE(8,*) QIN

          PRINT*,'WANT TO RUN AGAIN?  1 FOR YES, 2 FOR NO '
          READ(5,*) IQUES
          IF(IQUES.EQ.1) GOTO 5

501   FORMAT('0',2X,'TB  = ',F7.1,' QIN =    ',F7.2,' U/UMFC = ',F7.2,
     *         ' HB     = ',F8.3)
502   FORMAT(' ',2X,'TIW = ',F7.1,' QH20 =   ',F7.2,' CSCFM  = ',F7.2,
     *         ' A/F    = ',F8.3)
503   FORMAT(' ',2X,'TP  = ',F7.1,' QCAIR =  ',F7.2,' U/UMFA = ',F7.2,
     *         ' HA     = ',F8.3)
504   FORMAT(' ',2X,'TOW = ',F7.1,' QHTAIR = ',F7.2,' ASCFM  = ',F7.2,
     *         ' UABEDS = ',F8.3)
721   FORMAT('0',X,'  QIN    TB     RATIO  QCRAD    QCAIR     QCWALL',
     * /,X,F6.2,F9.1,F6.2,3(2X,F6.2) )
722   FORMAT('0',X,' QHTCONVI  QRADI   QHTAIR    QHTCONVO   QRADO ',
     * /,3X,5(F6.2,3X) )
723   FORMAT('0',X,'QH20 = : ',F6.2)
724   FORMAT(' ',X,'**********************************',/)


          STOP
          END
```

```
      SUBROUTINE PROP( T,RHO,CP,MU,K,PR,IFLAG )

C     This routine evaluates the properties of air using look-up tables
C     from Incorpera and DeWitt, Fundamentals of Heat and Mass Transfer,
C     John Wiley and Sons, New York (1985):  767.
C     Last update:  June 23, 1989 by Jim Foley.

      DOUBLE PRECISION T,RHO,CP,MU,K,PR
      INTEGER IFLAG
      DOUBLE PRECISION TEMP(25),DENS(25),HEAT(25),VISC(25),COND(25)
      DOUBLE PRECISION PRAN(25),X
      INTEGER I
      IFLAG = 0


      DATA (TEMP(I),I=1,22) /   200.0D0,  250.0D0,  300.0D0,  350.0D0,
     *      400.0D0,  450.0D0,  500.0D0,  550.0D0,  600.0D0,  650.0D0,
     *      700.0D0,  750.0D0,  800.0D0,  850.0D0,  900.0D0,  950.0D0,
     *     1000.0D0, 1100.0D0, 1200.0D0, 1300.0D0, 1400.0D0, 1500.0D0
     /

      DATA(DENS(I),I=1,22) / 1.7458D0, 1.3947D0, 1.1614D0, .9950D0,
     *     .8711D0, .7740D0,  .6964D0,  .6329D0,  .5804D0, .5356D0,
     *     .4975D0, .4643D0,  .4354D0,  .4097D0,  .3868D0, .3666D0,
     *     .3482D0, .3166D0,  .2902D0,  .2679D0,  .2488D0, .2322D0 /

      DATA (HEAT(I),I=1,22) /  1007.0D0, 1006.0D0, 1007.0D0, 1009.0D0,
     *     1014.0D0, 1021.0D0, 1030.0D0, 1040.0D0, 1051.0D0, 1063.0D0,
     *     1075.0D0, 1087.0D0, 1099.0D0, 1110.0D0, 1121.0D0, 1131.0D0,
     *     1141.0D0, 1159.0D0, 1175.0D0, 1189.0D0, 1207.0D0, 1230.0D0
     /

      DATA (VISC(I),I=1,22) /  132.5D-7, 159.6D-7, 184.6D-7, 208.2D-7,
     *     230.1D-7, 250.7D-7, 270.1D-7, 288.4D-7, 305.4D-7, 322.5D-7,
     *     338.8D-7, 354.6D-7, 369.8D-7, 384.3D-7, 398.1D-7, 411.3D-7,
     *     424.4D-7, 449.0D-7, 473.0D-7, 496.0D-7, 530.0D-7, 557.0D-7
     /
```

```
 DATA (COND(I),I=1,22)/ 18.1D-3, 22.3D-3, 26.3D-3, 30.0D-3,
*     33.8D-3, 37.3D-3, 40.7D-3, 43.9D-3, 46.9D-3, 49.7D-3,
*     52.4D-3, 54.9D-3, 57.3D-3, 59.6D-3, 62.0D-3, 64.3D-3,
*     66.7D-3, 71.5D-3, 76.3D-3, 82.0D-3, 92.0D-3, 100.D-3 /

 DATA (PRAN(I),I=1,22)/ .737D0, .720D0, .707D0, .700D0,
*       .690D0, .686D0, .684D0, .683D0, .685D0, .690D0,
*       .695D0, .702D0, .709D0, .716D0, .720D0, .723D0,
*       .726D0, .728D0, .728D0, .719D0, .703D0, .685D0 /

 IF (T.LE.TEMP(1)) THEN

      IFLAG = 1
      RHO = DENS(1)
      CP = HEAT(1)
      MU = VISC(1)
      K = COND(1)
      PR = PRAN(1)
      RETURN

ELSE

      IF (T.GE.TEMP(22)) THEN

           IFLAG = 2
           RHO = DENS(22)
           CP = HEAT(22)
           MU = VISC(22)
           K = COND(22)
           PR = PRAN(22)
           RETURN

      ELSE
           CONTINUE
      ENDIF
ENDIF

DO 100 I=1,21
```

```
         IF(T.GE.TEMP(I).AND.T.LT.TEMP(I+1)) J=I
100   CONTINUE

      X = ( T-TEMP(J) ) / ( TEMP(J+1)-TEMP(J) )

      CP  = ( HEAT(J+1)-HEAT(J) )*X + HEAT(J)
      RHO = ( DENS(J+1)-DENS(J) )*X + DENS(J)
      MU  = ( VISC(J+1)-VISC(J) )*X + VISC(J)
      K   = ( COND(J+1)-COND(J) )*X + COND(J)
      PR  = ( PRAN(J+1)-PRAN(J) )*X + PRAN(J)

      RETURN
      END
```

```
      SUBROUTINE MINFLU ( U, RHOAIR,CPAIR,KAIR,MUAIR,EO,DP,
     *                    RHOS, HEIGHT, PI, AR, UMF, KEO, HGC )

C     This routine evalutes the minimum fluidization velocity of a
C     bed of particles given the particle and gas stream properties.
C     It also calculates bed height, Archimedes number, conductivity
C     of the fluidized bed, and the convection coefficient from gas
C     to container wall.
C     Last update:  Jim Foley, June 23, 1989.


      DOUBLE PRECISION U, RHOAIR, CPAIR, KAIR, MUAIR, EO, DP
      DOUBLE PRECISION RHOS, HEIGHT, PI, AR, UMF, KEO, HGC
      DOUBLE PRECISION G, KS, M, KMF, HF, HAV



      G = 9.806D0
      KS = 1.90D0
      M = 6.0D0
      AR = RHOAIR*(RHOS-RHOAIR)*G*(DP**3)/(MUAIR*MUAIR)
      UMF = ( 25.7D0*MUAIR/(RHOAIR*DP) )*( (DSQRT(1.0D0+
     *        5.53D-05*AR)) - 1.0D0 )
      HF = M*KAIR/DP
      KEO = KAIR*( (KS/KAIR)**( 0.28D0-0.757D0*DLOG10(EO)-
     *        0.057D0*DLOG10(KS/KAIR) ) )
      KMF = KEO + 0.10D0*RHOAIR*CPAIR*DP*UMF
      HAV = DSQRT( 4.0D0*KMF*RHOAIR*CPAIR*U/(PI*HEIGHT) )
      IF (U.EQ.0.0D0) THEN
         HGC = HF
      ELSE
         HGC = 1.0D0/( (1.0D0/HAV) + (1.0D0/HF) )
      ENDIF

      RETURN
      END
```

```
      SUBROUTINE COEFFA ( DP,UOVERUMF,HGC,HTOT,FLAGDP )

C     This routine evaluates the annular bed convective heat transfer
C     coefficient using data from Pflum and Brown.  Particle diameter
C     and the velocity ratio (u/umf) is input and the convection
C     coefficient is output.  FLAGDP is set to 99 if DP is improperly
C     specified.  Last update:  June 23, 1989 by Jim Foley.

      DOUBLE PRECISION DP,UOVERUMF,HGC,HTOT,X
      INTEGER FLAGDP,J

      FLAGDP=0
      J=0
      X = UOVERUMF

      IF (DP.GT.240.0D-06.AND.DP.LT.260.0D-06) J=1
      IF (DP.GT.490.0D-06.AND.DP.LT.520.0D-06) J=2

      IF (J.EQ.1) THEN          ! 250 MICRON PARTICLES

        IF (X.GE.1.00D0.AND.X.LT.1.34D0) THEN

          HPC = 90.30D0

        ELSE

          IF (X.GE.1.34D0.AND.X.LT.2.24D0) THEN

            HPC = 94.11D0*(X-1.34D0) + 90.3D0

          ELSE

            IF (X.GE.2.24D0.AND.X.LT.4.90D0) THEN

              HPC = -479.6D0 + 365.85D0*X - 32.864D0*X*X

            ELSE
```

```
        IF (X.GE.4.90D0.AND.X.LT.7.58D0) THEN
          HPC = -43.25D0 + 179.51D0*X - 13.009D0*X*X
        ELSE
          IF (X.GE.7.58D0.AND.X.LT.9.32) THEN
            HPC = -9.195D0*(X-7.58) + 570.0D0
          ELSE              ! X > 9.32
            HPC = 554.0D0
          ENDIF
        ENDIF
      ENDIF
    ENDIF
  ENDIF



ELSE
  IF (J.EQ.2) THEN          ! 500 MICRON PARTICLES
    IF(X.GE.1.00D0.AND.X.LT.1.36D0) THEN
      HPC = 290.22D0 - 442.1D0*X + 292.517D0*X*X
    ELSE
      IF (X.GE.1.36D0.AND.X.LT.2.11D0) THEN
        HPC = - 867.47D0 + 1173.25D0*X - 269.33D0*X*X
      ELSE
```

```
        IF (X.GE.2.11D0.AND.X.LT.3.18D0) THEN

          HPC = 102.0D0 + 263.125D0*X - 55.747D0*X*X

        ELSE      ! X > 3.18

          HPC = 375.0D0

        ENDIF
      ENDIF
    ENDIF

  ELSE              ! DP IMPROPERLY SPECIFIED

          FLAGDP = 99
          HPC = -999.0D0

  ENDIF

ENDIF

HTOT = HGC + HPC

RETURN
END
```

```
      SUBROUTINE COEFFC ( UAIR, CPAIR, RHOAIR, RMUAIR, RKAIR,
     *     DP, CPS, RHOS, EO, EMF, ZDEAD, WIDTH, AORIF,
     *     UMF, E, EB, UB, DB, HEIGHT, HGC, HPC, HTOT )

C-----------------------------------------------------------------
C
C   THIS ROUTINE WILL EVALUATE THE HEAT TRANSFER COEFFICIENTS FOR
C   A FLUIDIZED BED FOLLOWING THE MODEL OF XAVIER AND DAVIDSON.
C
C
C   CALL PARAMETERS:
C
C      UAIR              FLUIDIZING AIR SUPERFICIAL VELOCITY ( m/s )
C      CPAIR             AIR SPECIFIC HEAT ( J/kgK )
C      RHOAIR            AIR DENSITY ( kg/m3 )
C      RMUAIR            AIR DYNAMIC VISCOSITY ( Ns/m2 )
C      RKAIR             AIR THERMAL CONDUCTIVITY ( W/mK )
C      DP                PARTICLE DIAMETER ( m )
C      CPS               PARTICLE SPECIFIC HEIGHT ( m )
C      RHOS              PARTICLE DENSITY ( kg/m3 )
C      EO                BED VOIDAGE OF PACKED BED
C      EMF               BED VOIDAGE AT MINIMUM FLUIDIZATION
C      ZDEAD             PACKED BED HEIGHT ( m )
C      WIDTH             CHARACTERISTIC BED WIDTH ( m )
C      AORIF             DISTRIBUTOR AREA PER ORIFICE ( m2 )
C
C
C      OUTPUT PARAMETERS:
C
C
C
C      UMF               SUPERFICIAL AIR VELOCITY AT MIN. FLUIDIZATION
( m/s )
C      E                 BED VOIDAGE OF FLUIDIZED BED
C      EB                VOIDAGE CONTAINED IN BUBBLES
C      UB                BUBBLE RISE VELOCITY ( m/s )
```

```
C       DB                  AVERAGE BUBBLE DIAMETER ( m )
C       HEIGHT              FLUIDIZED BED HEIGHT ( m )
C       HGC                 GAS-CONVECTION HEAT TRANS. COEFF. ( W/m2K )
C       HPC                 PARTICLE-CONVECTION HEAT TRANS. COEFF. ( W/m2K
)
C       HTOT                TOTAL HEAT TRANSFER COEFF. ( W/m2K )
C
C
C-----------------------------------------------------------------------
C   FIRST VERSION BY TIM PEDERSEN,
C   REVISED BY JIM FOLEY, 6/20/89.


      IMPLICIT REAL*8 (A-H,O-Z)
      REAL*8 KMF,KEO,KS

      PI = 4.0D0*DATAN(1.0D0)
      G = 9.806D0
      RM = 6.0D0
      KS = 1.90D0

C     PARTICLE REYNOLDS NUMBER
      REP = UAIR*RHOAIR*DP/RMUAIR

      ZMF = ZDEAD*(1.0D0-EO)/(1.0D0-EMF)
      RHOCMF = RHOS*(1.0D0-EMF)*CPS

      AR = RHOAIR*(RHOS-RHOAIR)*G*(DP**3)/(RMUAIR*RMUAIR)
      UMF = (RMUAIR/(RHOAIR*DP))*(((1.0D0+5.53D-05*AR)**(0.5)-1.0D0)
     *     *25.7D0)

      KEO = RKAIR*(KS/RKAIR)**(0.28D0-0.757D0*DLOG10(EO)-0.057D0*
     *     DLOG10(KS/RKAIR))
      KMF = KEO+0.1D0*RHOAIR*CPAIR*DP*UMF

      DB = (0.54D0*(UAIR-UMF)**(0.4D0)*(ZDEAD+4.0D0*DSQRT(AORIF))
     *     **(0.8D0))/G**(0.2D0)
      PROD = DB/WIDTH
```

```
C     BUBBLE RISE VELOCITY:

C          IF        PROD > 0.6    SLUG FLOW
C          IF .125 < PROD < 0.6    BUBBLE FLOW WITH WALL EFFECTS
C          IF .125 > PROD          BUBBLE FLOW

      UB = 0.71D0*DSQRT(G*DB)
      IF( PROD .GE. 0.125D0 .AND. PROD .LE. 0.6D0 )
     *      UB = 1.13D0*0.71D0*DSQRT(G*DB)*DEXP(-PROD)
      IF( PROD .GT. 0.6D0 ) UB = 0.35*DSQRT(G*WIDTH)

      QUANT = UB/(UAIR-UMF+UB)
      EB = 1.0D0 - QUANT

      E = 1.0D0 - (1.0D0-EB)*(1.0D0-E0)*ZDEAD/ZMF
      HEIGHT = ZMF/QUANT

      HP = 2.0D0*DSQRT(2.0D0*KMF*RHOCMF*(UAIR-UMF)/(PI*DB) )
      HF = RM*RKAIR/DP
      HPC = (1.0D0/(1.0D0/HP+1.0D0/HF))*QUANT

      U=UMF
      HAV=DSQRT(4.0D0*KMF*RHOAIR*CPAIR*U/(PI*HEIGHT))
      HGC = 1.0D0/(1.0D0/HAV+1.0D0/HF)

      HTOT = HPC + HGC

      RETURN
      END
```

11 APPENDIX B. DERIVATION OF COMBUSTION MODEL

The two-phase theory of fluidization treats the combustion bed as being composed of a particle-dense phase (emulsion phase) and a particle-lean phase (bubble phase). It is assumed that all air flow in excess of minimum fluidization passes through the bubble phase.

The volume of bubble phase is the product of bed volume and bed voidage due to bubbles: $V_{b_{gas}} = \epsilon_b H_c A_c$. The volume of emulsion phase is then $V_e = (1-\epsilon_b) H_c A_c$. The volume of gas in the emulsion phase is $V_{e_{gas}} = \epsilon_{mf}(1-\epsilon_b) H_c A_c$. Bubble phase carbon monoxide and oxygen concentrations are based on bubble volume, and emulsion phase concentrations are based on emulsion air volume.

Emulsion phase

Conservation of species A (either oxygen or carbon monoxide) in the emulsion phase, using the entire emulsion phase as the control volume is:

$$\left[\begin{array}{c}\text{Rate of change}\\ \text{of species A in}\\ \text{emulsion phase}\end{array}\right] = \left[\begin{array}{c}\text{Flow of A}\\ \text{into emulsion}\\ \text{phase}\end{array}\right] - \left[\begin{array}{c}\text{Flow of A}\\ \text{out of}\\ \text{emulsion phase}\end{array}\right]$$

$$- \left[\begin{array}{c}\text{Diffusion of A}\\ \text{from emulsion to}\\ \text{bubble phase}\end{array}\right] + \left[\begin{array}{c}\text{Production of A}\\ \text{within emulsion}\\ \text{phase}\end{array}\right]$$

$$\left[\begin{array}{c}\text{Rate of change}\\ \text{of species A in}\\ \text{emulsion phase}\end{array}\right] = \frac{d}{dt}\left[\epsilon_{mf}(1-\epsilon_b)H_c A_c C'_{A_e}\right]$$

where C'_{A_e} is the concentration of species A in the emulsion phase $(moles/m^3)$.

$$\left[\begin{array}{c}\text{Flow of A}\\ \text{into emulsion}\\ \text{phase}\end{array}\right] = u_{mf}\left(\frac{T_o}{T_c}\right) A_c C'_{A_e}\left(\epsilon_{mf}(1-\epsilon_b)\right)$$

where $u_{mf}\left(\frac{T_o}{T_c}\right)$ is the velocity of minimum fluidization air referenced to the air inlet temperature, and C'_{A_o} is the inlet gas flow concentration of species A.

$$\left[\begin{array}{c}\text{Flow of A}\\ \text{out of}\\ \text{emulsion phase}\end{array}\right] = u_{mf} A_c C'_{A_e}\left(\epsilon_{mf}(1-\epsilon_b)\right)$$

$$\left[\begin{array}{c}\text{Diffusion of A}\\ \text{from emulsion to}\\ \text{bubble phase}\end{array}\right] = k_q a_b \epsilon_b \left(C_{A_e} - \bar{C}_{A_b}\right) H_c A_c$$

where k_q is the interphase mass transfer coefficient (m/s), a_b is the bubble area-to-volume ratio (m^2/m^3), and $\bar{C}_{A_b}$ is the height-average concentration of species A in the bubble phase.

$$\left[\begin{array}{c}\text{Production of A}\\ \text{within emulsion}\\ \text{phase}\end{array}\right] = \dot{G}_{A_e}$$

Substituting the above terms into the conservation equation, setting the time derivative term equal to zero for steady state, and rearranging terms yield the emulsion phase conservation equation:

$$\frac{1}{H_c}\left[u_{mf} C_{A_e} - u_{mf}\left(\frac{T_o}{T_c}\right) C_{A_o}\right] = \frac{\left(-k_q a_b \epsilon_b (C_{A_e} - \bar{C}_{A_b}) + \dfrac{\dot{G}_{A_e}}{H_c A_c}\right)}{\epsilon_{mf}(1-\epsilon_b)} \qquad (11.1)$$

Bubble phase

$$\left[\begin{array}{c}\text{Rate of change}\\ \text{of species A in}\\ \text{bubble phase}\end{array}\right] = \left[\begin{array}{c}\text{Flow of A}\\ \text{into bubble}\\ \text{phase}\end{array}\right] - \left[\begin{array}{c}\text{Flow of A}\\ \text{out of}\\ \text{bubble phase}\end{array}\right]$$

$$- \left[\begin{array}{c}\text{Diffusion of A}\\ \text{from bubble to}\\ \text{emulsion phase}\end{array}\right] + \left[\begin{array}{c}\text{Production of A}\\ \text{within bubble}\\ \text{phase}\end{array}\right]$$

The concentration of a species of gas in the bubble phase varies with height. Therefore, a semi-infinitesmal control volume with cross-sectional area A_c, and height dz, is used for the bubble phase conservation equation.

$$\left[\begin{array}{c}\text{Rate of change}\\ \text{of species A in}\\ \text{bubble phase}\end{array}\right] = \frac{d}{dt}\left[(\epsilon_b A_c C_{A_b})dz\right]$$

$$\left[\begin{array}{c}\text{Flow of A}\\ \text{into bubble}\\ \text{phase}\end{array}\right] = \left(u - u_{mf}\right)\epsilon_b C_{A_b} A_c$$

$$\left[\begin{array}{c}\text{Flow of A}\\ \text{out of}\\ \text{bubble phase}\end{array}\right] = \left(u - u_{mf}\right)\left(C_{A_b} + \frac{\partial C_{A_b}}{\partial z}dz\right)\epsilon_b A_c$$

$$\left[\begin{array}{c}\text{Diffusion of A}\\ \text{from bubble to}\\ \text{emulsion phase}\end{array}\right] = k_q a_b \epsilon_b \left(C_{A_b} - C_{A_e}\right) A_c dz$$

$$\left[\begin{array}{c}\text{Production of A}\\ \text{within bubble}\\ \text{phase}\end{array}\right] = \frac{\dot{G}_{A_b}}{H_c}dz$$

The steady state bubble species differential equation then becomes:

$$\frac{d}{dz}C_{A_b} = \frac{\left(-k_q a_b \epsilon_b (C_{A_b} - C_{A_e}) + \frac{\dot{G}_{A_b}}{H_c A_c}\right)}{\epsilon_b (u - u_{mf})} \tag{11.2}$$

The initial condition is the concentration of species A at $z = 0$:

$$C_{A_b}\Big)_{z=0} = C_{A_o} \tag{11.3}$$

12 APPENDIX C. COMBUSTION COMPUTER MODEL LISTING

```
C     This program solves the oxygen and carbon monoxide conservation
C     equations for the two-bed fluidized combustor.  It utilizes the
C     IMSL routine DIVPAG to solve the two first-order differential
C     equations for bubble phase oxygen and carbon monoxide concentration.
C     The subroutine FCN evaluates the two derivatives.  The subroutine
C     FCNJ is never called (it is needed by DIVPAG in case the Jacobian
C     needed to be evaluated).
C
C     Last update:  June 27, 1989 by Jim Foley.
C
      EXTERNAL DIVPAG,FCN,FCNJ
      INTEGER NEQ,NPARAM,IMETH,MXSTEP,IDO,PRFLAG,IFLAG
      PARAMETER (NEQ=2,NPARAM=50)
      DOUBLE PRECISION U,UMF,UB,DB,TIN,TBED,AB,EB,EMF,KQ,H
      DOUBLE PRECISION COB,COE,O2B,O2E,QIN,MDOTDC,PI,DIFFUS
      DOUBLE PRECISION H2OB,AREA,HINIT,ZSTEP,TRAT
      DOUBLE PRECISION TOL,O2EOLD,COEOLD,PERCENT,KA,KB,KC,K1
      DOUBLE PRECISION RATE,LOSS1,LOSS2,LOSS3,LHV,D,SH,NUM
      DOUBLE PRECISION YB(2),YPRIME(2),Z,MDOTOLD,TEST1,TEST2
      DOUBLE PRECISION TEST3,ZEND,Y1OLD,Y2OLD,SUM1,SUM2,QUEST
      DOUBLE PRECISION A(1,1),DYDPY(1,1),PARAM(NPARAM)
      DOUBLE PRECISION A1,A2,A3,A4,A5,A6,A7,A8,A9,A10,O2IN
      DOUBLE PRECISION B1,B2,B3,B4,B5
      CHARACTER*20 CASE

      COMMON/BLK1/B1,B4,A3,A4,O2E,COE

      READ(8,*) U
```

```
      READ(8,*) UMF
      READ(8,*) UB
      READ(8,*) DB
      READ(8,*) TIN
      READ(8,*) TBED
      READ(8,*) EB
      READ(8,*) EMF
      READ(8,*) H
      READ(8,*) QJUNK

      write(9,*)'ECHO PRINT:  U,UMF,UB,DB,TIN,TBED,EB,EMF,H,QIN'
      write(9,*)U,UMF,UB,DB,TIN,TBED,EB,EMF,H,QIN

      PRINT*,'WHICH COMBUSTION CASE? '
      READ(5,1) CASE
      WRITE(9,*) 'FOR COMBUSTION CASE: ',CASE
1     FORMAT(A20)

      print*,'WHAT IS QIN (kW)?'
      READ(5,*) QIN
      write(9,*)'QIN = ',QIN
      QIN = QIN*1.0D+03
      D = 0.0040D0

C     *****   INITIALIZE VARIABLES    **************

      SH = 1.420D0
      PI = 4.0D0*DATAN(1.0D0)
      NUM = 0.080D0*6.0D0/(PI*D*D*D*720.0D0)
      H2OB = 0.00100D0
      DIFFUS = 2.08D-04
      AREA = 0.0324D0
      AB = 6.0D0/DB
      LHV = 2.8891D+07

      KQ = UMF/3.0D0 + DSQRT( 4.0D0*DIFFUS*EMF*UB/(PI*DB) )
      K1 = 1.30D+14
      KA = 2.23900D0*DEXP( -941.10D0/TBED )
      KB = 0.20890D0*DEXP( 7654.70D0/TBED )
```

```
      KC = 0.05018D0*DEXP( 59561.0D0/TBED )
      RATE = K1*(KA**0.50D0) / ( (KB**0.50D0)*(KC**0.25D0) )

C     Make initial guesses for fuel feed rate and concentrations
      MDOTDC = 2.0D0*QIN*3600.0D0/LHV
      YB(1) = 0.00D0
      YB(2) = 0.008705D0
      O2IN = YB(2)
      COE = 0.0010D0
      O2E = 0.0003280D0

      A1 = UMF/H
      A2 = TIN*O2IN/TBED
      A3 = KQ*AB*EB
      A4 = EMF*(1.0D0-EB)
      A5 = 1.0D0/(H*AREA)
      A6 = 2.0D0*PI*NUM*SH*DIFFUS*D
      write(9,*)'A1,A2,A3,A4,A5,A6'
      write(9,*)A1,A2,A3,A4,A5,A6

      B1 = U - UMF
      B2 = -3.162D-05*RATE
      B3 = DSQRT(H2OB)
      B4 = 0.50D0*B2*EB*B3
      write(9,*)'B1,B2,B3,B4'
      write(9,*)B1,B2,B3,B4

      TOL = 1.0D-06
      HINIT = 1.0D-06
      IMETH = 1
      MXSTEP = 10000
      PARAM(1) = HINIT
      PARAM(12) = IMETH
      PARAM(4) = MXSTEP
      ZSTEP = H/50.0D0
      TRAT = TIN/TBED
      IDO = 1
      Z = 0.0D0
```

```
      IT = 0
      IFLAG = 99
      PRFLAG = 0

      DO 222 WHILE (IFLAG.EQ.99)

C        Perform integration with 50 calls to DIVPAG
         Z = 0.0D0
         IDO = 1
         SUM1 = 0.0D0
         SUM2 = 0.0D0
         DO 30 I = 1,50
            Y1OLD = YB(1)
            Y2OLD = YB(2)
            ZEND = DFLOAT(I)*ZSTEP
            CALL DIVPAG (IDO,NEQ,FCN,FCNJ,A,Z,ZEND,TOL,PARAM,YB)
            SUM1 = SUM1 + 0.5D0*(YB(1)+Y1OLD)*H/50.0D0
            SUM2 = SUM2 + 0.5D0*(YB(2)+Y2OLD)*H/50.0D0
C            IF(PRFLAG.EQ.1) write(6,*) Z,YB(1),YB(2)
 30      CONTINUE

C        Last call to DIVPAG, release workspace
         IDO = 3
         CALL DIVPAG (IDO,NEQ,FCN,FCNJ,A,Z,ZEND,TOL,PARAM,YB)

C        Calculate average bubble concentrations
         COB = SUM1/H
         O2B = SUM2/H

C        Calculate emulsion phase concentrations
         A8 = 5.5196D-06*MDOTDC
         A10 = 18.016D-06*MDOTDC
         QUEST = A6*COE + A7
         COEOLD = COE
         O2EOLD = O2E
         IF (QUEST.LT.A8) THEN
            O2E = ( ( A1*A2*A4 + A3*O2B ) /
     !              ( A1*A4 + A3 + A5*A6 ) )
            COE = ( ( A3*COB + A5*A9 + 2.0D0*A5*A6*O2E )/
```

```
!                ( A1*A4 + A3 ) )
          LOSS1 = ( 11.032D-06*MDOTDC - A6*(COE) )*3.9352D+08
       ELSE
          O2E = ( ( A1*A2*A4 + A3*O2B - A5*A8 ) /
!                 ( A1*A4 + A3 ) )
          COE = ( ( A3*COB + A5*A10 ) /
!                 ( A1*A4 + A3 ) )
          LOSS1 = 0.0D0
       ENDIF

C      Calculate percent burned in bed and coal feed rate
       LOSS2 = COE*UMF*AREA*EMF*(1-EB)*1.1053D+08
       LOSS3 = COB*(U-UMF)*AREA*EB*1.1053D+08
       MDOTOLD = MDOTDC
       MDOTDC = 3600.0D0* ( QIN + LOSS1 + LOSS2 + LOSS3 )/ LHV
       PERCENT = QIN / (QIN+LOSS1+LOSS2+LOSS3)


C      Test for convergence
       TEST1 = DABS( (COEOLD-COE)/COE )
       TEST2 = DABS( (O2EOLD-O2E)/O2E )
       TEST3 = DABS( (MDOTOLD-MDOTDC)/MDOTDC )
       IF (PRFLAG.EQ.1) IFLAG = 0
       PRFLAG = 1
       IF (TEST1.GT.1.0D-04) PRFLAG = 0
       IF (TEST2.GT.1.0D-04) PRFLAG = 0
       IF (TEST3.GT.1.0D-04) PRFLAG = 0
       IT = IT + 1

C      Don't exceed 150 iterations
       IF (IT.GT.150) IFLAG = 0

 222   CONTINUE

       WRITE(9,*) 'COE,O2E,COB,O2B'
       WRITE(9,*) COE,O2E,COB,O2B
       WRITE(9,*) 'ITERATIONS = ',IT
       WRITE(9,*) ' '
       WRITE(9,*) 'LOSS1,LOSS2,LOSS3'
```

```
      WRITE(9,*) LOSS1,LOSS2,LOSS3
      WRITE(9,*) ' '
      WRITE(9,*) 'MDOTDC,PERCENT'
      WRITE(9,*) MDOTDC,PERCENT

      END

C     ************************************************************
      SUBROUTINE FCN (NEQ,Z,YB,YPRIME)
C     ************************************************************
C
C     This subroutine evaluates the derivatives of YB
C
      INTEGER NEQ
      DOUBLE PRECISION Z,YB(2),YPRIME(2)
      DOUBLE PRECISION A3,A4,B1,B4,O2E,COE

      COMMON/BLK1/B1,B4,A3,A4,O2E,COE

      YPRIME(1) = ( - A3*(YB(1)-(COE)) + 2.0DO*B4*YB(1)*
     !        ( DABS(YB(2))**0.25DO ) )  / (B1*A4)
      YPRIME(2) = ( - A3*(YB(2)-(O2E)) +   B4*YB(1)*
     !        ( DABS(YB(2))**0.25DO ) )  / (B1*A4)

      RETURN
      END

C     ************************************************************
      SUBROUTINE FCNJ (NEQ,X,Y,DYDPY)
C     ************************************************************
C
C     This subroutine is never called
C
      INTEGER NEQ
      DOUBLE PRECISION X,Y(2),DYDPY(*)
      RETURN
      END
```

13 APPENDIX D. COMBUSTION MASS BALANCES

Fuel composition

C = 0.7788

H = 0.0376

N = 0.0149

S = 0.0300

CaO = 0.01149

O = 0.0257

Ash = 0.1015

W_c = *lbm* of dry coal per *lbm* of fuel

W_l = *lbm* of added limestone per *lbm* of fuel

W_w = *lbm* of water (inherent + added) per *lbm* of fuel

Gas analysis

X_{CO} = mole fraction of CO in dry exhaust gas

X_{CO_2} = mole fraction of CO_2 in dry exhaust gas

X_{O_2} = mole fraction of O_2 in dry exhaust gas

X_{N_2} = mole fraction of N_2 in dry exhaust gas

= $1 - X_{CO} - X_{CO_2} - X_{O_2} - X_{SO_2}$

X_{SO_2} = mole fraction of SO_2 in dry exhaust gas

Carbon in fly-ash

Y_c = *lbm* of carbon per *lbm* of dry fly-ash

Air flow rate

SCFM = standard cubic feet per minute of air flow

= primary + secondary + tertiary air flow

Calculations

$$A_1 = (W_c)(CaO)/56.08 \tag{13.1}$$

$$A_2 = (W_l)/100.091 \tag{13.2}$$

$$A_3 = (W_c)(S)/32.06 \tag{13.3}$$

$$A_4 = (W_c)\left(\frac{O}{32.0} + \frac{CaO}{112.16}\right) + \frac{1.5W_l}{100.091} + \frac{0.5W_w}{18.016} \tag{13.4}$$

$$A_5 = \frac{X_{CO}}{2.0} + X_{CO_2} + X_{O_2} + X_{SO_2} \tag{13.5}$$

$$A_6 = \frac{N}{28.016} \tag{13.6}$$

$$N_{H_2O} = \frac{(H)(W_c)}{2.016} + \frac{W_w}{18.016} \tag{13.7}$$

Initial guess of carbon conversion

$$\eta = 1.0 - \frac{(Y_c)(Ash)}{C(1.0 - Y_c)} \tag{13.8}$$

The following equations are solved iteratively:

$$N_{dg} = \left[\frac{\eta W_c C}{12.011} + \frac{W_l}{100.091}\right]\left(\frac{1}{X_{CO} + X_{CO_2}}\right) \tag{13.9}$$

$$N_{CaSO_4} = A_3 - X_{SO_2} N_{dg} \tag{13.10}$$

$$N_{CaO} = A1 + A2 - N_{CaSO_4} \tag{13.11}$$

$$N_{O_2} = \frac{N_{dg} X_{N_2} - W_c A_6}{3.76 W_c} \tag{13.12}$$

$$\eta = 1.0 - \frac{[136.14 N_{CaSO_4} + 56.08 N_{CaO} + (W_c)(Ash)]Y_c}{CW_c(1.0 - Y_c)} \tag{13.13}$$

Then the excess air is:

$$x = \frac{(N_{O_2} - 0.07477)(100)}{0.07477} \tag{13.14}$$

The mass flow rate of fuel is:

$$\dot{m}_{dc} = \frac{(0.03276)SCFM}{N_{O_2} W_c} \tag{13.15}$$

$$\frac{kgNO}{GJ} = \frac{(0.0010099)Y(ppmNO)}{W_c} \tag{13.16}$$

$$\frac{kgS}{GJ} = \frac{(0.0010792)Y(ppmSO_2)}{W_c} \tag{13.17}$$

EXAMPLE - for Run B-3 with briquettes

$W_c = 0.7763$

$W_l = 0.1297$

$W_w = 0.0940$

$Y_c = 0.200$

$X_{CO} = 0.00024$

$X_{CO_2} = 0.1324$

$X_{O_2} = 0.0497$

$X_{N_2} = 0.8165$

$X_{SO_2} = 0.00117$

SCFM = 19.92 + 5.38 − 5.0 = 30.30

$A_1 = 0.0001591$

$A_2 = 0.001296$

$A_3 = 0.0007264$

$A_4 = 0.005256$

$A_5 = 0.19392$

$A_6 = 0.0005318$

Z = 0.019696

Solve equations iteratively:

N_{dg}	=	0.360 moles dry gas per *lbm* fuel
N_{CaSO_4}	=	0.000305 moles $CaSO_4$ per *lbm* fuel
N_{CaO}	=	0.00115 moles CaO per *lbm* fuel
η	=	0.924 = carbon conversion efficiency
N_{O_2}	=	0.1006 moles O_2 per *lbm* fuel

Fuel mass flow rate:

$\dot{m}_f$ = 12.71 *lbm* fuel per hr

$\dot{m}_{dc}$ = 9.87 *lbm* dry coal per hr

Excess air:

x = 34.59%

Emissions:

$\frac{kg\ NO}{GJ}$	=	0.160
$\frac{kg\ S}{GJ}$	=	0.586